HEINRICH HEINE
UNIVERSITÄT DÜSSELDORF

The role of the PsbS protein in the regulation of energy dissipation in vascular plants and green algae

Inaugural-Dissertation

for attaining the title of Doctor (Dr. rer. nat.)
in the Faculty of Mathematics and Natural Sciences
at Heinrich Heine University Düsseldorf

Presented by

Viviana Andrea Correa Galvis

From Bogotá, Colombia

Düsseldorf, November 2015

From the Institute of Plant Biochemistry,
Heinrich Heine University Düsseldorf

Printed with permission from the Faculty of Mathematics and Natural Sciences,
Heinrich Heine University Düsseldorf

Supervisor: Prof. Dr. Peter Jahns
Co-Supervisor: Prof. Dr. Rüdiger Simon.

Date of Oral Examination: December 7th 2015.

Para Cecilia e Iván.
Porque ustedes son mis raíces,
mi origen ,mi orgullo y mi punto de
retorno al que siempre vuelvo
cuando necesito la fuerza
para seguir adelante

Mit allen Augen sieht die Kreatur
das Offene. Nur unsre Augen sind
wie umgekehrt und ganz um sie gestellt
als Fallen, rings um ihren freien Ausgang…

Die achte Elegie
Duineser Elegien
Rainer Maria Rilke

STATEMENT OF DECLARATION

I, Viviana Andrea Correa Galvis, hereby declare that I have fully and independently written the submitted dissertation without additional unauthorized support and consultation beyond that permitted and specified in the dissertation to include the necessary and appropriate cited literary resources. The dissertation in its present or similar form has not been previously submitted under the same or otherwise specified institution and department name. Previous unsuccessful oral examinations have not been registered or attempted.

Düsseldorf, November 9th 2015

Table of Contents

1. GENERAL INTRODUCTION

1.1 PHOTOSYNTHESIS AS THE BASIS OF LIFE

The definition of the word “life” is *per se* complicated. However, one could use one intrinsic characteristic of life for its definition. There is one feature common to all living organisms: they transform energy in order to organize it, so in that sense, life is a form of organized energy. Evolution of living organisms is also the evolution of all those processes that enabled them to capture energy and to organize it. Photosynthesis is the process converting sun light energy into chemical energy of organic compounds, and thus represents one of the most important (if not the most important) biological developments. In oxygenic photosynthesis, light energy drives the generation of oxygen (from water oxidation) and the synthesis of carbohydrates (from carbon dioxide) (Taiz and Zeiger, 2010).

Photosynthesis in eukaryotic organisms occurs in the thylakoid membrane of the chloroplast (Fig. 1A). Thylakoids are a membrane system composed of stacked (grana) and unstacked (stroma lamellae) regions, which surrounds an additional compartment, the thylakoid lumen. The overall process of photosynthesis is divided into light reactions (light-dependent electron and proton transport) and dark reactions (carbon fixation through the Calvin-Bassham cycle). The light reactions use the energy of absorbed photons to reduce $NADP^+$ to NADPH through electron transport. Coupled to the electron transport, a proton gradient across the thylakoid membrane is built up, which provides the driving force for the synthesis of ATP. Both products, ATP and NADPH, are used in the Calvin-Bassham cycle (dark reactions) for the production of triose phosphates and hence carbohydrates. The light reactions take place in the thylakoid membrane, whereas the dark reactions are localized in the chloroplast stroma (Fig. 1A).

1.1.1 The photosynthetic electron transport chain

Electron and proton transport are driven by the photosynthetic electron transport chain located in the thylakoid membrane (Fig. 1B). This chain is mainly composed of three integral protein complexes: photosystem II (PSII), cytochrome b_6f-complex ($Cytb_6f$), and photosystem I (PSI), which are linked by two mobile electron carriers, plastoquinone (PQ) and plastocyanin (PC) (Hervás et al., 2003).

Both photosystems contain on the luminal side of their reaction centers a special chlorophyll a (Chl a) pair: P680 in PSII and P700 in PSI (Mazor et al., 2015; Suga et al., 2015; Zouni et al., 2001) .

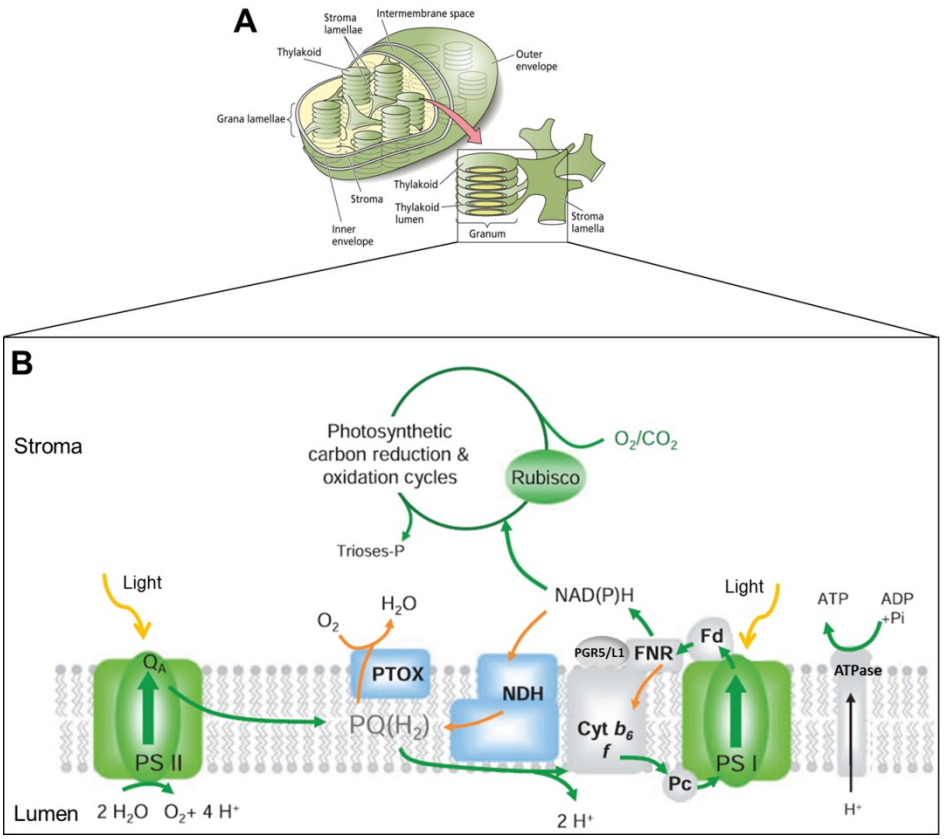

Figure 1. Light and dark reactions of photosynthesis. In the thylakoid membrane of the chloroplast **(A)**, light energy is captured and converted into chemical energy in the light-driven electron transport (light reactions) **(B)**. Chemical energy is stored in from of NADPH and ATP, which both are used for carbon assimilation in the chloroplast stroma (dark reactions). PSII = photosystem II; $Cytb_6f$ = cytochrome b_6f complex; PSI = photosystem I; $PQ(H_2)$ = plasto(hydro)quinone; PC = plastocyanin; Fd = ferredoxin; FNR = ferredoxin-NADP reductase; NDH = NADH dehydrogenase complex; PGR5/L1 = proton gradient regulation 5/L1 protein POTX = plastid terminal oxidase. Green arrows indicate linear electron flow, and orange arrows indicate cyclic electron flow and chlororespiration. Adapted from (Taiz and Zeiger, 2010)and (Rumeau et al., 2007).

Excitation of P680 and P700, respectively, induces a charge separation in the reaction center and by that electron transfer to the stromal side of the thylakoid membrane (Fig. 1B). Thereby oxidized $P680^+$ (in PSII) and $P700^+$ (in PSI) are formed. In PSII the electron gap is filled with electrons originating from the water oxidizing complex (WOC) which is accompanied by proton release from oxidized water into the lumen. The electrons are transferred from PSII to $Cytb_6f$ through plastohydroquinone (PQH_2). $Cytb_6f$ oxidizes PQH_2 to PQ and reduces plastocyanin (PC), again coupled to proton release into the lumen. In PSI, charge separation induces electron transfer to ferredoxin (Fd) and finally to the reduction of $NADP^+$ to NADPH by the ferredoxin-NADP reductase (FNR). The electron gap in $P700^+$ is filled by electron transfer from $Cytb_6f$ to PSI via PC. Electron transport together with the accumulation of protons in the lumen generate the proton motive force (*pmf* = $\Delta pH + \Delta\Psi$) across the thylakoid membrane, which is used by the CF_0/CF_1-ATPase (ATP-synthase) to form ATP along with the efflux of protons from the lumen into the stroma (Nelson and Junge,

2015). This sequence of electron transfer from H_2O (at PSII) to $NADP^+$ (at PSI) is known as linear electron flow (LEF). Additionally, electrons can be recycled around PSI, through cyclic electron flow (CEF). In CEF, electrons can be re-directed from Fd to PQ via the PROTON GRADIENT REGULATION proteins PGR5 and PGRL1 (DalCorso et al., 2008; Munekage et al., 2004) and/or by the NAD(P)H dehydrogenase-like (NDH) complex (Ifuku et al., 2011). Furthermore reducing power can be transferred from NADPH to PQ through chlororespiration. Chlororespiration has been mainly described for green algae (such as *Chlamydomonas reinhardtii*) and requires a NADPH-dehydrogenase (Jans et al., 2008) that transfers reducing power from NADPH to PQ using a plastid terminal oxidase (PTOX) as terminal plastoquinol oxidase (Cournac et al., 2000; Houille-Vernes et al., 2011). CEF and chlororespiration are supposed to balance the ATP/NADPH ratio by increasing the accumulation of protons in the lumen to drive ATP synthesis without new production of NADPH (Fig. 1B).

1.2 THE PHOTOSYNTHETHIC MACHINERY

1.2.1 PSII Supercomplexes

Light capture is achieved by energy transfer from a net of pigment protein complexes (known as light harvesting complexes, LHC) to the reaction center. LHCII proteins and PSII reaction centers are organized in the grana stacks in the thylakoid membrane as PSII-LHCII supercomplexes (Fig. 2).

In higher plants, the light harvesting proteins belong to the Lhc gene family (Jansson, 1999) and can be divided into two main groups: Major LHCII and minor LHCII antenna complexes. Major antenna complexes are oligomeric trimers composed of various combinations of three similar proteins named Lhcb1, Lhcb2 and Lhcb3, encoded by the *LHCB1.1–1.5, LHCB2.1–2.4* and *LHCB3.1* genes, respectively (Jansson, 1999). The trimers are found in a ratio of 8:3:1 for Lhcb1:Lhcb2:Lhcb3, respectively (Jansson, 1994). The minor antenna complexes CP29, CP26 and CP24 are encoded by the *LHCB4, LHCB5* and *LHCB6* genes, respectively (Jansson, 1999), and occur as monomers only (Dekker and Boekema, 2005); Fig. 2). In the green algae *C. reinhardtii*, four major types of LHCII proteins, termed type I–IV, have been described. LHCBM3, 4, 6, 8 and 9 belong to type I, LHCBM5 to type II, LHCBM2 and 7 to type III and LHCBM1 to type IV (Teramoto et al., 2002). In contrast to land plants, only the two minor LHCII proteins CP29 and CP26 (encoded by *LHCB4* and *LHCB5*, respectively) are present in *C. reinhardtii*, while CP24 is absent (Minagawa and Takahashi, 2004).

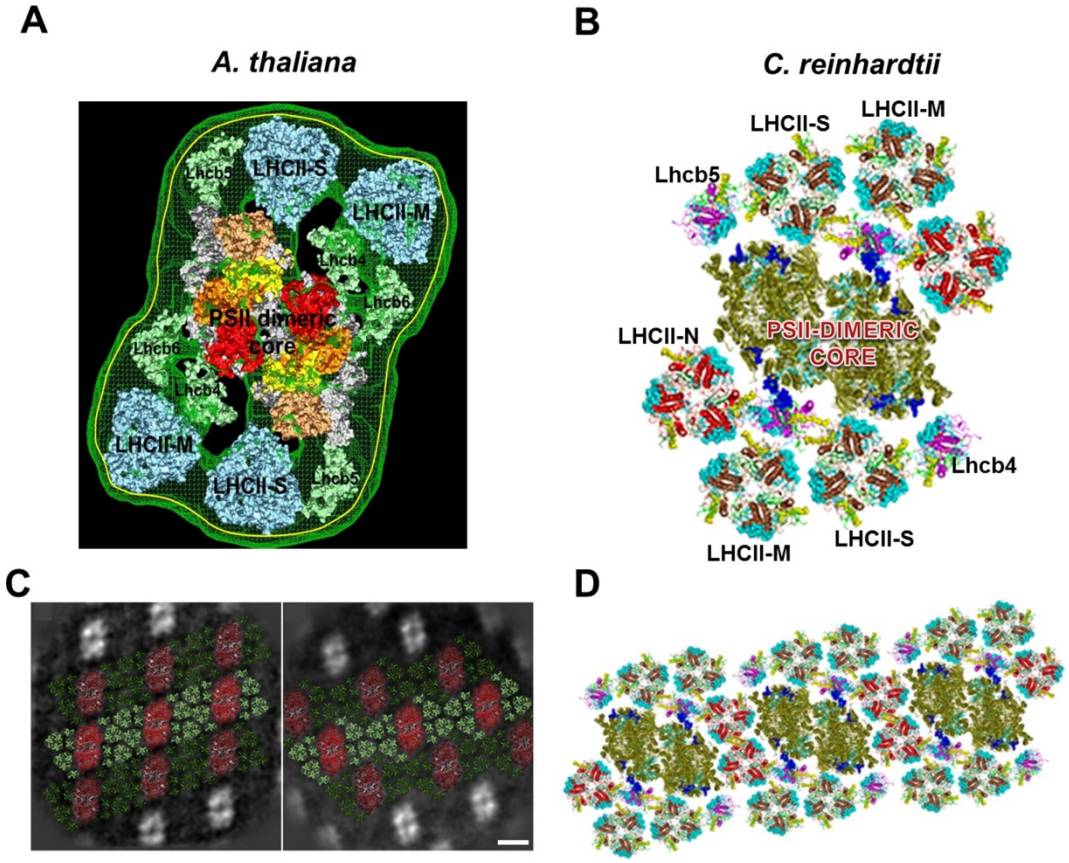

Figure 2. Structure of the PSII-LHCII supercomplexes in plants and green algae. (A) Model for the $C_2S_2M_2$ PSII-LHCII supercomplex in *A. thaliana*. D1, D2, CP47, CP43 and PsbO are in yellow, orange, red, sandy brown and purple, respectively. All other subunits in grey. LHCII-M and LHCII-S trimers are shown in blue and the minor complexes CP29 (Lhcb4), CP26 (Lhcb5) and CP24 (Lhcb6) in green (Pagliano et al., 2014). **(B)** $C_2S_2M_2N_2$ PSII-LHCII supercomplex in *C. reinhardtii*. PSII core, LHCII-S and -M, LHCII-N, CP29 (Lhcb4) and CP26 (Lhcb5) are in lime green, brown, red and magenta, respectively (Drop et al., 2014). **(C, D)** Crystalline arrays of the PSII-LHCII supercomplexes in the thylakoid membrane **(C)** Example of two arrays of supercomplexes in *A. thaliana*. Scale bar: 100 nm (Kouřil et al., 2012) **(D)** Model for the organization of $C_2S_2M_2N_2$ supercomplexes in *C. reinhardtii* (Drop et al., 2014).

In the PSII-LHCII supercomplex of higher plants, LHC proteins are arranged around PSII in a highly organized manner. LHCII trimers are classified as strongly (S), moderately (M) or loosely (L) bound to the PSII dimeric core complex related to their detergent-dependent susceptibility (Barera et al., 2012; Boekema et al., 1999). A dimeric core (C_2) can associate two LHCII S-trimers forming the C_2S_2 supercomplex. Further association of the M-trimers gives rise to the $C_2S_2M_2$ supercomplex (Dekker and Boekema, 2005; Pagliano et al., 2014). In spinach, the supercomplex can additionally bind a third LHCII trimer, denoted as L-trimer (Dekker and Boekema, 2005). The dimeric PSII core complex (C_2) strongly binds two copies of the monomeric complexes CP29 and CP26, and two LHCII trimers (S-trimer) in order to form the C_2S_2 supercomplex (Caffarri et al., 2009). Two LHCII-M trimers containing exclusively Lhcb1 and Lhcb3 are additionally bound to C_2S_2 via CP24, giving rise to the

$C_2S_2M_2$ supercomplex (Caffarri et al., 2009; Pagliano et al., 2014). $C_2S_2M_2$ represents the basic supercomplex unit of the PSII-LHCII organization in *A. thaliana* (Fig. 2A).

In *C. reinhardtii,* besides LHCII-S and M trimers, an additional trimer, termed LHCII-N, has been found as an intrinsic component of the PSII-LHCII supercomplex (Drop et al., 2014). Since CP24 is not present in this alga it is possible that the presence of a LHCII-N stabilizes the binding of LHCII-M to the core (Drop et al., 2014). Conversely, LHCII-N binding can be stabilized by LHCII-M as well. Consequently, PSII supercomplexes may be organized as $C_2S_2M_2N_2$, C_2S_2MN, C_2SMN supercomplexes, according to their distribution after separation by sucrose gradient ultracentrifugation. However, the distribution of each LHC protein within each trimer is still unclear (Drop et al., 2014). $C_2S_2M_2N_2$ likely constitutes the basic supercomplex unit in *C. reinhardtii* (Fig. 2B).

The different supercomplexes typically show a random distribution in the thylakoid grana region, however, under certain conditions it is possible to observe semi-crystalline arrays by single particle electron microscopy (Fig. 2C). This organization has some implications on the energy transfer mechanism. For example, the association of several $C_2S_2M_2$ supercomplexes implies that the captured energy is predominantly transferred among the peripheral antenna rather than among the PSII core complexes, thus optimizing light harvesting (Kouřil et al., 2012).

1.2.2 Light Harvesting Antenna Proteins

All harvesting antenna proteins show a very similar overall structure composed of three transmembrane helices and two small amphipathic helices. Each Lhcb1-3 monomer binds 14 chlorophyll (Chl) molecules (8 Chl a and 6 Chl b) and 4 xanthophylls (1 neoxanthin, 2 lutein and 1 violaxanthin) (Fig. 3) (Liu et al., 2004; Standfuss et al., 2005). Two lutein molecules are bound to the two central binding sites, termed L1 and L2. Neoxanthin and violaxanthin are located at the N1 and V1 sites, respectively, at the periphery of the complex (Caffarri et al., 2001; Croce et al., 1999). The close proximity of the Chl molecules (Fig. 3A) in the protein allow for fast energy transfer in the complex (Croce and van Amerongen, 2011). Four Chl a binding sites are located in the center of the molecule (602, 603, 610 and 612) (Fig. 3E), with Chl 602/603 absorbing at around 675 nm and Chl 610/612 at 680 nm (Croce and van Amerongen, 2011). Monomeric CP29 contains 13 Chl molecules (8 Chl a, 4 Chl b and a Chl a/b mixed binding site at position 610), and three xanthophyll binding sites for 1 lutein (L1), 1 violaxanthin (L2) and 1 neoxanthin (N1) (Pan et al., 2011).

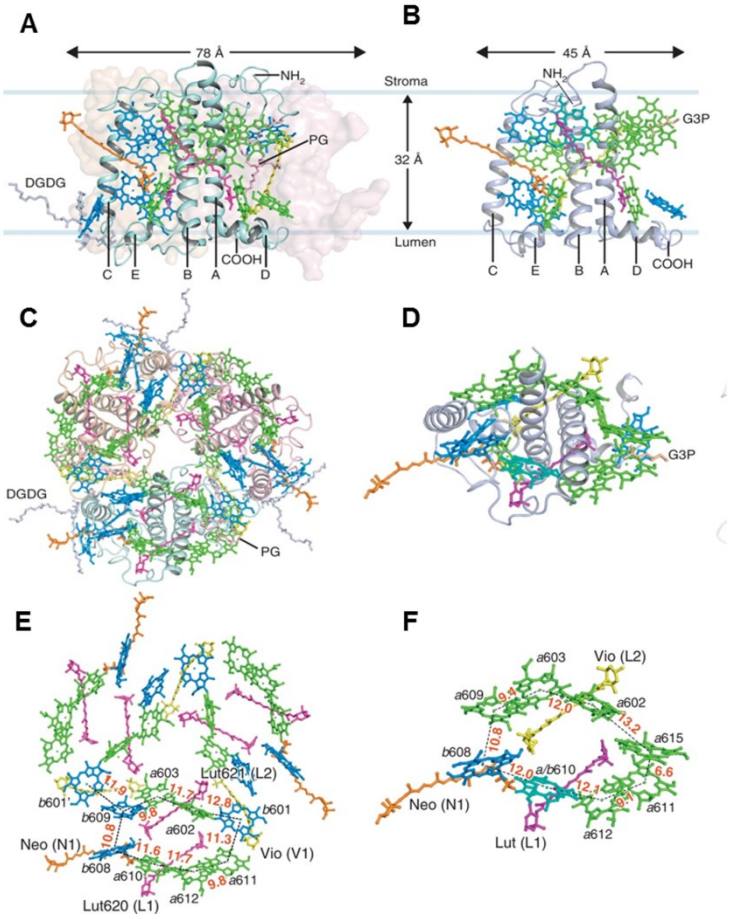

Figure 3. Structure of monomeric and trimeric LHCII proteins. **(A, B)** side view of major LHCII (A) and CP29 (B). Letter A to E denote transmembrane (A, B, C) and amphipathic (D, E) helices. **(C, D)** Top view from the stromal side on trimeric LHCII (C) and CP29 (D). **(E, F)** Pigment molecules within major LHCII trimers (E) and CP29 (F). Green, Chl a; blue, Chl b; cyan, Chl a/b610 in CP29; magenta, lutein (Lut); yellow, violaxanthin (Vio); orange, neoxanthin (Neo); pink, phosphatidyl glycerol (PG) in major LHCII; pale-blue, digalactosyl diacylglycerol (DGDG) in major LHCII; wheat, glyceraldehyde 3-phosphate (G3P) in CP29. Adapted from (Pan et al., 2013).

Some differences have been observed between the monomeric and trimeric LHC structures, which provide information about the features that define the formation of heterotrimers. The amino acid sequence WYXXXR in position 16–21 of major LHCII is essential for trimer formation (Hobe et al., 1995). This motif is conserved in Lhcb1, Lhcb2 and Lhcb3, but not in CP24, CP25 or CP26. The motif contributes to the binding of phosphatidyl glycerol in the thylakoid membrane at the trimer interphase, as well as the N-terminal domain that is essential for its positioning (Pan et al., 2013). The Chl binding sites are conserved across the LHC family (Croce and van Amerongen, 2011), except for Chl b601 and Chl b605 which are present in major LHCII but absent in CP29, while Chl a615 in CP29 is lacking in major LHCII proteins. Moreover, sites 609 and 614 are occupied by Chl b and Chl a, respectively, in major LHCII, and reversely in CP29 (Chl a at position 614 and Chl b at position 609) (Pan et al., 2013). The differential arrangement of pigments in trimeric and

monomeric proteins is supposed to contribute to an efficient energy equilibration within the trimer and to facilitate the energy transfer between major and minor LHCs (Pan et al., 2013).

1.2.3 Photosystem II reaction center

The active PSII reaction center (PSII-RC) is organized as a dimer with a calculated mass of about 700 kDa. Each monomer contains 17 transmembrane subunits, 3 peripheral units and various cofactors (Ferreira et al., 2004; Guskov et al., 2009; Umena et al., 2011) (Fig. 4A). Additionally, each monomer comprises 35 chlorophylls, 2 pheophytins, 11 b-carotenes, 2 plastoquinones,1 heme irons, 1 non-heme iron, 4 manganese atoms,1 bicarbonate ion, 4 calcium atoms, 3 Cl^- ions and more than 20 lipids (Umena et al., 2011).

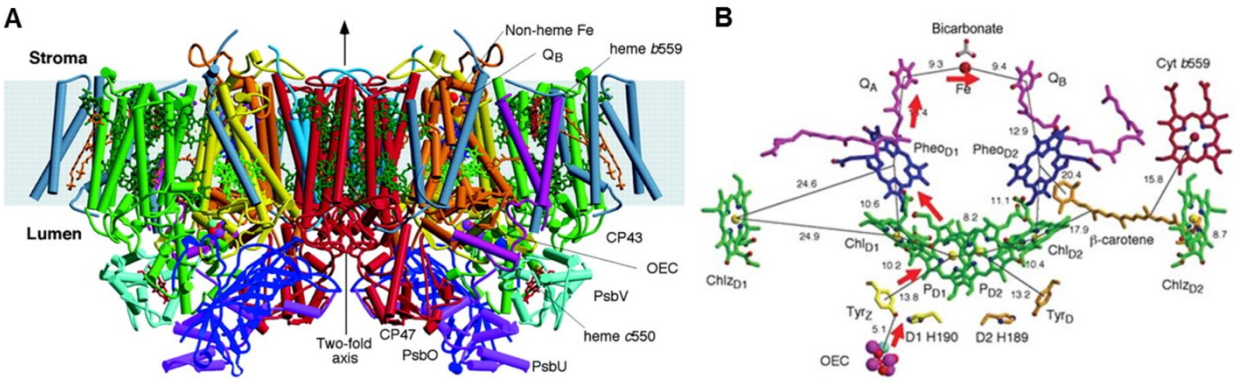

Figure 4. Structure of photosystem II and the oxygen evolving complex. **(A)** Side view of the dimeric PSII RC: D1 (yellow), D2 (orange), CP47 (red), CP43 (green), Cyt $_{b559}$ (wine red), PsbL, PsbM, and PsbT (medium blue) PsbH, PsbI, PsbJ, PsbK, PsbX, PsbZ, and PsbN (gray). Extrinsic proteins: PsbO (blue), PsbU (magenta), and PsbV (cyan). **(B)** Organization of the electron transfer cofactors present in the PSII RC: Chl (green); pheophytin (blue), heme (red), Q_A and Q_B (purple). The components of the oxygen-evolving center (OEC) are shown as red (oxygen atoms), magenta (Mn ions) and cyan (Ca^{2+}) balls. Red arrows represent electron transfer processes. Adapted from (Barber, 2012) and reprinted with permission from Ferreira et al. 2004. (AAAS).

The heart of the PSII reaction center core (PSII RC) consists of two homologous proteins, D1 (*PSBA*) and D2 (*PSBD*), which bind all cofactors required for charge separation (including 6 Chl a, 2 pheophytin a, and the acceptor quinones Q_A and Q_B). The D1/D2 heterodimer is connected to the core antenna proteins CP43 (*PSBC*) and CP47 (*PSBB*) which each contain six transmembrane helices. CP43 binds 13 Chl a and CP47 16 Chl a molecules (Ferreira et al., 2004). Additionally, a number of low molecular subunits are bound to the PSII RC named PsbL, PsbM, PsbT, PsbH, PsbI, PsbJ, PsbK, PsbX, PsbZ, PsbN and $Cytb_{559}$. $Cytb_{559}$ binds a high potential heme cytochrome, whose function is not yet understood (Ferreira et al., 2004). Excitation of the RC via Chl bound to CP47 and CP43 leads to the reduction of pheophytin (Pheo) in the D1/D2 heterodimer and thus to the first stable charge separated state $P680^+Pheo^-$. The electron from $Pheo^-$ is first donated to the

primary quinone acceptor Q_A and then to Q_B. After accumulation of two electrons at Q_B, the resulting in PQH_2 is released from the PSI-RC and diffuses towards $Cytb_6f$. $P680^+$ is reduced by a redox-active tyrosine of the D1 protein, which extracts an electron from the Mn_4O_5Ca cluster of the oxygen evolving complex (OEC). The OEC is located on the luminal side of PSII and is stabilized by PsbO, PSbP and PsbQ in plants and green algea, and by PsbO, PsbU, and PsbV in red algae and cyanobacteria (Barber, 2012; Ferreira et al., 2004).

1.2.4 Photosystem I

The PSI reaction center (PSI-RC) is organized as monomer with two major core proteins PsaA and PsaB and three extrinsic subunits (PsaC, D and E) being the central functional unit. The PsaA/B heterodimer binds all redox factors required for charge separation (including the Fx 4Fe-4S iron-sulphur cluster), while the stromal subunit PsaC binds the two terminal iron–sulfur clusters FeS_A and FeS_B, and forms together with PsaD and PsaE the docking site of the electron acceptor ferredoxin (Nelson and Junge, 2015). The PSI-RC is surrounded by the minor proteins PsaF, PsaG, PsaH, PsaI, PsaJ, PsaK and PsaL (Fig. 5). PsaA binds 40 Chl and PsaB 39 Chl, while 1-3 Chl molecules per subunit are bound by PsaJ, PsaK, PsaL, PsaG, and PsaH (Nelson and Yocum, 2006). PsaH might contribute to direct binding of PC at the luminal side (Mazor et al., 2015). Like PSII, also PSI is surrounded by peripheral Chl a/b binding antenna complexes (LHCI, Lhca1-6). Lhca proteins bind in total 52 Chl a and 9 Chl b molecules, as well as 10 carotenoids and 4 lipids, and are separated from PSI-RC by a half-moon shaped cleft that is docked at the F-subunit side of the RC (Mazor et al., 2015). PSI-LHCI complexes from *C. reinhardtii* are much larger than those of green plants, containing 11 Lhca proteins, with each of them binding 10 Chl (Kargul et al., 2003).

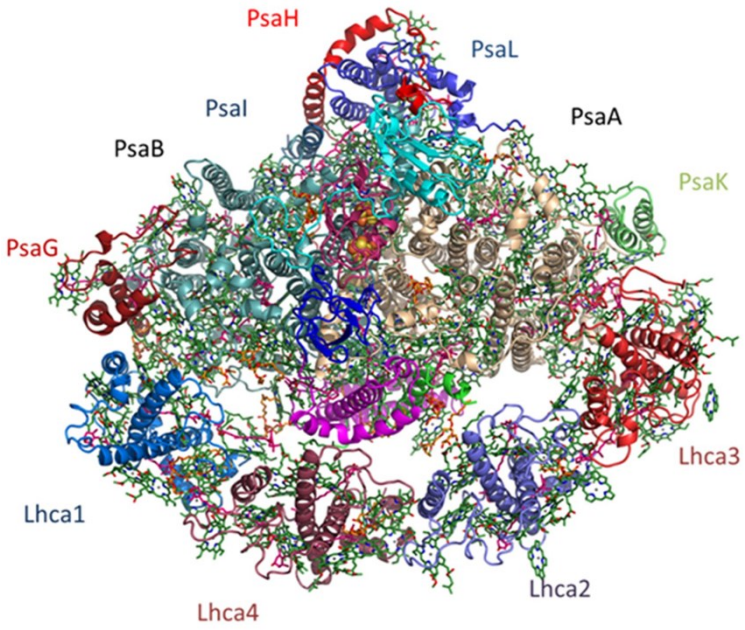

Figure 5. Structure of the photosystem I complex. The scheme represents the stromal view of the PSI-LHCI complex. Subunits PsaC, PsaD, and PsaE, are bound in the middle of the complex, coloured cyan, pink, and blue, respectively. The PsaF (magenta) and PsaJ (green) subunits are connected in the middle of LHCI. The two iron-sulfur clusters of PsaC can be distinguished as yellow and orange clusters in the middle of the complex. Adapted from (Mazor et al., 2015).

1.3 SENSING AND ACCLIMATION OF EXCESS LIGHT ENERGY

Under most natural conditions, the rate of light absorption exceeds the capacity of light utilization in photosynthesis (Li et al., 2009), which inevitably leads to the accumulation of excess light energy in the antenna of both photosystems. The accumulation of light energy that cannot be used for chemical work or electron transfer bears a high risk of cellular damage. If the energy of excited Chl molecules in the antenna proteins (^{1}Chl*) is not transferred to the PSII-RC core, the lifetime of ^{1}Chl* is increased and by that the probability of the formation of long-lived Chl triplet states (^{3}Chl*). ^{3}Chl* is known to transfer its energy rapidly to oxygen, by that forming $^1O_2$*, a highly reactive oxygen species that can unspecifically oxidize proteins, DNA and lipids (Müller et al., 2001). Photosynthetic organisms have developed a number of strategies to avoid damage by excess light such as the reduction of light absorption, the detoxification of ROS or the dissipation of excess light energy as heat. The absorption of excess light energy can be reduced in land plants by chloroplast movement, which is controlled by photon flux receptors as phototropins and neochromes (Suetsugu et al., 2005; Wada et al., 2003). In *C. reinhardtii,* rhodopsins have been shown to serve important functions in phototaxis, which allows cells to coordinate their swimming in relation to the light availability (Govorunova et al., 2004). The scavenging of ROS and the repair of oxidative damage caused by ROS include non-enzymatic antioxidants such as α-tocopherol (Kobayashi and DellaPenna, 2008), glutathione, ascorbate, and

enzymes such as superoxide dismutase (SOD), ascorbate peroxidase (APX) and glutathione reductase (GR) (Asada, 2006) or peroxiredoxins (Dietz, 2011). The third strategy involves the dissipation of energy in form of heat, known as non-photochemical quenching (NPQ).

1.3.1 Non-photochemical quenching

NPQ describes a photoprotective mechanism active in the antenna of PSII, which dissipates excitation energy as heat at the level of ^{1}Chl*, by that preventing the formation of singlet oxygen in PSII (Krause and Jahns, 2004). Four different components contribute to NPQ, called qE, qZ, qT and qI, which can be activated on different time scales (Nilkens et al., 2010) and thus allow optimal acclimation to different environmental conditions. The qE component represents the most rapidly inducible and most flexible NPQ mechanism and will be introduced in detail below.

qZ represents the zeaxanthin (Zx) dependent quenching and is activated under saturating light conditions. Zx develops slowly in the light (10-30 min) concomitant with Zx formation, and it typically relaxes within 10-60 min in the dark, in parallel with reconversion of Zx to violaxanthin (Nilkens et al., 2010). So far, qZ has been only reported in vascular plants.

qT represents the reversible movement of LHCII proteins between PSII and PSI. qT is regulated by protein phosphorylation catalyzed by a membrane-bound kinase, STATE TRANSITION7 (STN7 in higher plants; STT7 in *C. reinhardtii*) (Bonardi et al., 2005; Depège et al., 2003). qT is not a direct non-photochemical quenching of energy, but rather regulates the distribution of excitation energy between PSII and PSI. The transition from state 1 (preferential excitation of PSI, LHCII bound to PSII) to state 2 (preferential excitation of PSII, LHCII bound to PSI) is triggered when the plastoquinone (PQ) pool is reduced, which leads to activation of the Stt7/STN7 kinase and hence phosphorylation of LHCII. Phosphorylated LHCII then dissociates from PSII and binds to PSI (Rochaix, 2014). In *A. thaliana*, qT occurs under low and moderate light (Tikkanen et al., 2006) and its relative contribution to the overall NPQ is rather low (Nilkens et al., 2010). In contrast, state transitions (and thus qT) in *C. reinhardtii* represent a major component of the quenching response acting along with qE to balance the excess energy under high light (Allorent et al., 2013).

The qI component of NPQ is related to the photoinhibition of PSII upon long term high light illumination. The qI mechanism is not fully understood, but requires the inactivation of the D1 protein and Zx formation (Jahns et al., 2009). Since inactive PSII-RCs are efficient quenchers of absorbed light energy, the inactivation of the D1 protein is supposed to play an important regulatory and photoprotective role (Krause and Jahns, 2004; Lee et al., 1999). Recovery from photoinhibition (and thus the relaxation of qI) requires the degradation and *de novo* synthesis of the D1 protein (Gururani et al., 2015).

1.3.2 Energy-dependent quenching (qE)

qE is the dominating NPQ component under most conditions (Krause and Jahns, 2004; Müller et al., 2001; Nilkens et al., 2010) and is activated after a few seconds upon illumination. It constitutes a feedback de-excitation that provides a fitness advantage in field conditions by enhancing the tolerance to rapid variations in light intensity (Kulheim et al., 2002). qE is strictly dependent on the ΔpH across the thylakoid membrane due to the light-driven accumulation of protons in the lumen (Briantais et al., 1979). In land plants and mosses, it also requires the presence of the PsbS protein and the synthesis of the xanthophyll Zx (Alboresi et al., 2010; Li et al., 2000; Niyogi et al., 1998). In green algae (*C. reinhardtii*), however, qE depends on the light induced expression of the LHCSR proteins (Peers et al., 2009).

PsbS protein

The PsbS protein in *A. thaliana* (also known as CP22) is a 22 kDa member of the LHC protein superfamiliy and encoded by the *NPQ4* gene, which localizes to chromosome 1 (Li et al., 2000). Although PsbS is a constitutively expressed protein, the level of *PSBS* messenger RNA is increased several fold in response to high light (Li et al., 2000). PsbS is essential for qE induction (Li et al., 2000) and the protein is imported into the chloroplast in a SRP independent manner and accumulates in the thylakoid membrane independently of PSII (Niyogi et al., 2005; Rutschow et al., 2008). Unlike typical LHC proteins with three transmembrane α-helices, the PsbS protein has four helices. Helices 1 and 3 as well as helices 2 and 4 have very similar amino acid sequences and are located in mirrored positions (Fan et al., 2015; Li et al., 2000; Li et al., 2002) (Fig. 6). The rather compact structure of the protein is thought to contribute to a certain degree of flexibility among the PSII-LHCII complexes and prevents the binding of chlorophyll and carotenoid molecules (Dominici et al., 2002; Fan et al., 2015). The activation of PsbS relies on the protonation of two luminal glutamate residues (E55 and E159 in *S. oleraceae;* E122 and E226 in *A. thaliana*) upon drop of the luminal pH under high light illumination (Fan et al., 2015; Li et al., 2004). Extensive intermolecular interactions involving the hydrophobic transmembrane regions of helices 2 and 3 (Fig. 6), along with a distinct conformation of the two luminal loops contribute to the formation of a stable dimer (Fan et al., 2015). The dynamics of the monomeric and dimeric state of PsbS is critical to understand the function of PsbS and its interactions with members of the PSII-LHCII upon qE activation.

In *C. reinhardtii,* the PsbS protein is encoded by two genes, *PSBS1* and *PSBS2* located on chromosome 1 (Anwaruzzaman et al., 2004). Based on the predicted structure, PsbS in *C. reinhardtii* is supposed to contain four transmembrane helices and two glutamate

residues on the luminal side as its *A. thaliana* counterpart (Anwaruzzaman et al., 2004). However, PsbS expression has been only detected at the transcript level (Mettler et al., 2014; Miller et al., 2010) and hence PsbS has been defined as not essential for qE in green algae.

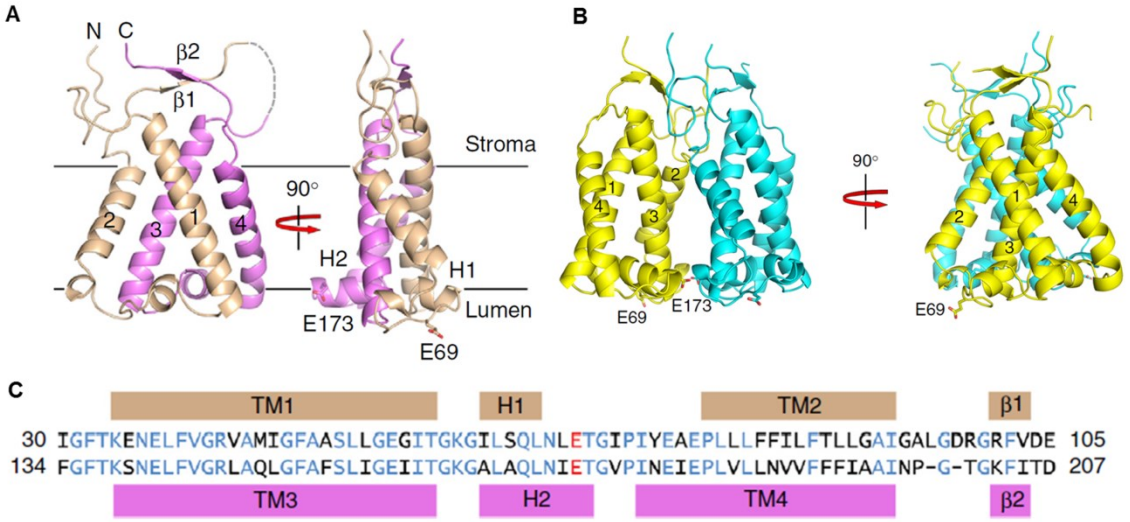

Figure 6. Model for the structure of spinach PsbS. (A) Side view on PsbS from the membrane plane, indicating the transmembrane domains (left) and the localization of the glutamate residues involved in sensing the lumen pH (right). **(B)** PsbS dimer. The scheme illustrates the hydrophobic interactions between TM2 and TM3 of two PsbS monomers **(C)** Sequence alignment between the two halves of PsbS highlighting the transmembrane and luminal loops as well as the pH sensing glutamates (red). Adapted from (Fan et al., 2015).

LHCSR protein

In *C. reinhardtii*, qE quenching is only induced after several hours of constant high light illumination. The activation of qE is tightly correlated with the high light dependent induction of two nuclear encoded proteins, LHCSR3 and LHCSR1 (Peers et al., 2009). LHCSR encoding genes are present in green algae and mosses but absent in vascular plants and red algae (Koziol et al., 2007; Teramoto et al., 2002). LHCSR3 is a 26.1 kDa protein encoded by two genes *LHCSR3.1, LHCSR3.2*. LHCSR1 has 87 % identity with LHCSR3 and is encoded by a single gene *LHCSR1* (Peers et al., 2009). LHCSR3 has a higher contribution to qE than LHCSR1, since the single *LHCSR3* mutant (*npq4* mutant in *C. reinhardtii*) shows more than 80 % reduction of maximum qE levels. The residual quenching found in the LHCSR3-deficient *npq4* mutant corresponds to the contribution of LHCSR1 (Peers et al., 2009). LHCSR proteins are, in contrast to PsbS, chlorophyll *a*/*b* and xanthophyll-binding proteins (Bonente et al., 2011). LHCSR3 is responsive to low luminal pH and is a strong quencher of Chl excited states, exhibiting very fast fluorescence decays (Bonente et al.,

2011). Furthermore LHCSR3 binds to the PSII-LHCII supercomplex at low luminal pH (i.e upon high light acclimation) forming a PSII-LHCII-LHCSR3 supercomplex mediated by the PSII PSBR subunit (Tokutsu and Minagawa, 2013; Xue et al., 2015).

According to the current understanding of qE in *C. reinhardtii,* high light induces the synthesis of LHCSR3, which acts as a pH sensor as well as a quencher. Conformational changes at the C-terminal subdomain of the protein, induced by lumen acidification, switch the protein from a light-harvesting to a photo-protective state (Liguori et al., 2013), thereby promoting energy dissipation in the PSII-LHCII super complexes (Minagawa and Tokutsu, 2015). Furthermore, LHCSR3 becomes phosphorylated in high light (Allorent et al., 2013; Bonente et al., 2011) and associates in higher amounts to the PSI-LHCI-FNR complexes in the *STT7*-kinase mutant (Bergner et al., 2015).

Zeaxanthin synthesis

Apart from activation of qE, acidification of the thylakoid lumen further activates the enzyme violaxanthin de-epoxidase (VDE) which converts the pigment violaxanthin (Vx) to Zx via the intermediate antheraxanthin (Ax) in the de-epoxidation reactions of the so-called xanthophyll cycle (Yamamoto, 1979). The activity of the lumen-localized VDE, and hence Zx formation, is strictly regulated by the pH of the thylakoid lumen, since VDE is only activated at a luminal pH below 6.2 (Hager and Holocher, 1994; Pfundel and Dilley, 1993; Yamamoto et al., 1971). The de-epoxidation reactions are known to occur in the lipid phase of the membrane, thus the conversion of Vx to Zx requires first the release of Vx from the xanthophyll binding sites in the antenna proteins and finally the rebinding of Zx by the antenna proteins (Jahns et al., 2009). The reconversion of Zx to Vx in the dark or under low light is catalyzed by the Zx epoxidase (ZEP). The ZEP is localized in the stroma and requires O_2, FAD and NADPH as co-factors (Siefermann and Yamamoto, 1975; Takeguchi and Yamamoto, 1968). Zx formation has been shown to enhance the qE capacity in *A. thaliana* as derived from analyses of the VDE-deficient *npq1* mutant, which exhibits a reduced qE capacity compared to wild-type plants (Niyogi et al., 1998).

Conversely, the *npq2* mutant (deficient in ZEP activity), which constitutively accumulates Zx, has a faster but not higher NPQ induction compared to the wild type (Niyogi et al., 1998). The specific role of Zx in qE is still under debate. Zx can either have an indirect role as an allosteric modulator of qE, or be directly involved in the quenching process through direct energy transfer from a neighboring Chl, resulting in formation of a Zx^+/Chl^- charge transfer state (Avenson et al., 2008; Holt et al., 2005; Jahns et al., 2009). In *C. reinhardtii,* Zx formation has only a minor impact on qE (Niyogi et al., 1997), underlining again the different regulation of qE in green algae in comparison to land plants.

2. AIMS OF THE WORK

Thermal energy dissipation of excess energy (NPQ = non-photochemical quenching) is a photoprotective mechanism that is rapidly induced under high light conditions. This rapid response is known as the pH-regulated qE mechanism of NPQ. In land plants, qE is supposed to require the interaction of the PsbS protein with components of the LHCII-PSII supercomplexes in the thylakoid membrane. However, the interaction partners of PsbS in either the qE inactive (dark) or the qE active (light) state are unknown. In green algae, qE requires the light induced expression of another protein, LHCSR3. The function of PsbS, however, is completely unknown. The aim of the present work was to address two key topics:

1. Identification of the interaction partners of the PsbS protein during NPQ induction in higher plants.
2. Determination of the factors that regulate PsbS expression and identification of the role of PsbS in *Chlamydomonas reinhardtii*.

3. HYPOTHESES

1) Manuscript 1 describes a study on the reactivity of several chemical cross-linkers in active thylakoids. This work was performed in order to establish an effective assay that allows the identification of PsbS interaction partners. Based on the effects of each cross-linker to inhibit NPQ induction, specifically the PsbS-dependent qE quenching, the conditions in which chemical cross-linking can be used to sequester PsbS with its interaction partners in the dark (qE inactive) and light state (qE active) were established.
2) Manuscript 2 presents evidence for PsbS interactions with specific members of the LHCII antenna and the PSII core in *A. thaliana*. Based on localization studies, combined with chemical cross-linking and mass spectrometric quantification of specific PsbS bound proteins, a model for the PsbS function on qE activation is proposed. In the dark-adapted state (qE inactive), dimeric PsbS is located in proximity to Lhcb1 (a member of the LHCII antenna). Upon illumination, PsbS undergoes monomerization and interacts with Lhcb1 and with the PSII core via CP47 and CP43. The enhanced interaction of PsbS with LHCII trimers is accompanied by the detachment and/or aggregation of LHCII proteins, a key process required for qE activation.
3) Manuscript 3 describes the expression and potential function of PsbS in *C. reinhardtii.* The work presents evidence that PsbS is a light induced protein, whose accumulation under high light is further controlled by CO_2 availability. PsbS accumulation occurred in parallel with the induction of LHCSR3-dependent NPQ, suggesting that PsbS might be involved in the activation of the qE capacity in *C. reinhardtii.*

Based on the results presented in this work, PsbS functions as an enhancer of protein rearrangements at the PSII-LHCII supercomplexes. These rearrangements constitute the molecular switch that is required for the activation of energy quenching under excess light, which makes PsbS a regulator of qE (Fig. 7). In green algae, quenching of excess energy as heat is only triggered under specific conditions, which are rarely present in aquatic environments. However, a quenching mechanism can be activated under excess light as observed in land plants. The PsbS expression patterns determined in the present work, suggest a role of PsbS as modulator of molecular changes required for the activation of energy quenching in green algae (Fig. 7A). In terrestrial environments, qE is a constitutive, PsbS-dependent process that contributes to photoprotection in plants. The activation, dynamics, and capacity of qE are strictly regulated by the pH-regulated activity of PsbS. PsbS regulates the protein rearrangements required for the quenching via specific interactions (Fig. 7B) and its activity is crucial for qE induction.

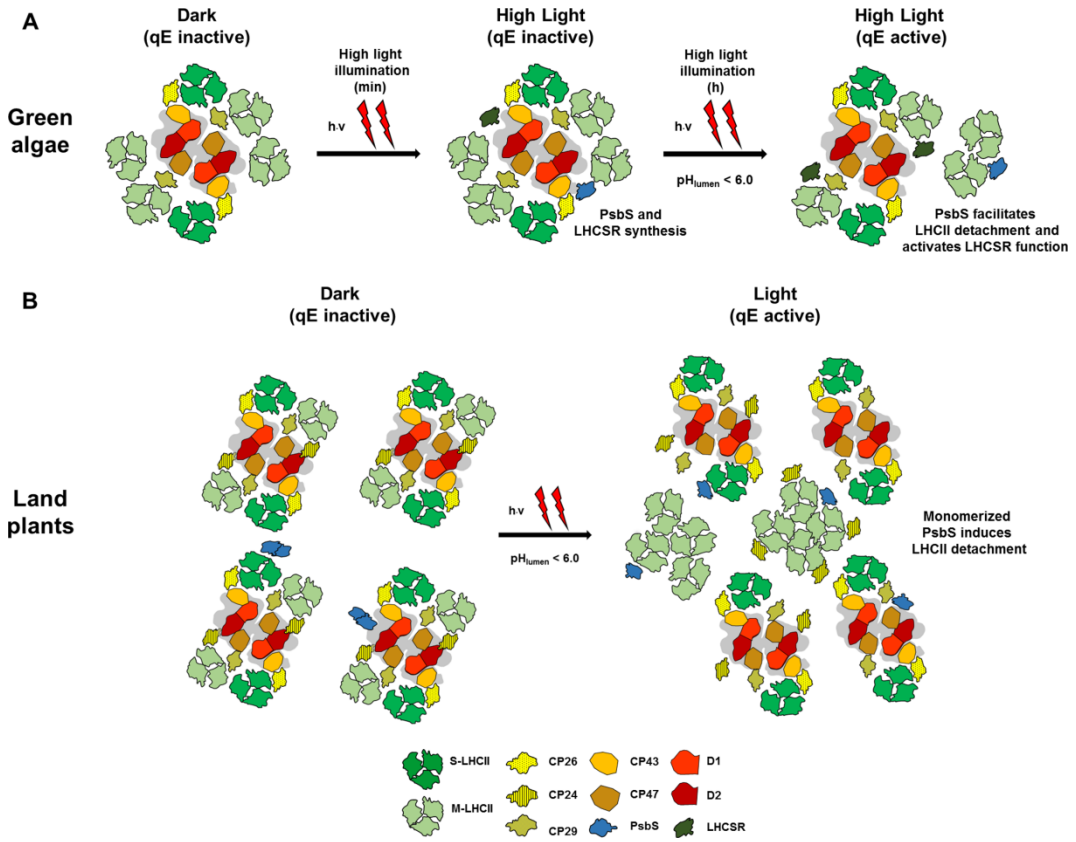

Figure 7. PsbS function on the activation of non-photochemical quenching. **(A)** Light induced expression of PsbS (blue) in *C. reinhardtii* might promote detachment and rearrangement of LHCII trimers necessary to trigger a full quenching capacity by LHCSR (dark green) and antenna proteins. **(B)** In *A. thaliana,* dimeric PsbS (blue) interacts in the dark with PSII-LHCII supercomplexes predominantly through the S-trimers of LHCII, and with the PSII core (CP47/D2/CP43). In the light, monomerized PsbS induces the detachment of trimeric LHCII from the PSII core through interaction of PsbS with LHCII M-trimers, by that activating energy quenching.

4.1 SUMMARY

Sunlight drives photosynthesis, the biological process that oxidizes water to molecular oxygen and fixes CO_2 into complex carbohydrates. Under most natural conditions, however, the absorbed light energy exceeds the capacity of light utilization in photosynthesis, giving rise to the formation of reactive oxygen species and thus photo-oxidative damage of the chloroplast. Non-photochemical quenching of excitation energy (NPQ) in the antenna of photosystem II (LHCII) allows the harmless dissipation of excess light energy as heat and thereby avoids oxidative damage to the photosynthetic apparatus. The energy dependent-quenching mechanism (qE) represents the dominating NPQ component under most conditions.

In *Arabidopsis thaliana,* NPQ is a constitutive mechanism and depends on the ΔpH-dependent activation of the PsbS protein, the rearrangement of LHCII complexes and the xanthophyll zeaxanthin (Zx). PsbS is supposed to activate NPQ through specific, light-regulated interactions with PSII antenna proteins. In this work, an effective assay using chemical cross-linking was developed to sequester PsbS with its interaction partners in dark (qE inactive) and light states (qE active). The localization and protein interactions of PsbS in thylakoid membranes were determined by mass spectrometric analyses of proteins co-purified with PsbS after chemical cross-linking. The analyses provided evidence that PsbS is localized in PSII supercomplexes and that the light activation of qE is based on the monomerization of dimeric PsbS, and an increased interaction of PsbS with Lhcb1, the major component of trimeric LHCII.

In the green algae *Chlamydomonas reinhardtii,* NPQ has to be activated upon high light acclimation and essentially requires the accumulation of the LHCSR proteins. Expression of the PsbS protein in *C. reinhardtii* has not been reported so far. In this work, it is shown that PsbS is a light induced protein that accumulates under high light and is further controlled by CO_2 availability. At high CO_2, PsbS was only transiently expressed under high light and was degraded after 1 h. PsbS accumulation correlated with an enhanced NPQ capacity in high light acclimated cells grown at low CO_2. However, PsbS could not complement the function of LHCSR in LHCSR-deficient mutants. These data suggest that PsbS might be involved in the regulation of the qE capacity in *C. reinhardtii* by promoting conformational changes required for NPQ activation in the antenna of photosystem II, similar to its counterpart in land plants.

4.2 ZUSAMMENFASSUNG

Sonnenenergie ist die Triebkraft der Photosynthese, der biologische Prozess, in dem Wasser zu molekularem Sauerstoff oxidiert und CO_2 fixiert und zu komplexen Zuckern verarbeitet wird. Unter den meisten natürlichen Bedingungen wird jedoch mehr Lichtenergie absorbiert als für Photosynthese genutzt werden kann. Die überschüssig absorbierte Energie kann zur Bildung reaktiver Sauerstoffspezies und letztendlich zur Schädigung des Chloroplasten führen. Durch die nicht-photochemische Löschung von Anregungsenergie (NPQ) in der Antenne (LHCII) von Photosystem II wird überschüssige Energie in Form von Wärme abgeführt und so der Photosyntheseapparat vor oxidativer Schädigung geschützt. Unter den meisten Bedingungen stellt der Energie-abhängige Mechanismus (qE) die dominierende Komponente des NPQ dar.

In *Arabidopsis thaliana* kann der qE Mechanismus unabhängig von den Wachstumsbedingungen jederzeit im Starklicht aktiviert werden. Die Licht-Aktivierung von qE ist von der pH-regulierten Aktivierung des PsbS Proteins, der ebenfalls pH-regulierten Synthese des Xanthophylls Zeaxanthin (Zx), sowie von Konformationsänderungen der LHCII Komplexe abhängig. Vermutlich aktivieren dabei spezifische, licht-regulierte Interaktionen des PsbS Proteins mit Antennenproteinen des PSII das NPQ. In dieser Arbeit wurde ein effektiver Ansatz, der auf der chemischen Vernetzung von Proteinen beruht, entwickelt, um Interaktionspartner des PsbS Proteins im dunkeladaptierten (qE inaktiven) und lichtadaptierten (qE aktiven) Zustand zu identifizieren. Anhand von massenspektrometrischen Analysen von Proteinen, die nach der chemischen Vernetzung zusammen mit PsbS aufgereinigt wurden, konnten sowohl die Lokalisation, als auch die Interaktionspartner von PsbS in der Thylakoidmembran bestimmt werden. Basierend auf diesen Analysen konnte PsbS am PSII Superkomplex lokalisiert werden. Die Licht-Aktivierung von qE geht mit der Monomerisierung des dimeren PsbS einher, wobei insbesondere die Interaktion von PsbS mit Lhcb1, der dominierenden Komponente der trimeren LHCII Komplexe, verstärkt wird.

In der Grünalge *Chlamydomonas reinhardtii* kann NPQ nur in Zellen aktiviert werden, die an Starklicht akklimatisiert sind. Für die Ausbildung des NPQ ist hier das LHCSR Protein essentiell. Die Expression des PsbS Proteins in *C. reinhardtii* konnte bisher nicht nachgewiesen werden. In dieser Arbeit konnte gezeigt werden, dass PsbS ein lichtinduziertes Protein ist, welches unter Starklicht Bedingungen akkumuliert und ferner von der CO_2 Verfügbarkeit kontrolliert wird. Bei hoher CO_2 Verfügbarkeit wird PsbS lediglich transient exprimiert und unter Starklicht bereits nach einer Stunde abgebaut. Bei niedriger CO_2 Verfügbarkeit korreliert eine erhöhte NPQ Kapazität mit der Akkumulation von PsbS in Starklicht-akklimatisierten Zellen. In LHCSR Mangelmutanten wurde jedoch gezeigt, dass die

Funktion des LHCSR Proteins nicht durch die des PsbS Proteins komplementiert werden kann. Auf dieser Grundlage kann vermutet werden, dass PsbS in *C. reinhardtii* an der Regulation der qE Kapazität involviert ist. Hierbei könnte PsbS Konformationsänderungen, die für die Aktivierung des NPQ in der PSII Antenne benötigt werden, unterstützen, analog zu der Funktion in höheren Pflanzen.

5. REFERENCES

Alboresi, A., Gerotto, C., Giacometti, G.M., Bassi, R., and Morosinotto, T. (2010). *Physcomitrella patens* mutants affected on heat dissipation clarify the evolution of photoprotection mechanisms upon land colonization. Proc. Natl. Acad. Sci. USA 107, 11128-11133.

Allorent, G., Tokutsu, R., Roach, T., Peers, G., Cardol, P., Girard-Bascou, J., Seigneurin-Berny, D., Petroutsos, D., Kuntz, M., Breyton, C., et al. (2013). A dual strategy to cope with high light in *Chlamydomonas reinhardtii*. Plant Cell 25, 545-557.

Anwaruzzaman, M., Chin, B., Li, X., Lohr, M., Martinez, D.A., and Niyogi, K.K. (2004). Genomic analysis of mutants affecting xanthophyll biosynthesis and regulation of photosynthetic light harvesting in *Chlamydomonas reinhardtii*. Photosynth Res 82, 265–276.

Asada, K. (2006). Production and scavenging of reactive oxygen species in chloroplasts and their functions. Plant Physiol 141, 391-396.

Avenson, T.J., Ahn, T.K., Zigmantas, D., Niyogi, K.K., Li, Z., Ballottari, M., Bassi, R., and Fleming, G.R. (2008). Zeaxanthin radical cation formation in minor light-harvesting complexes of higher plant antenna. J Biol Chem 283, 3550-3558.

Barber, J. (2012). Photosystem II: the water-splitting enzyme of photosynthesis. Cold Spring Harb Symp Quant Biol 77, 295-307.

Barera, S., Pagliano, C., Pape, T., Saracco, G., and Barber, J. (2012). Characterization of PSII-LHCII supercomplexes isolated from pea thylakoid membrane by one-step treatment with alpha- and beta-dodecyl-D-maltoside. Philos. Trans. R. Soc. Lond., B, Biol. Sci. 367, 3389-3399.

Bergner, S.V., Scholz, M., Trompelt, K., Barth, J., Gabelein, P., Steinbeck, J., Xue, H., Clowez, S., Fucile, G., Goldschmidt-Clermont, M., et al. (2015). STATE TRANSITION7-Dependent Phosphorylation Is Modulated by Changing Environmental Conditions, and Its Absence Triggers Remodeling of Photosynthetic Protein Complexes. Plant Physiol 168, 615-634.

Boekema, E.J., van Roon, H., Calkoen, F., Bassi, R., and Dekker, J.P. (1999). Multiple Types of Association of Photosystem II and Its Light-Harvesting Antenna in Partially Solubilized Photosystem II Membranes. Biochemistry 38, 2233-2239.

Bonardi, V., Pesaresi, P., Becker, T., Schleiff, E., Wagner, R., Pfannschmidt, T., Jahns, P., and Leister, D. (2005). Photosystem II core phosphorylation and photosynthetic acclimation require two different protein kinases. Nature 437, 1179-1182.

Bonente, G., Ballottari, M., Truong, T.B., Morosinotto, T., Ahn, T.K., Fleming, G.R., Niyogi, K.K., and Bassi, R. (2011). Analysis of LhcSR3, a protein essential for feedback de-excitation in the green alga *Chlamydomonas reinhardtii*. PLoS Biol 9, e1000577.

Briantais, J.M., Vernotte, C., Picaud, M., and Krause, G.H. (1979). A quantitative study of the slow decline of chlorophyll a fluorescence in isolated chloroplasts. Biochim. Biophys. Acta 548, 128-138.

Caffarri, S., Croce, R., Breton, J., and Bassi, R. (2001). The major antenna complex of photosystem II has a xanthophyll binding site not involved in light harvesting. J Biol Chem 276, 35924-35933.

Caffarri, S., Kouřil, R., Kereïche, S., Boekema, E.J., and Croce, R. (2009). Functional architecture of higher plant photosystem II supercomplexes. EMBO J 28, 3052-3063.

Cournac, L., Josse, E.M., Joet, T., Rumeau, D., Redding, K., Kuntz, M., and Peltier, G. (2000). Flexibility in photosynthetic electron transport: a newly identified chloroplast oxidase involved in chlororespiration. Philos. Trans. R. Soc. Lond., B, Biol. Sci. 355, 1447-1454.

Croce, R., Remelli, R., Varotto, C., Breton, J., and Bassi, R. (1999). The neoxanthin binding site of the major light harvesting complex (LHCII) from higher plants. FEBS Lett 456, 1-6.

Croce, R., and van Amerongen, H. (2011). Light-harvesting and structural organization of Photosystem II: from individual complexes to thylakoid membrane. J Photochem Photobiol B 104, 142-153.

Dal Corso, G., Pesaresi, P., Masiero, S., Aseeva, E., Schunemann, D., Finazzi, G., Joliot, P., Barbato, R., and Leister, D. (2008). A complex containing PGRL1 and PGR5 is involved in the switch between linear and cyclic electron flow in Arabidopsis. Cell 132, 273-285.

Dekker, J.P., and Boekema, E.J. (2005). Supramolecular organization of thylakoid membrane proteins in green plants. Biochim Biophys Acta 1706, 12-39.

Depège, N., Bellafiore, S., and Rochaix, J.-D. (2003). Role of Chloroplast Protein Kinase Stt7 in LHCII Phosphorylation and State Transition in Chlamydomonas. Science 299, 1572-1575.

Dietz, K.J. (2011). Peroxiredoxins in plants and cyanobacteria. Antioxid Redox Signal 15, 1129-1159.

Dominici, P., Caffarri, S., Armenante, F., Ceoldo, S., Crimi, M., and Bassi, R. (2002). Biochemical properties of the PsbS subunit of photosystem II either purified from chloroplast or recombinant. J Biol Chem 277, 22750-22758.

Drop, B., Webber-Birungi, M., Yadav, S.K., Filipowicz-Szymanska, A., Fusetti, F., Boekema, E.J., and Croce, R. (2014). Light-harvesting complex II (LHCII) and its supramolecular organization in *Chlamydomonas reinhardtii*. Biochim Biophys Acta 1837, 63-72.

Fan, M., Li, M., Liu, Z., Cao, P., Pan, X., Zhang, H., Zhao, X., Zhang, J., and Chang, W. (2015). Crystal structures of the PsbS protein essential for photoprotection in plants. Nat. Struct. Mol. Biol. 22, 729-735.

Ferreira, K.N., Iverson, T.M., Maghlaoui, K., Barber, J., and Iwata, S. (2004). Architecture of the Photosynthetic Oxygen-Evolving Center. Science 303, 1831-1838.

Govorunova, E.G., Jung, K.-H., Sineshchekov, O.A., and Spudich, J.L. (2004). Chlamydomonas Sensory Rhodopsins A and B: Cellular Content and Role in Photophobic Responses. Biophys J 86, 2342-2349.

Gururani, M.A., Venkatesh, J., and Tran, L.S. (2015). Regulation of Photosynthesis during Abiotic Stress-Induced Photoinhibition. Mol Plant 8, 1304-1320.

Guskov, A., Kern, J., Gabdulkhakov, A., Broser, M., Zouni, A., and Saenger, W. (2009). Cyanobacterial photosystem II at 2.9-A resolution and the role of quinones, lipids, channels and chloride. Nat. Struct. Mol. Biol. 16, 334-342.

Hager, A., and Holocher, K. (1994). Localization of the xanthophyll-cycle enzyme violaxanthin de-epoxidase within the thylakoid lumen and abolition of its mobility by a (light-dependent) pH decrease. Planta 192, 581-589.

Hervás, M., Navarro, J.A., and De la Rosa, M.A. (2003). Electron Transfer between Membrane Complexes and Soluble Proteins in Photosynthesis. Acc. Chem. Res 36, 798-805.

Hobe, S., Foerster, R., Klingler, J., and Paulsen, H. (1995). N-Proximal Sequence Motif in Light-Harvesting Chlorophyll a/b-Binding Protein Is Essential for the Trimerization of Light-Harvesting Chlorophyll a/b Complex. Biochemistry 34, 10224-10228.

Holt, N.E., Zigmantas, D., Valkunas, L., Li, X.-P., Niyogi, K.K., and Fleming, G.R. (2005). Carotenoid Cation Formation and the Regulation of Photosynthetic Light Harvesting. Science 307, 433-436.

Houille-Vernes, L., Rappaport, F., Wollman, F.-A., Alric, J., and Johnson, X. (2011). Plastid terminal oxidase 2 (PTOX2) is the major oxidase involved in chlororespiration in Chlamydomonas. Proc. Natl. Acad. Sci. USA 108, 20820-20825.

Ifuku, K., Endo, T., Shikanai, T., and Aro, E.M. (2011). Structure of the chloroplast NADH dehydrogenase-like complex: nomenclature for nuclear-encoded subunits. Plant Cell Physiol 52, 1560-1568.

Jahns, P., Latowski, D., and Strzalka, K. (2009). Mechanism and regulation of the violaxanthin cycle: the role of antenna proteins and membrane lipids. Biochim Biophys Acta 1787, 3-14.

Jans, F., Mignolet, E., Houyoux, P.A., Cardol, P., Ghysels, B., Cuine, S., Cournac, L., Peltier, G., Remacle, C., and Franck, F. (2008). A type II NAD(P)H dehydrogenase mediates light-independent plastoquinone reduction in the chloroplast of Chlamydomonas. Proc. Natl. Acad. Sci. USA 105, 20546-20551.

Jansson, S. (1994). The light harvesting chlorophylla/b binding proteins. Biochim Biophys Acta 1184, 1-19.

Jansson, S. (1999). A guide to the Lhc genes and their relatives in Arabidopsis. Trends in Plant Science 4, 1360-1385.

Kargul, J., Nield, J., and Barber, J. (2003). Three-dimensional reconstruction of a light-harvesting complex I-photosystem I (LHCI-PSI) supercomplex from the green alga *Chlamydomonas reinhardtii*. Insights into light harvesting for PSI. J Biol Chem 278, 16135-16141.

Kobayashi, N., and DellaPenna, D. (2008). Tocopherol metabolism, oxidation and recycling under high light stress in Arabidopsis. Plant J 55, 607-618.

Kouřil, R., Dekker, J.P., and Boekema, E.J. (2012). Supramolecular organization of photosystem II in green plants. Biochim Biophys Acta 1817, 2-12.

Koziol, A.G., Borza, T., Ishida, K., Keeling, P., Lee, R.W., and Durnford, D.G. (2007). Tracing the evolution of the light-harvesting antennae in chlorophyll a/b-containing organisms. Plant Physiol 143, 1802-1816.

Krause, G.H., and Jahns, P. (2004). Non-photochemical Energy Dissipation Determined by Chlorophyll Fluorescence Quenching: Characterization and Function. In Chlorophyll a Fluorescence, G. Papageorgiou, and Govindjee, eds. (Springer Netherlands), pp. 463-495.

Kulheim, C., Agren, J., and Jansson, S. (2002). Rapid regulation of light harvesting and plant fitness in the field. Science 297, 91-93.

Lee, H.-Y., Chow, W.S., and Hong, Y.-N. (1999). Photoinactivation of photosystem II in leaves of *Capsicum annuum*. Physiol Plant 105, 376-383.

Li, X., Björkman, O., Shih, C., Grossman, A.R., Rosenquist, M., Jansson, S., and Niyogi, K.K. (2000). A pigment-binding protein essential for regulation of photosynthetic light harvesting. Nature 403, 391-395.

Li, X.P., Gilmore, A.M., Caffarri, S., Bassi, R., Golan, T., Kramer, D., and Niyogi, K.K. (2004). Regulation of photosynthetic light harvesting involves intrathylakoid lumen pH sensing by the PsbS protein. J Biol Chem 279, 22866-22874.

Li, X.P., Müller-Moulé, P., Gilmore, A.M., and Niyogi, K.K. (2002). PsbS-dependent enhancement of feedback de-excitation protects photosystem II from photoinhibition. Proc. Natl. Acad. Sci. USA 99, 15222-15227.

Li, Z., Wakao, S., Fischer, B.B., and Niyogi, K.K. (2009). Sensing and responding to excess light. Annu Rev Plant Biol 60, 239-260.

Liguori, N., Roy, L.M., Opacic, M., Durand, G., and Croce, R. (2013). Regulation of light harvesting in the green alga *Chlamydomonas reinhardtii*: the C-terminus of LHCSR is the knob of a dimmer switch. J Am Chem Soc 135, 18339-18342.

Liu, Z., Yan, H., Wang, K., Kuang, T., Zhang, J., Gui, L., An, X., and Chang, W. (2004). Crystal structure of spinach major light-harvesting complex at 2.72 A resolution. Nature 428, 287-292.

Mazor, Y., Borovikova, A., and Nelson, N. (2015). The structure of plant photosystem I super-complex at 2.8 A resolution. elife 4, e07433.

Mettler, T., Muhlhaus, T., Hemme, D., Schottler, M.A., Rupprecht, J., Idoine, A., Veyel, D., Pal, S.K., Yaneva-Roder, L., Winck, F.V., et al. (2014). Systems Analysis of the Response of Photosynthesis, Metabolism, and Growth to an Increase in Irradiance in the Photosynthetic Model Organism *Chlamydomonas reinhardtii*. Plant Cell. 26, 2310-2350.

Miller, R., Wu, G., Deshpande, R.R., Vieler, A., Gartner, K., Li, X., Moellering, E.R., Zauner, S., Cornish, A.J., Liu, B., et al. (2010). Changes in transcript abundance in *Chlamydomonas reinhardtii* following nitrogen deprivation predict diversion of metabolism. Plant Physiol 154, 1737-1752.

Minagawa, J., and Takahashi, Y. (2004). Structure, function and assembly of Photosystem II and its light-harvesting proteins. Photosynth Res 82, 241-263.

Minagawa, J., and Tokutsu, R. (2015). Dynamic regulation of photosynthesis in *Chlamydomonas reinhardtii*. Plant J 82, 413-428.

Müller, P., Li, X.-P., and Niyogi, K.K. (2001). Non-Photochemical Quenching. A Response to Excess Light Energy. Plant Physiol 125, 1558-1566.

Munekage, Y., Hashimoto, M., Miyake, C., Tomizawa, K.-I., Endo, T., Tasaka, M., and Shikanai, T. (2004). Cyclic electron flow around photosystem I is essential for photosynthesis. Nature 429, 579-582.

Nelson, N., and Junge, W. (2015). Structure and energy transfer in photosystems of oxygenic photosynthesis. Annu Rev Biochem 84, 659-683.

Nelson, N., and Yocum, C.F. (2006). Structure and function of photosystems I and II. Annu Rev Plant Biol 57, 521-565.

Nilkens, M., Kress, E., Lambrev, P., Miloslavina, Y., Müller, M., Holzwarth, A.R., and Jahns, P. (2010). Identification of a slowly inducible zeaxanthin-dependent component of non-photochemical quenching of chlorophyll fluorescence generated under steady-state conditions in Arabidopsis. Biochim Biophys Acta 1797, 466-475.

Niyogi, K.K., Björkman, O., and Grossman, A.R. (1997). Chlamydomonas Xanthophyll Cycle Mutants Identified by Video Imaging of Chlorophyll Fluorescence Quenching. Plant Cell 9, 1369-1380.

Niyogi, K.K., Grossman, A.R., and Björkman, O. (1998). Arabidopsis Mutants Define a Central Role for the Xanthophyll Cycle in the Regulation of Photosynthetic Energy Conversion. Plant Cell 10, 1121-1134.

Niyogi, K.K., Li, X.P., Rosenberg, V., and Jung, H.S. (2005). Is PsbS the site of non-photochemical quenching in photosynthesis? J Exp Bot 56, 375-382.

Pagliano, C., Nield, J., Marsano, F., Pape, T., Barera, S., Saracco, G., and Barber, J. (2014). Proteomic characterization and three-dimensional electron microscopy study

of PSII-LHCII supercomplexes from higher plants. Biochim Biophys Acta 1837, 1454-1462.

Pan, X., Li, M., Wan, T., Wang, L., Jia, C., Hou, Z., Zhao, X., Zhang, J., and Chang, W. (2011). Structural insights into energy regulation of light-harvesting complex CP29 from spinach. Nat. Struct. Mol. Biol. 18, 309-315.

Pan, X., Liu, Z., Li, M., and Chang, W. (2013). Architecture and function of plant light-harvesting complexes II. Curr Opin Struct Biol 23, 515-525.

Peers, G., Truong, T.B., Ostendorf, E., Busch, A., Elrad, D., Grossman, A.R., Hippler, M., and Niyogi, K.K. (2009). An ancient light-harvesting protein is critical for the regulation of algal photosynthesis. Nature 462, 518-521.

Pfundel, E.E., and Dilley, R.A. (1993). The pH Dependence of Violaxanthin Deepoxidation in Isolated Pea Chloroplasts. Plant Physiol 101, 65-71.

Rochaix, J.D. (2014). Regulation and dynamics of the light-harvesting system. Annu Rev Plant Biol 65, 287-309.

Rumeau, D., Peltier, G., and Cournac, L. (2007). Chlororespiration and cyclic electron flow around PSI during photosynthesis and plant stress response. Plant Cell Environ. 30, 1041-1051.

Rutschow, H., Ytterberg, A.J., Friso, G., Nilsson, R., and van Wijk, K.J. (2008). Quantitative proteomics of a chloroplast SRP54 sorting mutant and its genetic interactions with CLPC1 in Arabidopsis. Plant Physiol 148, 156-175.

Siefermann, D., and Yamamoto, H.Y. (1975). NADPH and oxygen-dependent epoxidation of zeaxanthin in isolated chloroplasts. Biochem Biophys Res Commun 62, 456-461.

Standfuss, J., Terwisscha van Scheltinga, A.C., Lamborghini, M., and Kühlbrandt, W. (2005). Mechanisms of photoprotection and nonphotochemical quenching in pea light-harvesting complex at 2.5 Å resolution. EMBO J 24, 919-928.

Suetsugu, N., Mittmann, F., Wagner, G., Hughes, J., and Wada, M. (2005). A chimeric photoreceptor gene, NEOCHROME, has arisen twice during plant evolution. Proc. Natl. Acad. Sci. USA 102, 13705-13709.

Suga, M., Akita, F., Hirata, K., Ueno, G., Murakami, H., Nakajima, Y., Shimizu, T., Yamashita, K., Yamamoto, M., Ago, H., et al. (2015). Native structure of photosystem II at 1.95 A resolution viewed by femtosecond X-ray pulses. Nature 517, 99-103.

Taiz, L.,and Zeiger, E. (2002) Chapter 7. Photosynthesis: The Light Reactions. In Taiz, L.,Zeiger, E. (eds.): Plant Physiology, Third Edition. Sinauer Associates, Sunderland, MA,USA.

Takeguchi, C.A., and Yamamoto, H.Y. (1968). Light-induced 18O2 uptake by epoxy xanthophylls in New Zealand spinach leaves (*Tetragonia expansa*). Biochim. Biophys. Acta 153, 459-465.

Teramoto, H., Nakamori, A., Minagawa, J., and Ono, T.A. (2002). Light-intensity-dependent expression of Lhc gene family encoding light-harvesting chlorophyll-a/b proteins of photosystem II in *Chlamydomonas reinhardtii*. Plant Physiol 130, 325-333.

Tikkanen, M., Piippo, M., Suorsa, M., Sirpio, S., Mulo, P., Vainonen, J., Vener, A.V., Allahverdiyeva, Y., and Aro, E.M. (2006). State transitions revisited-a buffering system for dynamic low light acclimation of Arabidopsis. Plant Mol Bio 62, 779-793.

Tokutsu, R., and Minagawa, J. (2013). Energy-dissipative supercomplex of photosystem II associated with LHCSR3 in *Chlamydomonas reinhardtii*. Proc. Natl. Acad. Sci. USA 110, 10016–10021.

Umena, Y., Kawakami, K., Shen, J.R., and Kamiya, N. (2011). Crystal structure of oxygen-evolving photosystem II at a resolution of 1.9 A. Nature 473, 55-60.

Wada, M., Kagawa, T., and Sato, Y. (2003). Chloroplast movement. Annu Rev Plant Biol 54, 455-468.

Xue, H., Tokutsu, R., Bergner, S.V., Scholz, M., Minagawa, J., and Hippler, M. (2015). PSBR is required for efficient binding of LHCSR3 to photosystem II - light-harvesting supercomplexes in *Chlamydomonas reinhardtii*. Plant Physiol. 167, 1566-1578.

Yamamoto, H.Y. (1979). Biochemistry of the violaxanthin cycle in higher plants. In: Goodwin TW (ed) Carotenoids°C5. Pergamon, pp 639-648.

Yamamoto, H.Y., Wang, Y., and Kamite, L. (1971). A chloroplast absorbance change from violaxanthin de-epoxidation. A possible component of 515 nm changes. Biochem Biophys Res Commun 42, 37-42.

Zouni, A., Witt, H.-T., Kern, J., Fromme, P., Krauss, N., Saenger, W., and Orth, P. (2001). Crystal structure of photosystem II from *Synechococcus elongatus* at 3.8 Å resolution. Nature 409, 739-743.

6. MANUSCRIPTS

The Impact of Chemical Cross-linking on the Induction of Energy Dissipation: A Functional Study Towards the Linking of qE-related Proteins in Active Thylakoids

Viviana Correa Galvis and Peter Jahns

PsbS Interaction Partners Involved in the Activation of Energy Dissipation in *Arabidopsis thaliana*

Viviana Correa Galvis, Gereon Poschmann, Michael Melzer, Kai Stühler, and Peter Jahns

Expression of the PsbS Protein upon High Light Acclimation in *Chlamydomonas reinhardtii*

Viviana Correa Galvis, Petra Redekop, Annika Grieß, Viktor Koch, Ben Lucker, David Kramer, Krishna K. Niyogi, and Peter Jahns

The Impact of Chemical Cross-linking on the Induction of Energy Dissipation: A Functional Study Towards the Linking of qE-related Proteins in Active Thylakoids

Viviana Correa Galvis and Peter Jahns[1]

[1]Plant Biochemistry, Heinrich-Heine-University Düsseldorf, 40225 Düsseldorf, Germany

[1]Address correspondence to pjahns@hhu.de

ABSTRACT

Thermal dissipation of excess energy (= non-photochemical quenching, NPQ) is a photoprotective process that takes place in the antenna complexes of photosystem II (LHCII). The energy dependent-quenching mechanism (qE) represents the dominating NPQ component under most conditions. The protein interactions required for its activation are still unknown. However, it involves the delta pH-dependent activation of the PsbS protein, the xanthophyll zeaxanthin (Zx), and the rearrangement of LHCII complexes. In order to identify transient protein interactions involved in qE activation, the effect of chemical cross-linking on qE induction was analyzed. From a wide range of cross-linkers, only DTSSP [3,3-Dithio-bis-(sulfosuccinimidyl)propionate] had an effect on qE induction without inhibiting Zx conversion. This makes it the most suitable candidate for protein interaction studies that occur during qE induction in active thylakoids.

INTRODUCTION

Protein complexes are the functional units in biological processes. In order to understand their function and regulation, identification of their structural organization and the protein interactions that take place in an active state have become a major area of interest for biologists. The conventional approaches for studying protein-protein interactions in large protein complexes include the use of binary binding assays with pairs of protein subunits from the complex. However, this technique is unable to detect interactions that are rapidly activated and deactivated *in vivo*, or that include the cooperative work of several proteins.

Chemical cross-linking agents have been used to stabilize *in vivo* protein interactions since the 1960s (Spirin et al., 1965). However, studies of protein complexes in the thylakoid membrane using a cross-linking approach have been limited to enriched or solubilized complexes, as exemplified in several recent studies of photosystem II (PSII) core proteins (Liu et al., 2014; Mummadisetti et al., 2014). Such an approach is promising in systems where protein interactions are stable through the extraction and purification procedures and can provide valuable information in structural studies (Collins et al., 1996; Jansson et al., 1996; Rappsilber, 2011). To date, however, no studies have been reported that use chemical cross-linking *in vivo* to identify fast, transient protein-protein interactions in the chloroplast. In the thylakoid membrane, several light driven processes are related to the capture (light harvesting and energy transfer among the antennae) and use of energy (electron and proton transfer, ATP synthesis, carbon fixation), which require fast interactions between proteins (Nelson and Junge, 2015). Among those processes, the non-photochemical quenching of excess energy (NPQ) is a mechanism by which excess excitation energy, which cannot be used for photosynthesis, is dissipated as heat at the level of the PSII antennae (Horton, 2012). In vascular plants, NPQ consists of different components (namely qE, qZ and qI), whose time-dependent activation occurs on a scale of seconds to a few minutes (Nilkens et al., 2010). The qE mechanism represents the predominant NPQ component under moderate light stress conditions (Jahns and Holzwarth, 2012). qE is strictly regulated by the thylakoid lumen pH (Briantais et al., 1979), which facilitates its rapid (within seconds) activation/deactivation. This allows organisms to cope with sudden fluctuations in light intensity that frequently occur in natural environments. Aside from a low pH, the maximum qE capacity requires the presence of the xanthophyll zeaxanthin (Zx), which is formed via the - likewise pH-regulated - deepoxidation reactions of the xanthophyll cycle (Jahns et al., 2009). Activation of qE essentially depends on the PsbS protein (Li et al., 2000), which acts as a sensor of the thylakoid lumen pH via two protonable glutamate residues located on the luminal side of the protein (Li et al., 2004). Protonation of these two residues activates qE through PsbS-controlled conformational changes in the PSII antennae. The exact mechanism of qE and the interaction partners of PsbS are still a matter of debate, although it

is known that a protein rearrangement at the level of the PSII antennae is required for its execution (Johnson et al., 2011). Consequently, elucidating individual protein associations and/or interactions among the PSII-LHCII complex components (including PsbS) is an essential step towards better understanding energy dissipation processes. In this work, the effect of several chemical cross-linkers added to active thylakoids prior to NPQ induction was analyzed as a first step towards an assay that allows for identification of transient protein interactions during the light activation of NPQ.

RESULTS

Impact of chemical cross-linking on qE induction and Zx conversion

A series of chemical cross-linkers were selected based on a revision of previous studies that have successfully used them to link thylakoid membrane proteins (Table 1). In order to identify a chemical cross-linker that could rapidly bind to thylakoid membrane proteins, specifically those related to qE, we evaluated the impact of each cross-linker at selected concentrations on qE induction. At least eight different concentrations were selected based on the studies listed in Table 1. To do so, each cross-linker was shortly incubated (5-10 s) with isolated thylakoids in the dark, and its impact on qE was monitored by following the changes in Chl fluorescence (Krause and Jahns, 2004). In this way, we selected the concentration at which chemical cross-linking strongly reduces qE induction when compared to non-treated thylakoids (Fig. 1A) without pronounced side-effects. In general, qE impairment could be achieved by adding the cross-linker at very high high concentrations, but this could lead to strong aggregation of proteins or full inhibition of electron and proton transport. Therefore, the selected concentration was defined as the concentration at which a pronounced impact on qE was observable without the occurrence of any protein aggregation.

Table 1. **Properties of used cross-linkers.** All cross-linkers were selected according to previous protein interaction studies[a] via chemical cross-linking of thylakoid membrane proteins. Additional references[b] provide information on specific cross-linker properties.

Cross-linker	Spacer arm (Å)	Cleavage	Target groups	Solubility	References
Glutaraldehyde	5	Uncleavable	Amino Thiol Phenol Imidazole	Water soluble	(Armbrust et al., 1996)[a] (Habeeb and Hiramoto, 1968)[b]
Formaldehyde	2.3-2.7	Cleavable	Amino	Water soluble Membrane permeable	(Ytterberg et al., 2006)[a] (Sutherland et al., 2008)[b]
EDC [1-ethyl-l-3-[3-(dimethylamino)propyl] carbodiimide]	0	Uncleavable	Carboxy	Water insoluble	(Armbrust et al., 1996)[a] (Liu et al., 2014)[a] (Collins et al., 1996)[a] (Seidler, 1996)[a]
EGS [ethylene glycol bis(succinimidyl succinate)]	16.1	Cleavable	Amino	Water soluble	(Oh-oka et al., 1989)[a]
S-MBS (m-maleimidobenzoyl-N-hydroxysulfo-succinimide ester)	7.3	Uncleavable	Amino Thiol	Water soluble	(Nilsson et al., 1999)[a]
DTSSP [3,3-Dithio-bis-(sulfosuccinimidyl)pro-pionate]	12	Cleavable	Amino	Water soluble	(Liu et al. 2011)[a] (Liu et al. 2014)[a] (Jansson et al., 1996)[a] (Bergantino et al., 2003)[a]

The concentrations at which qE is impaired or reduced varies among the different cross-linkers, depending on their specific properties. However, all selected cross-linkers significantly affected qE induction when applied at higher concentrations. Glutaraldehyde, EDC and DTSSP showed a substantial impact on NPQ induction at reasonable concentrations, with DTSSP-treated samples showing the lowest qE after 10 min of illumination compared to other cross-linkers (Fig. 1A).

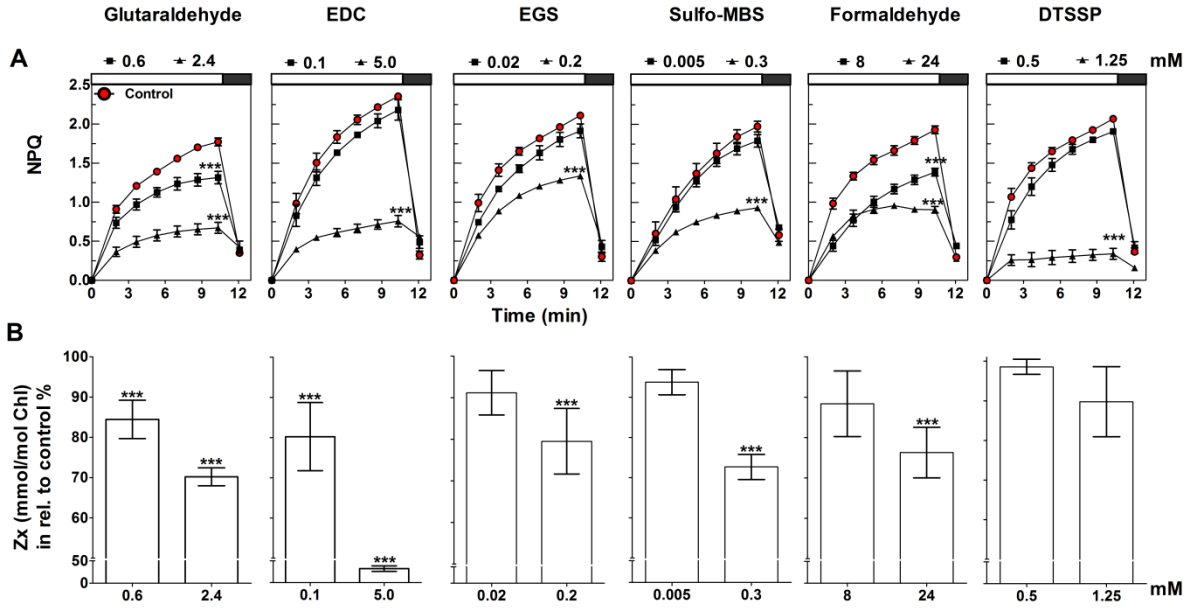

Figure 1. Impact of chemical cross-linking on NPQ and zeaxanthin conversion in *Spinacea oleracea*. (A) NPQ induction; **(B)** Zeaxanthin conversion (Zx). Isolated thylakoids (60 µg Chl) were incubated for 5-10 s with six different cross-linkers in the dark and the Chl fluorescence was measured upon illumination (825 µmol photons m^{-2} s^{-1} red light) for 10 min, followed by 2 min of relaxation in the dark. The pigment content was measured after 10 min of illumination. Data represent means ± SD (n = 3). *** Significant differences in qE values and the Zx content (Zx mmol/ml Chl) between each cross-linker treatment and the control (Student *t-test*).

The inhibition of NPQ induction indicates that the cross-linker affects directly (by linking proteins together, thereby restricting their mobility) and/or indirectly (inhibition of electron transport or ΔpH formation) the conformational changes required for quenching. A direct effect on NPQ by chemical cross-linking is a useful tool to sequester protein interactions directly related to qE. To test which of the cross-linkers had a specific direct effect on NPQ, Zx synthesis during illumination was analyzed. Zx synthesis is catalyzed by the violaxanthin de-epoxidase (VDE), which converts violaxanthin (Vx) to Zx via the intermediate antheraxanthin (Yamamoto, 1979). VDE activity, and hence Zx formation, is strictly regulated by the pH of the thylakoid lumen and is activated at a luminal pH below 6.2 (Hager and Holocher, 1994; Pfundel and Dilley, 1993; Yamamoto et al., 1971). Consequently, those cross-linkers that directly affect the quenching induction but not the Zx conversion are likely

to have little to no effect on electron and proton transport. Among all cross-linkers tested, formaldehyde and DTSSP had the lowest effect on Zx conversion when added at concentrations that strongly inhibit the qE induction (below 30 % of control values, Fig. 1B). Although EDC and Glutaraldehyde had a more pronounced effect on NPQ than formaldehyde (Fig. 1A), both strongly affected the Zx conversion (below 30 % of control values, Fig. 1B). Consequently, DTSSP and formaldehyde are the most promising cross-linkers for studying qE-specific protein interactions without affecting electron and proton transport and were therefore selected for further characterization.

Chemical cross-linking in relation to the PsbS protein: Impact on qE in active thylakoids of wild type and *npq4 Arabidopsis thaliana* plants

In addition to a low pH and the presence of Zx, activation of qE depends on the PsbS protein (Li et al., 2000). If one of the two cross-linkers is capable of inhibiting specifically the function of PsbS during dark incubation, the NPQ induction curve in the presence of the cross-linker should (i) resemble the PsbS-lacking phenotype and (ii) have no additional impact on NPQ induction in PsbS-lacking thylakoid membranes. Analysis of NPQ induction in thylakoids isolated from WT and *npq4* (PsbS knockout mutant) *Arabidopsis thaliana* plants revealed that incubation with DTSSP in the dark indeed led to a *npq4*-like phenotype and did not affect NPQ induction in PsbS-deficient *npq4* thylakoids. In contrast, formaldehyde induced a slow increase in Chl fluorescence in the absence of PsbS (Fig. 2). The latter indicates a PsbS-independent action of formaldehyde in *A. thaliana*. Furthermore, DTSSP had no significant effect on Zx conversion and thus on the de-epoxidation state (DEPS) (Fig. 3). Conversely, incubation with formaldehyde significantly affected both the DEPS and the total Zx conversion (Fig. 3). Thus, only cross-linking with DTSSP showed a qE-specific effect in *A. thaliana* thylakoids.

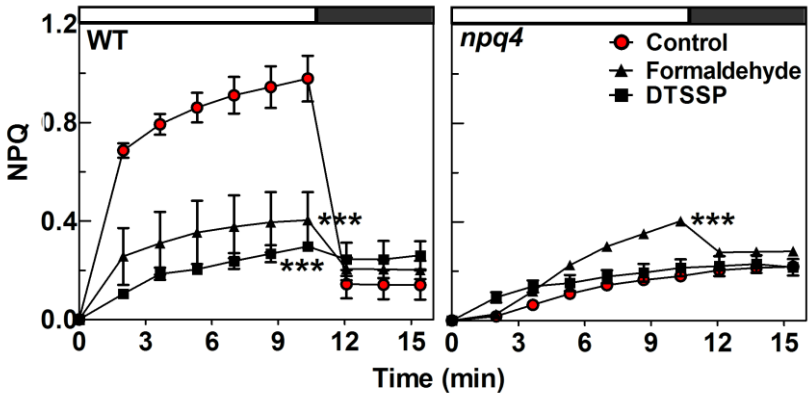

Figure 2. Impact of chemical cross-linking on NPQ induction in *A. thaliana*. Isolated thylakoids (equivalent to 60 µg Chl) from wild type (WT) and PsbS-deficient mutant (*npq4)* plants were incubated for 5-10 s with formaldehyde (24 mM) or DTSSP (1.25 mM) in the dark prior to Chl fluorescence measurements. Data represent means ± SD (n = 3). *** Significant differences in qE values between each cross-linker treatment and the control (Student *t-test*).

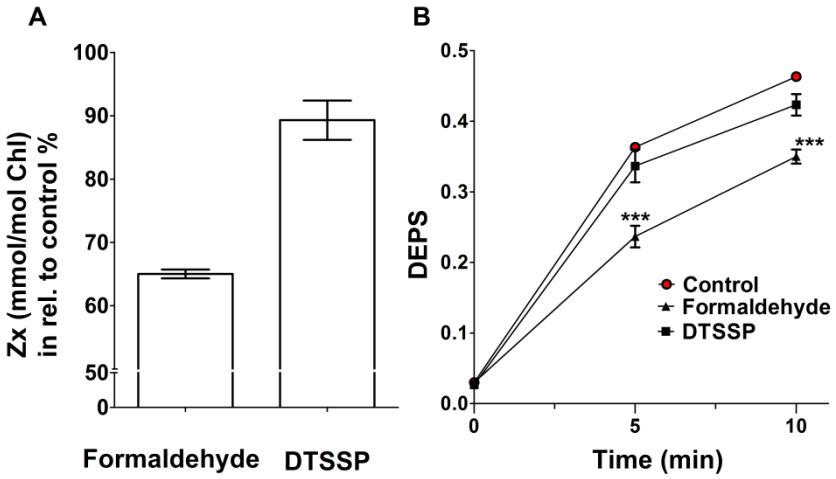

Figure 3. Impact of chemical cross-linking on Zx synthesis. Isolated thylakoids (60 µg Chl) isolated from WT *A. thaliana* plants were incubated for 5-10 s with each cross-linker in the dark followed by illumination at 825 µmol photons m^{-2} s^{-1} red light. Conversion of Vx to Zx was analyzed by comparing the pigment content before (0 min), during (5 min), and after (10 min) the illumination period. **(A)** Zx content after 10 min; **(B)** De-epoxidation state (DEPS): (Zx+1/2Ax)/(Zx+Ax+Vx). Data represent means ± SD (n = 3). *** Significant differences between DEPS values at 5 and 11 min of each cross-linker treatment and the control (Student *t-test*).

Impact of DTSSP on proton transport

The nearly unchanged light-induced Zx conversion in the presence of DTSSP (Figs. 1 and 3) indicates that lumen acidification and hence electron and proton transport was not affected by this cross-linker. We further studied the impact of DTSSP on the formation of the ΔpH across the membrane by measuring the effect of DTSSP on 9-aminoacridine (9-AA) fluorescence quenching, which is commonly use as an indicator of the transthylakoid ΔpH (Schuldiner et al., 1972). Cross-linking with DTSSP reduced 9-AA quenching to approximately 40 % of the level of untreated thylakoids (Fig. 4A, Table 2).

Table 2. Impact of DTSSP on the light induced ΔpH. DTSSP was added in the dark, 5-10 s before illumination at two different red light intensities, 70 and 825 µmol photons m^{-2} s^{-1}. The ΔpH across the thylakoid membrane was estimated from the light-induced quenching of 9-AA fluorescence according to Schuldiner et al. (1972). 9-AA quenching is given in % of controls illuminated at 825 µmol photons m^{-2} s^{-1}. Data represent mean values ± SD of three independent experiments.

Parameter	Sample treatment			
	825 µE		70 µE	
	control	+ DTSSP	control	+ DTSSP
9-AA quenching (in %)	100	40.1 ± 2.0	96.5 ± 0.6	3.5 ± 0.6
Estimated ΔpH	3.6 ± 0.1	2.9 ± 0.1	3.3 ± 0.1	2.0 ± 0.3

This reduction corresponded to a decrease in the ΔpH by 0.7 pH units from 3.6 in controls to 2.9 in DTSSP-treated samples (Table 2), which might explain the slightly reduced synthesis of Zx (Fig. 4C). To test this hypothesis, we reduced the actinic light intensity to 70 µmol photons m^{-2} s^{-1}. In control thylakoids, this led to only marginally reduced 9-AA fluorescence quenching (Fig. 4B, Table 2), while Zx synthesis was reduced to similar values as in DTSSP-treated thylakoids (Fig. 4D). This implies that the observed reduction in Zx synthesis In DTSSP-treated samples is likely due only to a slight reduction in the ΔpH. Strikingly, however, 9-AA fluorescence quenching was completely abolished when DTSSP-treated thylakoids were illuminated at this low light intensity of 70 µmol photons m^{-2} s^{-1} (Fig. 4B, Table 2). Zx synthesis remained unchanged in comparison with the higher actinic light intensity (Fig. 4D). Clearly, 9-AA fluorescence cannot be used as a reliable indicator of the ΔpH in DTSSP-treated thylakoids, possibly related to the interference of DTSSP with 9-AA.

Changes on proton gradient	**Dark**			**Light**
	825 µE	**70 µE**	**13 µE**	**825 µE**
Decrease in 9-AA Fluorescence (% relat. to control)	59,9 ± 2	96,5 ±0,6	81,5 ± 16,4	87,8 ± 3,5
Reduction in Δ pH units	0,7 ± 0,1	1,3 ± 0,3	0,8 ±0,5	1,0 ±0,3
Reduction in Δ pH units (% relat. to control)	23,1 ± 3,4	40,2 ± 7,6	30,3 ± 0,2	33,7 ± 6,7

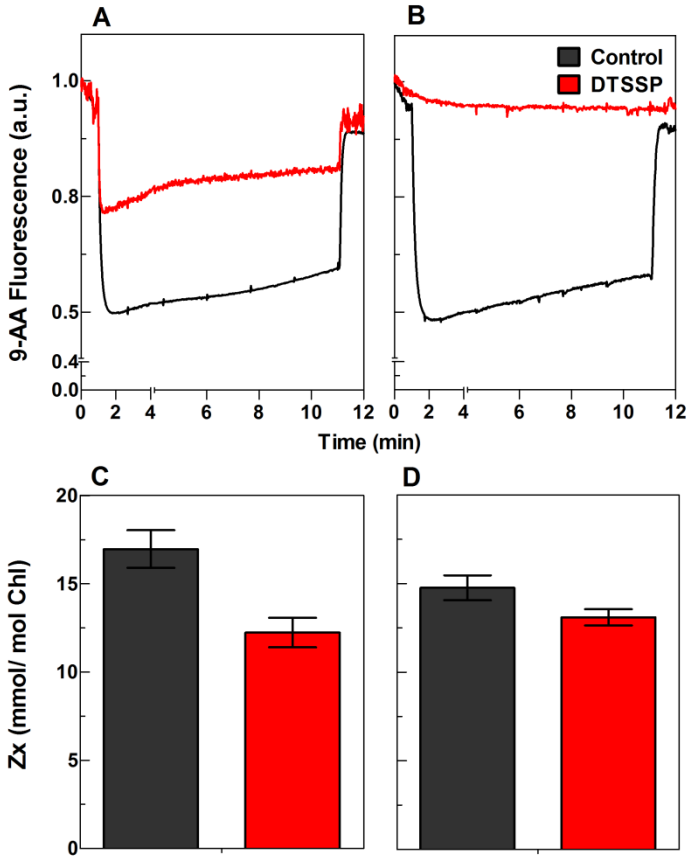

Figure 4. Impact of chemical cross-linking with DTSSP on proton transport. (A, B) Impact of DTSSP on 9-AA fluorescence quenching upon illumination of thylakoids at an intensity of **(A)** 825 µmol photons m^{-2} s^{-1} or (B) 70 µmol photons m^{-2} s^{-1}. Representative single curves are shown. **(C, D)** Impact of DTSSP on Zx synthesis. Light-induced formation of Zx was derived from the pigment content after **(C)** 10 min illumination at an intensity of 825 µmol photons m^{-2} s^{-1} or **(D)** 70 µmol photons m^{-2} s^{-1}. Data represent means ± SD (n =3). No significant differences in Zx conversion were found between the two light intensities or the cross-linker/control treatments (one way ANOVA, p value >0.05).

DISCUSSION

All chemical cross-linkers evaluated in this work had an effect on qE induction upon illumination following dark acclimation (qE inactive) of samples. This indicates that chemical cross-linking of isolated thylakoids can generally be used as a tool to affect the reactions required for qE induction, either at the level of electron transport or at the level of qE-specific protein interactions.

qE is activated upon acidification of the lumen and requires protonation of the PsbS protein (Li et al., 2004), which likely interacts with LHCII proteins upon activation of energy quenching (Kereïche et al., 2010). In this sense, an effect of chemical cross-linking on qE induction might be due to a direct modification of the PsbS protein. EDC has been used to stabilize PsbS dimers in readily-formed crystals in acidic solution (pH 3.0-5.0) as well as solubilized, high light-treated thylakoids (Fan et al., 2015). In our assays, however, EDC strongly inhibited Zx conversion upon illumination (Fig. 1B), which means that EDC either generally inhibits electron transport or interacts also specifically with other pH-regulated proteins, such as the VDE. The latter action would be in agreement with the notion that EDC has its optimal efficiency at low pH (between pH 4 and pH 6, according to the manufacturer's instructions). On the other hand, it is plausible that EDC generally inhibits electron transport reactions required for the buildup of a trans-thylakoid ΔpH, as earlier reported in enriched PSII fractions at different EDC concentrations (Collins et al., 1996). EDC has been shown to be an optimal cross-linker for structural studies (Cashman et al., 2014; Liu et al., 2014), and likely to generate inter-thylakoid cross-linking (Collins et al., 1996). These features make it very feasible to identify qE-specific interactions, so that several control parameters other than Chl fluorescence and Zx conversion must be additionally investigated to exclude qE-unspecific protein linking.

Only formaldehyde and DTSSP likely preferentially link proteins directly involved in qE activation, as determined by their low effect on Zx conversion (Fig. 1B). Formaldehyde is an inexpensive and commonly used protein cross-linker reported in protein interactions studies *in vivo* (Pertl-Obermeyer et al., 2014). However, it slightly increased the fluorescence quenching in thylakoids deficient in PsbS (*npq4* mutant, Fig. 2B) and did not impair qE induction as drastically as DTSSP (Figs. 1A and 2A). Thus, it is plausible that protein linking with formaldehyde is not optimal to characterize linking of qE-related and PsbS-dependent protein interactions that can be monitored by Chl fluorescence. Nevertheless, it will be of interest to determine if incubation of PsbS-depleted thylakoids with higher or identical concentrations as reported here, but with longer illumination periods, lead to full NPQ inhibition without inhibiting electron and proton transport. If so, this type of linking could serve as an indirect tool to detect protein interactions involved in a PsbS-independent quenching mechanism.

Previous studies applying chemical cross-linking of PsbS with DTSSP and with its uncleavable equivalent DSS demonstrated the stability of a PsbS dimer in a dark-adapted state under denaturizing conditions (Bergantino et al., 2003; Gerotto et al., 2015). These reports showed that DTSSP is a good candidate for PsbS linking, likely to be used for intermolecular cross-linking with other PSII-LHCII. In the present study, DTSSP had the strongest impact on qE induction and the lowest on Zx conversion when added in the dark (Figs. 1, 2 and 3), resembling the *npq4* qE phenotype. The fast reactivity of DTSSP makes it a good candidate for protein linking since qE activation/deactivation occurs in a very short time frame (ms to s). DTSSP is a water soluble cross-linker feasible for cross-linking membrane proteins on the surface of the lipid bilayer without interfering with processes that occur inside the membrane (i.e. electron transport) or on the luminal side (i.e. Zx conversion). This is particularly useful for linking membrane proteins that are in close proximity and require activation by electron and proton transport, such as PsbS and its interaction partners. Although it is plausible that some interactions occur inside the membrane among the transmembrane helices of PsbS and other LHC proteins, it was not possible to efficiently use the membrane permeable version of DTSSP, DSP [Dithiobis(succinimidyl propionate)]. DSP precipitated in solution, which impaired the analysis of its effects on NPQ induction in active thylakoids illuminated in a reaction medium (data not shown). Nevertheless, if the proteins were in direct contact through the membrane helices, their proximity should be reflected on the membrane surface side as well, so that they can also be linked with DTSSP.

DTSSP did not affect Zx synthesis, which indicates that proton and thus also electron transport was not impaired. To obtain further insight into the effect of cross-linking with DTSSP on proton transport, analysis of ΔpH formation was performed. Strikingly, DTSSP strongly reduced the 9-AA fluorescence without affecting Zx conversion (Fig. 4), indicating that 9-AA fluorescence cannot be used as an indicator of the ΔpH in the presence of DTSSP. Estimations of the ΔpH using 9-AA fluorescence depend on the ability of 9-AA to cross the membrane and to accumulate in the lumen in its protonated form upon increasing proton accumulation in the lumen in the light-adapted state. This leads to 9-AA fluorescence quenching, which is used to calculate the ΔpH across the thylakoid membrane (Schuldiner et al., 1972). 9-AA contains an amino group in its central aromatic ring. Since DTSSP binds amino groups, it is thus likely that DTSSP also reacts with the amino group of 9-AA, thereby decreasing the ability of 9-AA to cross the membrane upon illumination even though DTSSP linking was quenched prior 9-AA addition (see Materials and Methods). This interference can explain the lack of 9-AA fluorescence in DTSSP-treated samples (Fig. 4A, B; Table 2). Consequently, by analyzing 9-AA fluorescence quenching, it was not possible to determine whether DTSSP affects the build-up of the transmembrane ΔpH. However, since Zx

formation and qE-induction are known to have similar pH responses under *in vivo* conditions (Takizawa et al., 2007), only marginally impaired Zx formation in the presence of DTSSP excludes a pronounced effect of DTSSP on ΔpH formation. This makes DTSSP a very promising candidate for chemical cross-linking of proteins involved in qE activation.

Protein-protein interactions required for qE induction may thus be identified through chemical cross-linking with DTSSP, as described in this work. This assay can be performed in non-solubilized, fully active thylakoids, which provide more accurate insights into the interactions between PsbS and other PSII-LHCII proteins upon qE activation in the dark and also those occurring in the qE-active state (see manuscript 2).

MATERIALS AND METHODS

Plant material

Spinacea oleracea and *Arabidopsis thaliana* wild type (Col-0) and *npq4* mutant (Graßes et al., 2002) plants were grown under short-day conditions (8 h light / 16 h dark) on soil at 20 °C and a light intensity of 180-200 µmol photons m^{-2} s^{-1}. All experiments were performed with 5-6-week old plants.

Thylakoid membrane preparations

Detached leaves of dark-adapted plants were homogenized with extraction media (see manuscript 2). All steps were performed in the dark at 4 °C. To determine Chl content, 5 µl of isolated thylakoids were dissolved in 995 µl of 80 % aqueous acetone and centrifuged for 2 min at 10,000 x *g*. The Chl concentration was calculated according to Arnon (1949) using the extinction coefficients of Chl a and b at 645 and 663 nm.

Chlorophyll fluorescence measurements

All measurements were performed with dark adapted, freshly isolated thylakoids. Chl fluorescence was measured using a Dual-PAM-100 system (Walz, Germany). Thylakoids (60 µg Chl) in 2 ml reaction media (40 mM Hepes/ NaOH pH 8.0, 0.33 M Sucrose, 5 mM $MgCl_2$, 10 mM NaCl, 10 mM KCl, 20 mM sodium ascorbate, 40 µM Methyl viologen) were illuminated at 825 µmol photons m^{-2} s^{-1} red actinic light, unless specified otherwise, for 10 min, followed by 2-5 min of incubation in the dark. Saturation pulses (6000 µmol photons m^{-2} s^{-1}) were applied every 100 seconds and the NPQ was calculated as: (Fm/Fm') – 1 (Krause and Jahns, 2004). The effect of chemical cross-linking on NPQ was measured using the following reagents: Glutaraldehyde (Serva), S-MBS (m-maleimidobenzoyl-Nhydroxysulfo-succinimide ester) (Thermo Scientific), EDC [1-ethyl-3-(3-dimethylaminopropyl)carbodiimide hydrochloride] (Sigma-Aldrich), DTSSP [3,3-Dithio-bis-(sulfosuccinimidyl)propionate] (Merck-Millipore), formaldehyde and EGS (ethylene glycolbis(succinimidy1 succinate) (Applichem). Each cross-linker was added in the dark 5-10 s before starting measurements.

9-AA measurements

The light-induced proton gradient was measured through the fluorescence quenching of protonated 9-aminoacridine (9-AA) at 365 nm using the NADPH measuring head of the DUAL PAM-100 system. Thylakoids (15 µg Chl) were incubated in the dark in 2 ml reaction media (40 mM Hepes/ NaOH pH 7.5, 0.33 M Sorbitol, 5 mM $MgCl_2$, 10 mM NaCl, 50 µM Methyl viologen) and 5 µM 9-AA were added before illumination with red actinic light for 10 min. The ΔpH was calculated according to Schuldiner et al. (1972) by comparing stable

values of ground-state (F_0-Dark) and steady-state (F-Light) 9-AA fluorescence yields of dark-light and light-dark transitions. In DTSSP-treated samples, to avoid binding of DTSSP to the amino group of 9-AA, samples were incubated for 5 minutes in the dark with the cross-linker and the linking reaction was quenched with 25 mM (final concentration) Tris-HCl pH 8.5 before the addition of 9-AA.

Pigment analysis

To analyze light induced Zx formation, 200-300 µl thylakoid samples (treated as described for Chl fluorescence measurements) were diluted to 20 % (v/v) with acetone and the pigments were analyzed by reversed phase HPLC (Färber et al., 1997).

REFERENCES

Armbrust, T.S., Chitnis, P.R., Guikema, J.A. (1996). Organization of Photosystem I Polypeptides Examined by Chemical Cross-Linking. Plant Physiol **111** : 1307-1312.

Arnon, D.I. (1949). Copper enzymes in isolated chloroplasts. Polyphenoloxidase in Beta vulgaris. Plant Physiol **24**:1-15.

Bergantino, E., Segalla, A., Brunetta, A., Teardo, E., Rigoni, F., Giacometti, G.M., Szabò I. (2003). Light- and pH-dependent structural changes in the PsbS subunit of photosystem II. Proc. Natl. Acad.Sci. USA **100** :15265-15270.

Briantais, J.M., Vernotte, C., Picaud, M., Krause, G.H. (1979). A quantitative study of the slow decline of chlorophyll a fluorescence in isolated chloroplasts. Biochim. Biophys. Acta **548** :128-138.

Cashman, D.J, Zhu, T., Simmerman, R.F., Scott, C., Bruce B.D., Baudry, J. (2014). Molecular interactions between photosystem I and ferredoxin: an integrated energy frustration and experimental model. J Mol Recognit **27** (10):597-608.

Collins RF, Flint TD, Holzenburg A, Ford R.C. (1996). Structural changes in photosystem II after treatment with the zero-length bifunctional cross-linker 1-ethyl-3-(3-dimethylaminopropyl)carbodi-imide: an electron microscopic study. Biochem J **319** (2):585-589.

Demmig, B., Winter, K., Krüger, A., Czygan, F.C. (1987). Photoinhibition and Zeaxanthin Formation in Intact Leaves: A Possible Role of the Xanthophyll Cycle in the Dissipation of Excess Light Energy. Plant physiol **84** (2): 218-224.

Fan, M., Li, M., Liu, Z., Cao, P., Pan, X., Zhang, H., Zhao, X., Zhang, J., Chang, W. (2015). Crystal structures of the PsbS protein essential for photoprotection in plants. Nat. Struct. Mol. Biol **22** (9): 729-735.

Färber, A., Young, A.Y., Ruban, A., Horton, P., Jahns, P. (1997). Dynamics of Xanthophyll-Cycle Activity in Different Antenna Subcomplexes in the Photosynthetic Membranes of Higher Plants (The Relationship between Zeaxanthin Conversion and Nonphotochemical Fluorescence Quenching). Plant physiol **115**:1609-1618.

Gerotto, C., Franchin, C., Arrigoni, G., Morosinotto, T. (2015). In Vivo Identification of Photosystem II Light Harvesting Complexes Interacting with PHOTOSYSTEM II SUBUNIT S. Plant physiol. **168**:1747-1761.

Graßes, T., Pesaresi, P., Schiavon, F., Varotto, C., Salamini, F., Jahns, P., Leister, D. (2002). The role of ΔpH-dependent dissipation of excitation energy in protecting photosystem II against light-induced damage in Arabidopsis thaliana. Plant Physiol. Biochem. **40**:41-49.

Habeeb, A.F.S.A, Hiramoto, R. (1968). Reaction of proteins with glutaraldehyde Arch Biochem Biophys **126** (1):16-26.

Hager, A., Holocher, K. (1994). Localization of the xanthophyll-cycle enzyme violaxanthin de-epoxidase within the thylakoid lumen and abolition of its mobility by a (light-dependent) pH decrease. Planta **192** (4): 581-589.

Horton P (2012). Optimization of light harvesting and photoprotection: molecular mechanisms and physiological consequences. Philos Trans R Soc Lond B Biol Sci **367** (1608):3455-3465.

Jahns, P., and Holzwarth, A.R. (2012). The role of the xanthophyll cycle and of lutein in photoprotection of photosystem II. Biochim. Biophys. Acta **1817**:182-193.

Jahns, P., Latowski, D., Strzalka, K. (2009). Mechanism and regulation of the violaxanthin cycle: The role of antenna proteins and membrane lipids. Biochim. Biophys. Acta **1787**:3-14.

Jansson, S., Andersen, B., Scheller, H. (1996). Nearest-Neighbor Analysis of Higher-Plant Photosystem I Holocomplex. Plant physiol **112**:409-420.

Johnson, M.P., Goral, T.K., Duffy, C.D., Brain, A.P., Mullineaux, C.W., Ruban, A.V. (2011). Photoprotective energy dissipation involves the reorganization of photosystem II light-harvesting complexes in the grana membranes of spinach chloroplasts. Plant Cell **23**:1468-1479.

Kereïche, S., Kiss, A.Z., Kouřil, R., Boekema, E.J., Horton, P. (2010). The PsbS protein controls the macro-organisation of photosystem II complexes in the grana membranes of higher plant chloroplasts. FEBS Lett. **584** :759-764.

Krause, G.H., Jahns, P. (2004). Non-photochemical Energy Dissipation Determined by Chlorophyll Fluorescence Quenching: Characterization and Function. In: Papageorgiou G, Govindjee (eds) Chlorophyll a Fluorescence, **vol 19**. Advances in Photosynthesis and Respiration. Springer Netherlands, pp 463-495.

Li, X., Bjoerkman, O., Shih, C., Grossman, A.R., Rosenquist, M., Jansson, S., Niyogi, K.K. (2000). A pigment-binding protein essential for regulation of photosynthetic light harvesting. Nature **403** :391-395.

Li, X.P., Gilmore, A.M., Caffarri, S., Bassi, R., Golan, T., Kramer, D., Niyogi, K.K. (2004). Regulation of photosynthetic light harvesting involves intrathylakoid lumen pH sensing by the PsbS protein. J Biol Chem **279**:22866-22874.

Liu, H., Huang, R.Y.-C, Chen, J., Gross, M.L., Pakrasi, H.B. (2011). Psb27, a transiently associated protein, binds to the chlorophyll binding protein CP43 in photosystem II assembly intermediates. Proc. Natl. Acad.Sci. USA **108** (45):18536-18541.

Liu H., Zhang, H., Weisza, D.A., Vidavsky, I., Gross, M.L., Pakrasi, H.B (2014). MS-based cross-linking analysis reveals the location of the PsbQ protein in cyanobacterial photosystem II. Proc. Natl. Acad.Sci. USA **111** (12):4638-4643.

Mummadisetti, M.P., Frankel, L.K., Bellamy, H.D., Sallans, L., Goettert, J.S., Brylinski, M., Limbach, P.A., Bricker, T.M. (2014). Use of protein cross-linking and radiolytic footprinting to elucidate PsbP and PsbQ interactions within higher plant Photosystem II. Proc. Natl. Acad.Sci. USA **111** (45):16178-16183.

Nelson, N., Junge, W. (2015). Structure and energy transfer in photosystems of oxygenic photosynthesis. Annu Rev Biochem **84**:659-683.

Nilkens, M., Kress, E., Lambrev, P., Miloslavina, Y., Müller, M., Holzwarth, A.R., Jahns, P. (2010). Identification of a slowly inducible zeaxanthin-dependent component of non-photochemical quenching of chlorophyll fluorescence generated under steady-state conditions in Arabidopsis. Biochim. Biophys. Acta **1797**:466-475.

Nilsson, R., Brunner, J., Hoffman, N.E., Van Wijk, K.J. (1999). Interactions of ribosome nascent chain complexes of the chloroplast-encoded D1 thylakoid membrane protein with cpSRP54. EMBO J **18** (3):733–742.

Niyogi, K.K., Grossman, A.R., Björkman, O.(1998). Arabidopsis Mutants Define a Central Role for the Xanthophyll Cycle in the Regulation of Photosynthetic Energy Conversion. Plant Cell **10** (7):1121-1134.

Oh-oka, H., Takahashi, Y., Matsubara, H. (1989). Topological Considerations of the 9-kDa Polypeptide which Contains Centers A and B, Associated with the 14- and 19-kDa Polypeptides in the Photosystem I Complex of Spinach. Plant Cell Physiol **30** (6):869-875.

Pertl-Obermeyer, H., Schulze, W.X., Obermeyer, G. (2014). In vivo cross-linking combined with mass spectrometry analysis reveals receptor-like kinases and $Ca(^{2+})$ signalling proteins as putative interaction partners of pollen plasma membrane $H(^{+})$ ATPases. J Proteomics **108**:17-29.

Pfündel, E.E., Dilley, R.A. (1993). The pH Dependence of Violaxanthin Deepoxidation in Isolated Pea Chloroplasts. Plant physiol **101** (1):65-71.

Rappsilber, J. (2011). The beginning of a beautiful friendship: cross-linking/mass spectrometry and modelling of proteins and multi-protein complexes. J Struct Biol **173** (3):530-540.

Schuldiner, S., Rottenberg, H., Avron, M. (1972). Determination of ΔpH in Chloroplasts. Eur J Biochem **25** (1):64-70.

Seidler, A. (1996). Intermolecular and Intramolecular Interactions of the 33-kDa Protein in Photosystem II. Eur J Biochem **242** (3):485-490.

Spirin, A.S., Belitsina, N.V., Lerman, M.I. (1965). Use of formaldehyde fixation for studies of ribonucleoprotein particles by caesium chloride density-gradient centrifugation. J Mol Biol **14** (2):611-615.

Sutherland, B.W., Toews, J., Kast, J. (2008). Utility of formaldehyde cross-linking and mass spectrometry in the study of protein-protein interactions. J Mass Spectrom **43** (6):699-715.

Takizawa, K., Cruz, J.A., Kanazawa, A., Kramer, D.M. (2007). The thylakoid proton motive force in vivo. Quantitative, non-invasive probes, energetics, and regulatory consequences of light-induced pmf. Biochim Biophys Acta **1767:** 1233-1244.

Yamamoto, H.Y. (1979). Biochemistry of the violaxanthin cycle in higher plants. In: Goodwin TW (ed) Carotenoids℃5. Pergamon, pp 639-648.

Yamamoto, H.Y., Wang, Y., Kamite, L. (1971). A chloroplast absorbance change from violaxanthin de-epoxidation. A possible component of 515 nm changes. Biochem Biophys Res Commun **42** (1):37-42.

Ytterberg, A.J., Peltier, J.B., and van Wijk, K.J. (2006). Protein profiling of plastoglobules in chloroplasts and chromoplasts. A surprising site for differential accumulation of metabolic enzymes. Plant Physiol **140**: 984-997.

PsbS Interaction Partners Involved in the Activation of Energy Dissipation in *Arabidopsis thaliana*

Viviana Correa Galvis[a], Gereon Poschmann[b], Michael Melzer[c], Kai Stühler[b], and Peter Jahns[a,1]

[a]Plant Biochemistry, Heinrich-Heine-University Düsseldorf, 40225 Düsseldorf, Germany

[b]Molecular Proteomics Laboratory, Biologisch-Medizinisches Forschungszentrum, Heinrich-Heine-University Düsseldorf, 40225 Düsseldorf, Germany

[c]Physiology and Cell Biology, Leibniz Institute of Plant Genetics and Crop Plant Research (IPK), 06466 Gatersleben, Germany

Short title: PsbS Interactions During Energy Dissipation

[1]Address correspondence to pjahns@hhu.de

One sentence summary:

Protein-protein interactions involved in the light activation of energy dissipation in higher plants

ABSTRACT

The PsbS protein plays a central photoprotective role in plants as regulator of the pH-dependent dissipation of excess light energy (= NPQ) in the antenna of photosystem II (PSII). PsbS is supposed to activate NPQ through specific, light-regulated interactions with PSII antenna proteins. However, NPQ-specific interaction partners of PsbS in the thylakoid membrane are still unknown. In this study, we determined the localization and protein interactions of PsbS in thylakoid membranes in the NPQ inactive (dark) and NPQ active (light) state by mass spectrometric analyses of proteins co-purified with PsbS after chemical cross-linking. Our results corroborate a localization of PsbS in PSII supercomplexes and support the model that the light activation of NPQ is based on the monomerization of dimeric PsbS and an increased interaction with the Lhcb1 protein, the major component of trimeric light-harvesting complexes in PSII. Analysis of thylakoid protein complexes under non-denaturing conditions underscored the particular interaction of PsbS with LHCII trimers in the NPQ-active state. Our results are fully consistent with current models of the light-induced and pH-regulated reorganization of the PSII antenna during activation of NPQ.

INTRODUCTION

In natural environments, plants are frequently exposed to rapidly changing light intensities, which may vary in orders of magnitude on a second to minute time scale. Optimal photosynthesis under such conditions requires efficient light absorption under limiting light as well as efficient photoprotection under excess light conditions. Absorption of light energy in excess to what can be utilized in photosynthesis leads to the formation of reactive oxygen species (ROS) and subsequently to photo-oxidative damage of cellular components (Møller et al., 2007). Singlet oxygen has been shown to be the major ROS involved in lipid peroxidation under photo-oxidative stress conditions in plants (Triantaphylidès et al., 2008). To minimize photo-oxidative damage, plants have evolved a number of photoprotective mechanisms which either reduce ROS formation or deactivate formed ROS (Li et al., 2009). Among those, the dissipation of excess light energy as heat (= non-photochemical quenching, NPQ) is an important process aiming at the reduction of ROS formation. Several NPQ mechanisms (termed qE, qT, qZ and qI) can be activated on different time scales (Nilkens et al., 2010) allowing optimal acclimation to different environmental conditions. The pH-regulated qE mechanism represents the dominating NPQ component under moderate light stress conditions and represents an efficient mechanism to reduce singlet oxygen formation (Jahns and Holzwarth, 2012). The strict regulation of qE by the thylakoid lumen pH (Briantais et al., 1979) facilitates rapid (within seconds) activation/deactivation of this mechanism in response to rapidly changing light intensities. Aside from a low pH, the maximum qE capacity requires the presence of the xanthophyll zeaxanthin which is formed in the - likewise pH-regulated - deepoxidation reactions of the xanthophyll cycle (Jahns et al., 2009). Activation of qE essentially depends on the PsbS protein (Li et al., 2000) which acts as sensor of the pH in the thylakoid lumen (Li et al., 2004) and by that is supposed to control conformational changes in the antenna of photosystem II (PSII) (Horton et al., 2005). In fact, PsbS-dependent conformational changes such as the dissociation of a LHCII-CP24-CP29 complex (Betterle et al., 2009), the detachment of LHCII (Holzwarth et al., 2009) and/or the aggregation of LHCII (Horton et al., 2005) are supposed to contribute to qE. However, the structural basis of such conformational changes as well as the exact localization of PsbS and its (qE-specific) interaction partners in PSII remain unclear.

Studies carried out so far, support the view that PsbS is not specifically and strongly associated with a single site in PSII (Caffarri et al., 2009). PsbS has been found to be associated with LHCII (Nield et al., 2000) and with PSII (Fey et al., 2008; Haniewicz et al., 2013). On basis of spectroscopic data (Kiss et al., 2008) and structural analysis of grana membranes (Kereïche et al., 2010), Horton and co-workers proposed that PsbS acts at the contact site of LHCII and PSII core and by that controls the organization of PSII in the grana membranes. Such a view was supported by the observation that dimeric PsbS (present in

the dark or at neutral lumen pH) is rather associated with the PSII core, while monomeric PsbS (formed in light or at acidic lumen pH) associates with LHCII (Bergantino et al., 2003). Additionally, pull-down assays using solubilized thylakoid membranes provided evidence that PsbS interacts with subunits from all large protein complexes (PSII, PSI, cytochrome b6/f and ATP-Synthase) in the thylakoid membrane (Teardo et al., 2007). Whether these findings represent specific interactions of PsbS with these complexes, or might rather be due to unspecific interactions related to the assay conditions and the high hydrophobicity of PsbS (Aspinall-O'Dea et al., 2002; Dominici et al., 2002) has not been clarified so far. A recent study with the moss *Physcomitrella patens*, in which over-expressed and His-tagged PsbS was purified, provided further evidence for an interaction of PsbS with trimeric LHCII (Gerotto et al., 2015). However, no light-dependent (and thus qE-related) changes in this interaction were detectable under those conditions (Gerotto et al., 2015).

Knowledge of qE-specific interaction partners of PsbS is essential for understanding the molecular basis of the pH-regulation of qE. Here, we applied chemical cross-linking of thylakoid membrane proteins in quenched and un-quenched states in combination with co-immunoprecipitation (Co-IP) of PsbS-associated proteins and mass-spectrometric analyses to identify PsbS interaction partners. Our data show that PsbS interacts predominantly with LHCII trimers and PSII core proteins, with Lhcb1 being the most likely binding partner among those complexes. In the qE-active state, particularly interaction with LHCII was increased, suggesting a qE-specific interaction of PsbS with trimeric LHCII.

RESULTS

Localization of PsbS

Using a specific antibody raised against the PsbS protein of Arabidopsis, we localized the PsbS protein predominantly in the grana regions of the thylakoid membrane by immunogold labeling (Figure 1A; Supplemental Figure 1). About 75 % of the gold particles localized to grana stacks, 20 % to grana margins and less than 5 % to stroma lamellae. This localization of PsbS resembles the preferential accumulation of PSII. In the light acclimated state (20 min illumination at 600 µmoles photons m^{-2} s^{-1}), more pronounced labelling in the grana margins was detected, suggesting a reorganization of PsbS upon illumination (Figure 1A). Separation of the protein subcomplexes in the thylakoid membrane by mild detergent treatment and sucrose gradient centrifugation revealed that PsbS co-migrates in the dark predominantly with PSII-LHCII supercomplexes, while increased co-migration of PsbS with dimeric PSII core and trimeric LHCII was detectable in light-adapted samples (Figure 1B), indicating a light induced shift in the binding affinity of PsbS towards LHCII. Disassociation of the PSII-LHCII complexes by increasing the detergent concentration followed by blue native gel electrophoresis (BN-PAGE) revealed that the affinity of PsbS to trimeric LHC proteins is maintained upon illumination (Figure 2A). It should be noted, however, that PsbS protein was also detectable in all other fractions in the sucrose gradient (Figure 1B) suggesting either a random distribution of PsbS or artificial binding of PsbS related to its hydrophobic properties. To identify specific protein interactions of PsbS we therefore applied chemical cross-linking in combination with Co-IP analysis.

Chemical Cross-linking

We performed a cross-linking assay using the thiol-cleavable 12-Å cross-linker 3,3′-dithiobis(sulfosuccinimidylpropionate) (DTSSP) and established conditions under which the cross-linking specifically affected PsbS–dependent qE-quenching in active isolated thylakoids. Addition of DTSSP to dark-adapted thylakoids inhibited the activation of qE, and the resulting chlorophyll (Chl) fluorescence dynamics resembled that of the *npq4* mutant (Figure 1C). On the contrary, addition of DTSSP to light-activated thylakoids impaired the further increase of NPQ as well as NPQ relaxation in the dark (Figure 1C). However, addition of DTSSP did not show a pronounced effect on zeaxanthin synthesis (reduction of maximal levels below 20 %) (Figure 1D), indicating that lumen acidification and hence electron transport were not inhibited by cross-linking. We conclude that under these experimental conditions, cross-linking with DTSSP targets (among others) proteins involved in the pH-regulation of PsbS-dependent quenching. It is tempting to speculate, that DTSSP affects conformational changes and protein interactions required for qE activation (when added in the dark) and relaxation (when added in the light), without inhibition of the electron transport.

Protein analysis of cross-linked thylakoids under native conditions (BN-PAGE) revealed that a fraction of PsbS is present as a dimer in the dark, while only monomeric PsbS was detectable in the light (Figure 2A), in accordance with other studies (Bergantino et al., 2003; Gerotto et al., 2015). Sucrose gradient fractionation of cross-linked samples revealed a differential distribution particularly of PsbS and LHC proteins in light- and dark-adapted thylakoids (Figure 2B). Although PsbS was found to co-migrate predominantly with LHC proteins and PSII core proteins, no PsbS-containing cross-link products were detectable (Figure 2B). Therefore, we enriched the PsbS cross-linked proteins by immunoprecipitation of thylakoid proteins from samples cross-linked in the dark (qE inactive) and light (qE active) adapted state. The assay was performed in parallel with cross-linked samples of isolated thylakoids of *npq4* plants (as control for PsbS-independent protein purification) and WT thylakoids without addition of DTSSP (as control for cross-linking-independent protein purification).

Higher amounts of PsbS were eluted in non-cross-linked WT samples compared to DTSSP linked ones (Figures 3B, 3D and 4), suggesting that the column epitope has a better access to the protein when it is not bound to other proteins. Under non-denaturing conditions, PsbS was not found as part of a protein complex in non-cross linked WT elutes. Nevertheless, other proteins, such as Lhcb proteins, which were also present in cross-linked samples, were co-eluted in the absence of chemical cross-linking, though in relatively low amounts (Figures 3B and 4). The elutes from cross-linked WT thylakoids showed higher PsbS amounts in dark-adapted samples than in light-adapted samples (Figures 3 and 4). Immunoblot analysis of non-denatured elutes from WT cross-linked samples (where the DTSSP link is maintained) allowed the detection of a dimer in the dark (Figures 3A and C) as previously observed (Teardo et al., 2007). In the light, PsbS was found in two protein complexes detected by immunoblotting at ~ 70 and 130 kDa, while monomeric PsbS was no longer detectable (Figure 3A). Lhcb1 was identified as further additional component of those cross-linked products (Figure 3A) which supports the interaction of monomeric PsbS with trimeric LHCII in the light, in accordance with previous *in vitro* studies (Wilka et al., 2013). However, since PsbS detection in these complexes was only possible upon prolonged exposure of the blots and no defined signals at this molecular size were observable in silver stained gels (Figure 3A), we separated the proteins by denaturing electrophoresis (i.e. cleavage of the DTSSP link) to identify specific differences between PsbS co-eluted proteins (Figure 3B). Although the overall protein pattern between WT light and dark adapted samples did not change, the intensity of each band differed between the two conditions. Strikingly, enrichment of a complex at 50 kDa in the light adapted cross-linked WT elutes was observed (Figure 3B). Similar protein patterns were also found in non-linked WT elutes and cross-linked *npq4* elutes (except for the absence of PsbS in the mutant), but with clearly different

band intensities. These results suggest that PsbS is not specifically associated with single proteins but rather to different protein complexes, and that the degree of association is modulated by the proximity of PsbS to those complexes in either the dark- or the light-adapted state. To identify the protein complexes, which are specifically interacting with PsbS and to what extent this binding is enhanced upon illumination, we performed a quantitative mass spectrometric analysis of the whole elutes obtained after co-immunoprecipitation.

Mass Spectrometric Identification and Quantitative Analysis of PsbS Interacting Proteins

WT thylakoids (with and without cross-linking) and non-linked *npq4* thylakoids in both the dark-adapted (qE inactive) and the light-adapted (qE active) state were used as source material for PsbS co-immunoprecipitation. The resulting elutes of five independent replicates per condition were analyzed by quantitative mass spectrometry. Principal component analysis of relative protein quantities clearly separated cross-linked *npq4* and WT samples and cross-linked and unlinked WT sample groups (Supplemental Figure 2). In total, 120 detected proteins were defined as PsbS co-purified proteins due to a significantly higher abundance in the WT compared to the *npq4* samples (q-value WT/*npq4* < 0.01 and ratio WT/*npq4* > 1.5, Supplemental Table 1), from which 42 enclosed 97 % of the cumulated ion intensity excluding PsbS. From these 42 proteins, 29 were components of protein complexes involved in light harvesting and electron transport (Figure 4; Supplemental Table 1). The additional 13 low abundant proteins were related to light driven processes such as pigment biosynthesis or oxidative stress (Supplemental Table 1) and therefore not considered as specific PsbS interaction partners during qE induction.

The three components of the LHC trimers (Lhcb1, 2 and 3), PSII core proteins CP47, CP43 and D2, and the LHC minor proteins (CP26, CP24, CP29) showed, in that order, the highest cumulated ion intensity from all proteins co-eluted with PsbS (Figure 4; Supplemental Table 1). All these LHC and PSII core proteins were highly enriched in cross-linked samples (Figure 4) and showed at least one lysine modified with DTSSP in all WT samples, indicating that contact sites among/within them where maintained through all extraction and purification steps. The differences between their quantified values thus reflect the degree to which the individual proteins either directly interact with PsbS or with other PsbS-linked proteins in the dark- and light-adapted states. Notably, no DTSSP-related modification was detected for D1 and Cytb559 β, indicating a high affinity of both proteins to other cross-linked proteins (Supplemental Table 1).

The relative amount of each protein was strongly increased in cross-linked WT samples in comparison with the cross-linked *npq4* and non-linked WT samples (Figure 4), indicating a PsbS and cross-linking dependent purification of proteins. Furthermore, an increase was detectable in the light-adapted state, especially for LHCII major and minor

proteins, as compared to the dark-adapted state (Figure 5A and 5B), indicating a light-induced increase of the interaction of PsbS with PSII antenna proteins. To clarify whether this increase is related to a higher affinity of LHC proteins to PsbS in the light-adapted state, we estimated the amounts of LHC and PSII core proteins in relation to the detected PsbS levels (Figures 5D, 5E and 5F). Using a relative quantitative approach, the ratio of each protein per PsbS increased about twofold in the light-adapted state, with Lhcb3 (factor 3.1) and Lhcb1 (2.7) showing the highest enrichment and CP43 (1.6), CP47 (1.8), Lhcb2 (1.8) and D2 (1.9) the lowest. The ratio of Lhcb1:Lhcb2:Lhcb3 was estimated with 14:5:1 in dark samples and 12:3:1 in light-adapted ones. These ratios are clearly higher than the 8:3:1 ratio reported earlier for the occurrence of the three proteins in thylakoid membranes (Jansson, 1994; Peter and Thornber, 1991). This suggests that either predominantly the single Lhcb1 protein or LHCII-trimers not containing Lhcb3 are co-purified with PsbS.

In summary, these data suggest that in the qE inactive dark state, PsbS is present as dimer and located close to trimeric LHCII and PSII core proteins, without interacting specifically with one of the PSII proteins. In the qE active state, monomerization of PsbS leads to a reorganization of the PSII antenna, by that enhancing the interaction of PsbS with LHCII and PSII proteins, with Lhcb1 and thus trimeric LHCII being the most likely binding partner in the qE-active state.

DISCUSSION

Light-induced acidification of the thylakoid lumen acts as a trigger signal for the activation of quenching of excess light energy through changes in the structural organization of the PSII-LHCII (Betterle et al., 2009; Holzwarth et al., 2009; Johnson et al., 2011). Protonated PsbS (Li et al., 2004) enhances these conformational changes by promoting LHCII aggregation (Holzwarth et al., 2009; Johnson et al., 2011), implying a direct contact of PsbS with the LHCII-PSII complexes upon illumination. However, none of these interactions have been successfully tested in qE active thylakoids, due to the rapid relaxation of qE (within seconds) in the dark. In this work, we established a cross-linking assay which allowed the identification of light dependent interactions between PsbS and the PSII-LHCII components in isolated thylakoids.

Cross-linker properties

The inhibition of qE activation/relaxation by addition of the water soluble cross-linker DTSSP to isolated thylakoids (Figure 1C) occurred within a few seconds. This suggests that PsbS-controlled conformational changes required for qE activation and relaxation are effectively inhibited by chemical cross-linking when DTSSP is added in the dark and light, respectively, denoting that cross-linked membranes remain in a dark state-arrangement even after illumination (Figure 1C). Obviously, addition of DTSSP leads to a rapid stabilization of the organization of PSII in the thylakoid membrane in either the dark-adapted or light-adapted conformation. Strikingly, electron and proton transport was only marginally affected by cross-linking as monitored from zeaxanthin formation (Figure 1D). Due to the very rapid reaction of DTSSP, it is likely that the cross-linker interacts with stroma-exposed Lys residues at the grana margins and in grana partitions. This view is supported by the fact that all DTSSP-linking sites identified for PsbS were located on the stroma side of the protein (Supplemental Figure 3), and further suggests that, apart from interactions with proteins in the same membrane, PsbS could also interact with proteins of a neighboring grana stack. The implication of this type of interaction and its role on structural membrane changes upon qE induction might be of interest for further research.

PsbS dimer vs PsbS monomer

Previous studies with maize thylakoids have shown that PsbS is at least partially present as a dimer in the dark (Bergantino et al., 2003). In that work, the monomer/dimer ratio increased upon illumination so that at low luminal pH only the monomeric form was present: However, dimeric PsbS in dark samples could be dissociated by treating thylakoids with a high concentration of anionic detergent (Bergantino et al., 2003). Here, dimeric PsbS was detected in *A. thaliana* thylakoid membranes after chemical cross-linking in the dark (Figures 2 and 3), as reported for other plant species (Bergantino et al., 2003; Gerotto et al., 2015; Teardo et al., 2007) or when using very low concentrations of a non-ionic detergent in native

electrophoresis (Figure 3C). Thus dimer stability *in vitro* strongly depends on the solubilization and protein separation conditions. The fraction of monomeric PsbS found in dark-adapted membranes might thus be ascribed to the detergent treatment. We therefore assume that also in *A. thaliana*, PsbS is predominantly present as dimer in the dark-adapted state, while only monomeric PsbS exists in the light-adapted state. Light-induced monomerization of PsbS dimers can thus be expected to be crucial for the pH-induced activation of qE, as supposed earlier (Bergantino et al., 2003). The concept of light-induced monomerization of PsbS was recently challenged in a study where pre-illuminated thylakoids were cross-linked with 1-ethyl-3-(3-dimethylaminopropyl) carbodiimide (EDC) and mainly dimeric PsbS was determined (Fan et al., 2015). In that study, however, cross-linking was performed for up to 4 h after illumination and in presence of detergent (1 % n-dodecyl-β-d-maltopyranoside) so that reorganization of PsbS and/or artificial cross-linking of PsbS monomers cannot be excluded.

Identification of PsbS interaction partners

Our data strongly support the predominant interaction of PsbS with PSII core and LHCII proteins in both the dark-and light-adapted state, and an enhanced interaction with LHCII in the qE-active light state. This conclusion is corroborated by the distribution of PsbS in chloroplasts (Supplemental Figure 1), the co-migration of PsbS with PSII and LHCII containing proteins bands under native conditions (Figures 1B, 2 and 3) and the MS analysis of proteins co-purified with PsbS (Figures 4 and 5). So far, Co-IP based analyses of PsbS interaction partners have been performed with isolated thylakoids from *Zea mays* (Teardo et al., 2007) and *Physcomitrella patens* (Gerotto et al., 2015). In both cases, however, Co-IP was not combined with chemical cross-linking. In maize, PsbS was found to interact with all major protein complexes of the thylakoid membrane rather than specifically with PSII proteins, although also LHCII was among the identified interaction partners (Teardo et al., 2007). In the moss *P. patens*, however, LHCII proteins were assigned as the major PsbS interaction partners, albeit other thylakoid membrane proteins were co-eluted at reasonable amounts with His-tagged PsbS (Gerotto et al., 2015). Also in the present work, a number of proteins were co-eluted with PsbS in addition to the LHCII and main PSII core proteins, such as minor subunits of the PSII core and some components of the cytochrome b6f, PSI core, PSI antenna and ferredoxins (FNR) (Figure 4; Supplemental Table 1). These proteins were, however, present in a very low amount (around tenfold less than the most abundant proteins) and therefore were not included as direct interaction partner candidates during qE induction. Obviously, PsbS binds either unspecifically to other proteins during purification or some proteins are purified independent of any interaction with PsbS. In both cases, the experimental conditions applied for membrane solubilization and protein purification are likely determinants of the degree of unspecific protein purification. To estimate PsbS-independent

purification of proteins, we used thylakoids from the PsbS deficient mutant *npq4*, as has been also applied recently for *Physcomitrella* (Gerotto et al., 2015). To minimize unspecific PsbS interactions, we used cross-linked samples as starting material, which can be expected to reduce unspecific protein interactions during solubilization. Indeed, cross-linking led to a pronounced reduction of the overall amount of purified PsbS, likely related to the fact that both the cross-linking sites and the epitope recognized by the antibody are located on stroma-exposed regions of PsbS (Supplemental Figure 3). Furthermore, cross-linking enabled us to stabilize PSII in either the dark- or light-adapted state and thus to determine light-induced and qE-specific protein interactions, regardless of the following purification steps. In fact, only in cross-linked WT samples (but not in non-cross-linked WT and cross-linked *npq4* samples) we observed a pronounced increase of the amounts of co-purified LHCII proteins in the light-adapted state (Figure 4, Supplemental Table 1), supporting a qE-specific increase of the interaction of PsbS with LHCII.

Chemical cross-linking can occur either within or between proteins. Both types of linking are plausible, however only intermolecular links can be related to the functional role of PsbS in qE activation through protein interactions. The observed changes in the distribution of PsbS (and other PSII proteins) and the presence of the dimeric PsbS in the dark (Figures 2 and 3) are good indicators for DTSSP intermolecular cross-linking, allowing the identification of PsbS interaction partners (without discarding the possibility of additional intramolecular links). Although MS analyses identified the cross-linked proteins, we cannot decide whether the cross-link is due to a direct cross-link to PsbS or to other PsbS-linked proteins. The quantification of co-purified proteins by a relative quantitative approach indicated that overstoichiometric amounts of proteins in relation to PsbS were co-purified with PsbS (Figure 5). Since it is unlikely, that a single PsbS protein is linked to more than 1 or 2 other proteins at the same time, this may suggest that several proteins are cross-linked to each other. However, the by far highest abundance of Lhcb1 implies that this protein is the predominant direct binding partner of PsbS, supporting a close proximity of Lhcb1 and PsbS. The nearly threefold increase of the Lhcb1/PsbS ratio upon illumination likely reflects the light-induced monomerization of PsbS, resulting in an increased interaction between both proteins.

Model for the localization of PsbS in the dark- and light-adapted state

The PSII-LHCII-supercomplex in Arabidopsis is composed of a dimeric core (C_2), two strongly bound LHCII trimers (= S-trimers) and two moderately bound LHCII trimers (= M-trimers), giving rise to the $C_2S_2M_2$ supercomplex (Caffarri et al., 2009). The S-trimer has direct contact to the RC core through CP43, while the moderately bound M-trimers attach to PSII through the minor antenna complexes CP29 and CP24 (Kouřil et al., 2012). In addition to this basic $C_2S_2M_2$ unit, also some smaller complexes (such as C_2S_2M, C_2S_2, C_2S and C_2)

have been found, but no larger complexes containing additional loosely bound L-trimers (Caffarri et al., 2009). In stacked grana regions, where most of the functional PSII is located, a fraction of 5-10 % of PSII-supercomplexes is further organized in well-ordered arrays, so-called PSII megacomplexes (Kouřil et al., 2012; Kouřil et al., 2013). The extent of array formation was shown to decrease upon short- and long-term acclimation of chloroplasts to high light (Kirchhoff et al., 2007; Kouřil et al., 2013). All available structural data exclude a localization of PsbS within the PSII-LHCII supercomplexes, so that PsbS is likely associated only weakly with PSII supercomplexes or located between two different supercomplexes.

Our data support a localization of PsbS close to trimeric LHCII. The ratio of 14:5:1 determined for co-purified Lhcb1, Lhcb2 and Lhcb3, respectively, in the dark-adapted state (Figure 5) implies that predominantly Lhcb1 alone or LHCII S-trimers, which are devoid of Lhcb3, interact with PsbS in the qE-inactive state. We propose that, in the dark-adapted state, dimeric PsbS is located in proximity to the Lhcb1 protein of the S-trimer (Figure 6). In addition, PsbS, might interact with the RC core through CP43, the most easily accessible subunit (from outside of the supercomplex) among RC proteins. In the light-adapted, qE-active state, monomerization of PsbS increases the interaction with PSII proteins. Due to the increased amount of Lhcb3 purified in the light-adapted state (Figure 5), it is very likely that upon activation of qE particularly the interaction of PsbS with M-trimers (where Lhcb3 is located) is increased. We thus propose for the qE-active state (Figure 6), that the enhanced interaction of PsbS with M-trimers is accompanied by the detachment and/or aggregation of LHCII proteins, in agreement with current models for qE-quenching (Betterle et al., 2009; Holzwarth et al., 2009; Horton, 2012; Johnson et al., 2011). Whether LHCII aggregates contain M-trimers only or additionally minor PSII antenna complexes, cannot be decided on basis of our data. The model for the qE-active state (Figure 6) thus exemplarily shows two possible scenarios, one with aggregated M-trimers containing no minor antenna complexes and one with additional binding of CP24. The latter case is in accordance with the notion that PSII-LHCII supercomplexes, which do not contain M-trimers are also devoid of CP24 (Caffarri et al., 2009) and with the model favored by (Johnson et al., 2011). Monomerization of PsbS and detachment of M-trimers likely increases the probability for an interaction of PsbS with the RC core (particularly with CP47) and with the minor antenna protein CP29, which are both shielded by M-trimers in the dark-adapted state. This interpretation is supported by our data, showing that CP47 and CP29 show the largest increase among all RC core proteins and minor antenna proteins, respectively, upon qE-activation, when comparing the levels of co-purified proteins per PsbS in the dark and light state (Figure 5). To what extent the de-epoxidation of violaxanthin to zeaxanthin supports the detachment/aggregation of M-trimers or the protein interactions in the qE-active state remains to be clarified.

METHODS

Plant Material

Arabidopsis thaliana wild type (Col-0) and mutant (*npq4* = PsbS-deficient (Graßes et al., 2002); *L17* = PsbS overexpressing line (Li et al., 2002)) plants were grown under short-day conditions (8 h light / 16 h dark) on soil at 20 °C and a light intensity of 180-200 µmol photons m^{-2} s^{-1}. All experiments were performed with 5-6 weeks old plants.

Immunogold Labeling and Transmission Electron Microscopy

Dark adapted and illuminated leaves (20 min with 600 µmol photons m^{-2} s^{-1}) of WT plants were fixed and labeled as previously reported (Schwarz et al., 2014).

Thylakoid Membrane Preparations

Detached leaves of dark-adapted (end of night phase) plants were homogenized with extraction media (330 mM Sorbitol, 44 mM MES-NaOH pH 7.4, 1 mM $MgCl_2$, 1 mM $MnCl_2$, 10 mM NaCl, 5mM EGTA, 5 mM EDTA, 1.7 mM sodium ascorbate, 0.1 % BSA) by three 0.5 s pulses in a precooled blender. The homogenate was filtered through 4 layers of cheesecloth followed by 1 layer of nylon gaze (20 µm mesh size), centrifuged 3 min at 3850 x *g,* and resuspended carefully in 1 ml shock media (SM: 5 mM $MgCl_2$). After incubation for 15 s on ice, 1 ml of resuspension media (RM: 80 mM HEPES-NaOH pH 7.6, 660 mM sorbitol, 5mM $MgCl_2$, 10 mM NaCl, 2 mM KH_2PO_4) was added to the homogenate and then centrifuged for 5 min at 3850 x *g*. The pellet was resuspended in 1 ml 1:1 SM:RM. All steps were performed in the dark at 4 °C The Chl concentration was calculated as described (Arnon, 1949).

Chlorophyll Fluorescence Measurements

All measurements were done in dark adapted, freshly isolated thylakoids. Chl fluorescence was measured using a Dual-PAM-100 system (Walz, Germany). Thylakoids (equivalent to 60 µg Chl) in 2 ml reaction media (RM-A : 40 mM HEPES-NaOH pH 8.0, 0.33 M sucrose, 5 mM MgCl2, 10 mM NaCl, 10 mM KCl, 20 mM sodium ascorbate, 40 µM methyl viologen) were illuminated at 825 µmol photons m-2 s-1 red actinic light for 10 min followed by 5 min incubation in the dark. Saturation pulses (6000 µmol photons m-2 s-1) were applied every 100 seconds and the NPQ was calculated as (Fm/Fm') – 1. The effect of chemical cross-linking was measured adding 1.25 mM DTSSP (Merck-Millipore).

Pigment Analysis

For pigment extraction, 200-300 µl thylakoid samples (treated as described for Chl fluorescence measurements) were diluted to 20 % (v/v) with acetone and the pigments were analyzed by reversed phase HPLC (Färber et al., 1997).

Chemical Cross-linking and Co-immnoprecipitation

For cross-linking, isolated thylakoids (equivalent to 60 µg Chl) from WT and *npq4* plants were incubated either in the dark or in the light (825 µmol photons m^{-2} s^{-1}, actinic red light) under stirring in 2 ml reaction media (40 mM HEPES-NaOH pH 8.0, 0.33 M Sucrose, 5 mM $MgCl_2$, 10 mM NaCl, 10 mM KCl, 20 mM sodium ascorbate, 40 µM methyl viologen) with 1.25 mM DTSSP for 25 min. The reaction was stopped by adding 50 mM Tris pH 7.5 and further incubation for 15 min. For the light treatment, DTSSP was added to thylakoid samples after 5 min of illumination. Cross-linked thylakoids were spun down and resuspended in 2 ml CO-IP buffer (PBS,1 % α-DM [α-n-dodecyl-D-maltoside], protease inhibitors cocktail (Roche)) and incubated overnight with 500 µl sepharose beads bound to a specific anti-PsbS antibody (commissioned work Pineda Antibody-service). Unspecifically bound proteins were eluted as previously described (Teardo et al., 2007) with the following modifications: Proteins were eluted with a washing buffer (0.5 M NaCl, 0,05 % Tween 20 and 0.1 % Triton X-100). PsbS-linked proteins were eluted with 2 ml Pierce™ IgG Elution Buffer, pH 2.0 (Thermo Scientific), 0.05 % α-DM. Eluted proteins were concentrated by overnight precipitation with TCA (15 %) at 4 °C, spun down for 1 h at 17,000 x *g*. Pellets were resuspended in 75 µl ACA Buffer (750 mM ε-aminocaproic acid, 50 mM Bis-Tris, pH 7.0, 0.5 mM EDTA) and incubated for 1 h at 37 °C.

Electrophoresis and Western Blot

For immunoblots, samples were separated on a NuPAGE® Novex® 10 % Bis-Tris gel (Life Sciences) according to the manufacturer's protocol, without adding DTT to the sample buffer when analyzing proteins without breaking the DTSSP link. Proteins were immobilized and detected as previously described (Schwarz et al., 2014). PsbS was detected using the same antibody used for the co-immunoprecipitation.

Sucrose Density Gradient Ultracentrifugation and Blue Native Electrophoresis

Isolated thylakoids equivalent to 200 µg Chl were incubated either in the dark or in the light (825 µmol photons m^{-2} s^{-1}, actinic red light) under stirring in 2 ml RM-A for 25 min. DTSSP (4 mM) was added in the dark or after 5 min of illumination. Subsequently, membranes were pelleted and washed briefly with 5 mM EDTA in 10 mM HEPES, pH 7.5.

For ultracentrifgation, protein complexes in the thylakoid membrane were separated by sucrose density gradient centrifugation as described (Caffarri et al., 2009) with some modifications .The resulting thylakoids were solubilized in a medium containing 10 mM HEPES pH 7.5 and 0.6 % α-DM at a final concentration of 0.5 mg Chl/ml. Insolubilized material was removed by centrifugation at 17,000 x *g* for 10 min. Solubilized thylakoids corresponding to 100 µg Chl were loaded onto a sucrose gradient containing 0.65 M sucrose, 0.008 % α-DM in 10 mM HEPES pH 7.5, protease inhibitors cocktail (Roche), and fractionated by ultracentrifugation for 16 h at 4 °C at 130,000 x *g*. Proteins of the obtained bands were concentrated by TCA precipitation as described above and resuspended in 100 µl SDS sample buffer. Proteins were separated by loading 5 µl of each sample onto a SDS–PAGE (Laemmli, 1970).

For BN-PAGE, the resulting thylakoids were resuspended in ACA buffer (750 mM e-aminocaproic acid; 50 mM Bis-Tris, pH 7.0; 0.5 mM EDTA) at a final concentration of 1 µg Chl/µl and solubilized by adding α-DM (2 % final concentration) for 10 min at 4 °C. Insolubilized material was removed as above. Solubilized thylakoids were mixed with equal amounts of 2 x Blue Native Buffer (SERVA) and the volume corresponding to 2 µg Chl was loaded on a 4-16 % acrylamide native gel (SERVA). BN-PAGE was performed using a voltage gradient at 4 °C as follows: 10 min at 50 V, 30 min at 75 V, and 2 h at 200 V. For the second dimension, a single lane of the BN gel was incubated for 20 min in equilibration buffer (66 mM Na_2CO_3; 468 mM β-mercaptoethanol; 2 % SDS) and loaded on a 12.5 % SDS-PAGE as described (Laemmli, 1970). Immunoblot detection was performed as described above using our specific PsbS antibody and Agrisera® antibodies for all other proteins.

Mass Spectrometric Analysis

A quantitative mass spectrometric approach was used for the identification of proteins interacting directly or indirectly with PsbS.

Sample Preparation for Liquid Chromatography and Mass Spectrometric Analysis

After cross-linking and anti-PsbS based affinity purification of five technical replicates per samples group (1: *npq4* mutant, cross-linked in the light; 2: WT, cross-linked, in the light; 3*: npq4* mutant, cross-linked in the dark; 4: WT, cross-linked in the dark; 5: WT not cross-linked incubated in the light; 6: WT, not cross-linked incubated in the dark), protein samples were prepared for mass spectrometric analysis by first focusing them shortly in a 4-12 % polyacrylamide Bis-Tris gel (Life Technologies, Darmstadt, Germany). After silver staining, protein containing bands were excised, destained, reduced and alkylated with iodoacetamide as described (Poschmann et al., 2014) Subsequently, protein samples were digested with

0.1 µg trypsin (Serva, Heidelberg, Germany) in 50 mM NH_4HCO_3 overnight at 37 °C and resulting peptides extracted with 1:1 (v/v) 0.1 % TFA / acetonitrile.

Liquid Chromatography and Mass Spectrometry

After acetonitrile removal by vacuum concentration, peptides were subjected to reversed-phase liquid chromatography on an UltiMate 3000 UHPLC system (Thermo Scientific, Dreieich, Germany) online coupled to an Obitrap Elite high resolution mass spectrometer (Thermo Scientific, Bremen, Germany). Peptides were pre-concentrated at a flow rate of 6 µl / min on an Acclaim PepMap100 trap column (3 µm C18 particle size, 100 Å pore size, 75 µm inner diameter, 2 cm length, Thermo Scientific, Dreieich, Germany) for ten minutes using 0.1 % TFA as mobile phase. Subsequently, an analytical column (Acclaim PepMapRSLC, 2 µm C18 particle size, 100 Å pore size, 75 µm inner diameter, 25 cm length, Dionex/ Thermo Scientific) was used to separate peptides at a flow rate of 300 nl/min at 60 °C using a 2 h gradient from 4 to 40 % solvent B (solvent A: 0.1 % (v/v) formic acid in water, solvent B: 0.1 % (v/v) formic acid, 84 % (v/v) acetonitrile in water).

Peptides were injected into the mass spectrometer via a nano electrospray ionization source equipped with distal coated SilicaTip emitters (New Objective, Woburn, MA, USA). The source voltage was set to 1400 V and the capillary temperature to 275 °C. The Orbitrap Elite instrument was operated in positive mode, precursor scans carried out in the orbitrap analyzer with a resolution of 60,000 (at 400 m/z) over a 350-1700 m/z mass range using a maximum fill time of 200 ms and a target value for the automatic gain control of 1,000,000. Fragment spectra were recorded data dependently in the linear ion trap (LTQ) part of the instrument: The 20 most intense >1+ charged precursor ions with a minimal signal of 500 were isolated and fragmented using collision induced dissociation (CID). Fragment ions were accumulated with a maximal fill time of 300 ms and an automatic gain control target value of 10,000 and analyzed with an available mass range from 200 to 2,000 m/z at a resolution of 5,400 (at 400 m/z). Already fragmented precursor ions were excluded from the analysis for 45 seconds in the data dependent setting. The mass spectrometry proteomics data have been deposited to the ProteomeXchange Consortium (Vizcaíno et al., 2014) via the PRIDE partner repository with the dataset identifier PXD002160.

Data Analysis

Protein and peptide identification and label-free quantification was carried out using the MaxQuant software suite (version 1.5.0.30, MPI for Biochemistry, Planegg, Germany). Spectra were searched against 27416 protein entries from the TAIR database (TAIR10_pep_20110103_representative_gene_model_updated.fasta) with the predefined setting for orbitrap mass spectrometers: 20 ppm first search peptide tolerance; 4.5 ppm main

search peptide tolerance, 0.5 Da MS/MS match tolerance. Carbamidomethyl at cysteines was set as fixed and N-terminal acetylation as well as methionine oxidation and 3-(carbamidomethylthio)propanoyl of lysine residues as variable modification. Peptide identification was controlled by a decoy database approach using a false discovery rate of 1 %. Protein were accepted at a false discovery rate of 1 % and initially with at least one unique or razor peptide. Subsequently, proteins marked as contaminants, proteins which were only identified by a modified site and protein identifications based on only one peptide were not considered for further analysis.

Label-free quantification of precursor ions of unique and razor peptides was done using the label-free quantification algorithm implemented in MaxQuant (Cox et al., 2014) considering a “minimal ratio count” of two and “match between runs” enabled.

The protein data was split into two separate lists: list one comprising proteins with at least three valid values per cross-linked samples group and another list – list two - excluding proteins from list one and including proteins with five valid values in at least one group of the cross-linked samples. For the second list a “fill in” approach of missing values generated from a downshifted normal distribution was applied to be able to find PsbS co-purified proteins for which no quantitative information was available in the *npq4* samples.

Statistical calculations on logarithmized quantitative protein data were done with Perseus 1.5.0.15 (MPI for Biochemistry, Planegg, Germany) and the R statistical environment (version 3.1.1, The R Foundation for Statistical Computing, Vienna, Austria). First, PsbS co-purified proteins were identified by a two way ANOVA (wt/*npq4*, light/dark) from the samples subjected to crosslinking (p-value wt/*npq4* < 0.01 after correction by the method of Benjamini and Hochberg, ratio wt/*npq4* > 1.5). Within the resulting list of PsbS co-purified proteins, proteins differing in abundance between light and dark were identified by Student’s t-tests (followed by correction after Benjamini and Hochberg) before and after normalizing the protein abundance data of individual samples by the respective abundance of PsbS.

ACKNOWLEDGMENTS

This work was supported by the Deutsche Forschungsgemeinschaft (GRK 1525 to P.J.)

AUTHOR CONTRIBUTIONS

V.C.G., G.P. and P.J. designed the experiments; V.C.G. performed most of the research; G.P. and K.S. performed and analyzed the mass spectrometry data; M.M. performed the electron microscopy; V.C.G. and P.J. wrote the paper.

REFERENCES

Arnon, D.I. (1949). Copper enzymes in isolated chloroplasts. Polyphenoloxidase in Beta vulgaris. Plant Physiol **24**, 1-15.

Aspinall-O'Dea, M., Wentworth, M., Pascal, A., Robert, B., Ruban, A., and Horton, P. (2002). In vitro reconstitution of the activated zeaxanthin state associated with energy dissipation in plants. Proc. Natl. Acad.Sci. USA **99**, 16331-16335.

Bergantino, E., Segalla, A., Brunetta, A., Teardo, E., Rigoni, F., Giacometti, G.M., and Szabò I. (2003). Light- and pH-dependent structural changes in the PsbS subunit of photosystem II. Proc. Natl. Acad.Sci. USA **100**, 15265-15270.

Betterle, N., Ballottari, M., Zorzan, S., De Bianch, S., Cazzaniga, S., Dall'osto, L., Morosinotto, T., and Bassi, R. (2009). Light-induced dissociation of an antenna hetero-oligomer is needed for non-photochemical quenching induction. J Biol Chem **284**, 15255-15266.

Briantais, J.M., Vernotte, C., Picaud, M., and Krause, G.H. (1979). A quantitative study of the slow decline of chlorophyll a fluorescence in isolated chloroplasts. Biochim. Biophys. Acta **548,** 128-138.

Caffarri, S., Kouřil, R., Kereïche, S., Boekema, E.J., and Croce, R. (2009). Functional architecture of higher plant photosystem II supercomplexes. EMBO J. **28**, 3052-3063.

Cox, J., Hein, M.Y., Luber, C., Paron, I., Nagaraj, N., and Mann, M. (2014). Accurate Proteome-wide Label-free Quantification by Delayed Normalization and Maximal Peptide Ratio Extraction, Termed MaxLFQ. Mol. Cell Proteomics **13**, 2513-2526.

Dominici, P., Caffarri, S., Armenante, F., Ceoldo, S., Crimi, M., and Bassi, R. (2002). Biochemical properties of the PsbS subunit of photosystem II either purified from chloroplast or recombinant. J Biol Chem **277**, 22750-22758.

Fan, M., Li, M., Liu, Z., Cao, P., Pan, X., Zhang, H., Zhao, X., Zhang, J., and Chang, W. (2015). Crystal structures of the PsbS protein essential for photoprotection in plants. Nat. Struct. Mol. Biol. 22, 729-735.

Färber, A., Young, A.Y., Ruban, A., Horton, P., and Jahns, P. (1997). Dynamics of Xanthophyll-Cycle Activity in Different Antenna Subcomplexes in the Photosynthetic Membranes of Higher Plants (The Relationship between Zeaxanthin Conversion and Nonphotochemical Fluorescence Quenching). Plant physiol **115**, 1609-1618

Fey, H., Piano, D., Horn, R., Fischer, D., Schmidt, M., Ruf, S., Schröder, W.P., Bock, R., and Büchel, C. (2008). Isolation of highly active photosystem II core complexes with

a His-tagged Cyt b559 subunit from transplastomic tobacco plants. Biochim. Biophys. Acta **1777**, 1501-1509.

Gerotto, C., Franchin, C., Arrigoni, G., and Morosinotto, T. (2015). In Vivo Identification of Photosystem II Light Harvesting Complexes Interacting with PHOTOSYSTEM II SUBUNIT S. Plant physiol. **168**, 1747-1761.

Graßes, T., Pesaresi, P., Schiavon, F., Varotto, C., Salamini, F., Jahns, P., and Leister, D. (2002). The role of ΔpH-dependent dissipation of excitation energy in protecting photosystem II against light-induced damage in Arabidopsis thaliana. Plant Physiol. Biochem. **40**, 41-49.

Haniewicz, P., De Sanctis, D., Büchel, C., Schröder, W.P., Loi, M.C., Kieselbach, T., Bochtler, M., and Piano, D. (2013). Isolation of monomeric photosystem II that retains the subunit PsbS. Photosyn. Res. **118,** 199-207.

Holzwarth, A.R., Miloslavina, Y., Nilkens, M., and Jahns, P. (2009). Identification of two quenching sites active in the regulation of photosynthetic light-harvesting studied by time-resolved fluorescence. Chem Phys Lett **483**, 262-267.

Horton, P. (2012). Optimization of light harvesting and photoprotection: molecular mechanisms and physiological consequences.Philos. Trans. R. Soc. Lond., B, Biol. Sci. **367**, 3455-3465.

Horton, P., Wentworth, M., and Ruban, A. (2005). Control of the light harvesting function of chloroplast membranes: The LHCII-aggregation model for non-photochemical quenching. FEBS Lett. **579**, 4201-4206.

Jahns, P., and Holzwarth, A.R. (2012). The role of the xanthophyll cycle and of lutein in photoprotection of photosystem II. Biochim. Biophys. Acta **1817**, 182-193.

Jahns, P., Latowski, D., and Strzalka, K. (2009). Mechanism and regulation of the violaxanthin cycle: The role of antenna proteins and membrane lipids. Biochim. Biophys. Acta **1787**, 3-14.

Jansson, S. (1994). The light-harvesting chlorophyll a / b-binding proteins. Biochim. Biophys. Acta **1184**, 1-19.

Järvi, S., Suorsa, M., Paakkarinen, V., and Aro, E.M. (2011). Optimized native gel systems for separation of thylakoid protein complexes: novel super- and mega-complexes. Biochem. J. **439**, 207-214.

Johnson, M.P., Goral, T.K., Duffy, C.D., Brain, A.P., Mullineaux, C.W., and Ruban, A.V. (2011). Photoprotective energy dissipation involves the reorganization of photosystem

II light-harvesting complexes in the grana membranes of spinach chloroplasts. Plant Cell **23**, 1468-1479.

Kereïche, S., Kiss, A.Z., Kouřil, R., Boekema, E.J., and Horton, P. (2010). The PsbS protein controls the macro-organisation of photosystem II complexes in the grana membranes of higher plant chloroplasts. FEBS Lett. **584**, 759-764.

Kirchhoff, H., Haase, W., Wegner, S., Danielsson, R., Ackermann, R., and Albertsson, P.-A. (2007). Low-Light-Induced Formation of Semicrystalline Photosystem II Arrays in Higher Plant Chloroplasts. Biochemistry **46**, 11169-11176.

Kiss, A.Z., Ruban, A.V., and Horton, P. (2008). The PsbS protein controls the organization of the photosystem II antenna in higher plant thylakoid membranes. J Biol Chem **283**, 3972-3978.

Kouřil, R., Dekker, J.P., and Boekema, E.J. (2012). Supramolecular organization of photosystem II in green plants. Biochim. Biophys. Acta **1817**, 2-12.

Kouřil, R., Wientjes, E., Bultema, J.B., Croce, R., and Boekema, E.J. (2013). High-light vs. low-light: effect of light acclimation on photosystem II composition and organization in Arabidopsis thaliana. Biochim. Biophys. Acta **1827**, 411-419.

Laemmli, U.K. (1970). Cleavage of Structural Proteins during the Assembly of the Head of Bacteriophage T4. Nature **227**, 680-685.

Li, X., Björkman, O., Shih, C., Grossman, A.R., Rosenquist, M., Jansson, S., and Niyogi, K.K. (2000). A pigment-binding protein essential for regulation of photosynthetic light harvesting. Nature **403**, 391-395.

Li, X.P., Gilmore, A.M., Caffarri, S., Bassi, R., Golan, T., Kramer, D., and Niyogi, K.K. (2004). Regulation of photosynthetic light harvesting involves intrathylakoid lumen pH sensing by the PsbS protein. J Biol Chem **279**, 22866-22874.

Li, X.P., Muller-Moule, P., Gilmore, A.M., and Niyogi, K.K. (2002). PsbS-dependent enhancement of feedback de-excitation protects photosystem II from photoinhibition. Proc. Natl. Acad.Sci. USA 99, 15222-15227.

Li, Z., Wakao, S., Fischer, B.B., and Niyogi, K.K. (2009). Sensing and responding to excess light. Annu Rev Plant Biol **60**, 239-260.

Møller, I.M., Jensen, P.E., and Hansson, A. (2007). Oxidative modifications to cellular components in plants. Annu Rev Plant Biol 58, 459-481.

Nield, J., Funk, C., and Barber, J. (2000). Supermolecular structure of photosystem II and location of the PsbS protein. Philos. Trans. R. Soc. Lond., B, Biol. Sci. **355**, 1337-1344.

Nilkens, M., Kress, E., Lambrev, P., Miloslavina, Y., Müller, M., Holzwarth, A.R., and Jahns, P. (2010). Identification of a slowly inducible zeaxanthin-dependent component of non-photochemical quenching of chlorophyll fluorescence generated under steady-state conditions in Arabidopsis. Biochim. Biophys. Acta **1797,** 466-475.

Pagliano, C., Nield, J., Marsano, F., Pape, T., Barera, S., Saracco, G., and Barber, J. (2014). Proteomic characterization and three-dimensional electron microscopy study of PSII-LHCII supercomplexes from higher plants. Biochim. Biophys. Acta **1837**, 1454-1462.

Peter, G.F., and Thornber, J.P. (1991). Biochemical composition and organization of higher plant photosystem II light-harvesting pigment-proteins. **J Biol Chem** 266, 16745-16754.

Poschmann, G., Seyfarth, K., Besong Agbo, D., Klafki, H.W., Rozman, J., Wurst, W., Wiltfang, J., Meyer, H.E., Klingenspor, M., and Stühler, K. (2014). High-fat diet induced isoform changes of the Parkinson's disease protein DJ-1. J Proteome Res **13**, 2339-2351.

Schwarz, N., Armbruster, U., Iven, T., Brückle, L., Melzer, M., Feussner, I., and Jahns, P. (2014). Tissue-specific accumulation and regulation of zeaxanthin epoxidase in Arabidopsis reflect the multiple functions of the enzyme in plastids. Plant Cell Physiol **56** 346-357.

Teardo, E., De Laureto, P.P., Bergantino, E., Dalla Vecchia, F., Rigoni, F., Szabò, I., and Giacometti, G.M. (2007). Evidences for interaction of PsbS with photosynthetic complexes in maize thylakoids. Biochim. Biophys. Acta **1767**, 703-711.

Triantaphylidès, C., Krischke, M., Hoeberichts, F.A., Ksas, B., Gresser, G., Havaux, M., Van Breusegem, F., and Mueller, M.J. (2008). Singlet oxygen is the major reactive oxygen species involved in photooxidative damage to plants. Plant physiol **148**, 960-968.

Vizcaíno, J.A., Deutsch, E.W., Wang, R., Csordas, A., Reisinger, F., Rios, D., Dianes, J.A., Sun, Z., Farrah, T., Bandeira, N., et al. (2014). ProteomeXchange provides globally coordinated proteomics data submission and dissemination. Nat Biotechnol **32**, 223-226.

Wilk L, Grunwald M, Liao P, Walla PJ, Kühlbrandt W (2013) Direct interaction of the major light-harvesting complex II and PsbS in nonphotochemical quenching. Proc Natl Acad Sci USA **110**, 5452–5456.

FIGURE LEGENDS

Figure 1. Localization of PsbS. (A) Distribution of PsbS by immunogold labelling in dark- and light-adapted WT Arabidopsis chloroplasts. Distribution calculated from Dark-N_T= 120 and Light-N_T= 265 particles (for detailed images see Fig. S1). **(B)** Sucrose gradient fractionation of thylakoids membranes (100 µg Chl) incubated for 25 min in the dark- or light-adapted state. Each band was identified according to Caffari et al (Caffarri et al., 2009). The distribution of PsbS in each fraction was analyzed by loading equal volumes from each concentrated fraction in a SDS-PAGE (SI Methods) followed by immunoblot detection. **(C)** Impact of chemical cross-linking in dark- and light-adapted thylakoids on NPQ Induction and **(D)** Zeaxanthin conversion. DTSSP was added either in the dark or after 5 min of illumination (black arrow) and the pigment content was measured after 10 min of illumination. Data represent means ± SD (n =3). Light treatments in (B - D) were performed with 825 µmol photons m^{-2} s^{-1} red light.

Figure 2. **Distribution of PsbS among different subcomplexes of the thylakoid membrane**. Isolated thylakoids from Arabidopsis WT plants were incubated for 25 min in either the dark-adapted (qE inactive) or the light-adapted (qE active) state (for further details see SI methods). For the DTSSP treatments, the cross-linker was added at a concentration of 0.042 µmol DTSSP / µg Chl. **(A)** Solubilized thylakoids equivalent to 2 µg Chl were separated by BN-PAGE and protein complexes were identified as in (Järvi et al., 2011): (I) PSII–LHCII super complexes, (II) monomeric PSI and dimeric PSII, (III) monomeric PSII and Cyt b_6f, (IV) LHCII assembly, (V) trimeric LHC, and (VI) monomeric LHC. PsbS was detected by immunoblotting after separating the protein complexes in a second dimension. In control thylakoids, PsbS was found in bands of different molecular masses in the dark-adapted state, while PsbS co-migrated predominantly with trimeric LHCII in the light-adapted state. In cross-linked thylakoids, dimeric PsbS was found only in the dark-adapted state. **(B)** Sucrose gradient fractionation of cross-linked thylakoids membranes (100 µg Chl). The distribution of PsbS and representative proteins from minor Lhc, LHCII and PSII Core complexes was analyzed by loading equal volumes from each concentrated fraction in a SDS-PAGE followed by immunoblotting. As in **(A)**, dimeric PsbS was only detectable in dark-adapted samples.

Figure 3. Protein analysis of elutes used for MS analyses. PsbS co-eluted proteins were isolated from *npq4* and WT thylakoids after chemical cross-linking in dark (D) and light (L) states and subsequently separated under native (**A** and **C**) and denaturing (**B**) conditions. **(A)** Cross-linked samples (+DTSSP) from WT thylakoids were separated by native NU-PAGE thereby conserving the DTSSP link. PsbS and Lhcb1 containing bands were identified by

immunoblotting. In the dark-adapted state, dimeric and monomeric PsbS was detectable (black arrows). However, the fraction of dimeric PsbS was rather small and its detection required fivefold increased exposure time. In the light-adapted state, the amount of both monomeric and dimeric PsbS was strongly reduced, and PsbS accumulated in complexes of higher molecular mass, which also contained Lhcb1 (*). **(B)** Elutes from npq4 and WT samples were separated by NU-PAGE after sample denaturation (DTSSP link is cleaved). For WT thylakoids, also non cross-linked samples (-DTSSP) were analyzed. Under denaturing conditions, PsbS was detected by immunoblotting mainly in monomeric form. Dimeric PsbS (*) and PsbS bound to other proteins was detectable in low amounts after increasing exposure time (*). Each lane contained 10 µl of total elutes (Material and Methods). Representative data from 5 independent experiments are shown. **(C)** 20 µl concentrated elutes from Dark–Adapted thylakoids were separated by BN-PAGE (SERVA) and PsbS detected by immunoblotting. **(D)** Relative PsbS amounts (NII) in WT elutes as determined by mass spectrometry (n=5).

Figure 4. PsbS interaction partners. The scheme illustrates the relative amounts of individual proteins co-purified with PsbS from isolated thylakoid membranes incubated either in the dark-adapted (dark) or qE-active (light) state in the presence (+) or the absence (-) of the cross-linker DTSSP. Unspecific purification of proteins was evaluated from samples of the PsbS-deficient *npq4* mutant (material and methods). Protein amounts are expressed as normalized ion intensities (i.e. label free quantification (LFQ) values) of averages from 5 independent experiments for each condition. Detailed values are listed in the Supplemental Table 1.

Figure 5. Relative amounts of PsbS interaction partners. The relative amounts of the individual proteins of LHCII trimers, Lhcb1-3, **(A, D)**, minor LHC II proteins, Lhcb4-6 **(B, E)** and PSII core proteins CP43, CP47 and D2 **(C, F)**. PsbS co-eluted proteins in the WT are shown in relation to the values in PsbS-deficient *npq4* thylakoids **(A-C)** and in relation to the PsbS content **(D-F)**, in the dark-adapted (grey bars) or the light-adapted (white bars) state. Relative amounts were calculated for each replicate using the normalized ion intensity values (NII). Data represent mean values ± SD of 5 independent biological replicates. ***Significant difference (q-value < 0.05) between dark and light ratios.

Figure 6. Model for PsbS-induced conformational changes in PSII-LHCII supercomplexes. In the dark-adapted state dimeric PsbS (blue) is supposed to interact with PSII-LHCII supercomplexes predominantly through the S-trimers of LHCII and likely also with the RC core (CP47/D2/CP43). Acidification of the lumen drives the monomerization of PsbS

which induces the detachment of trimeric LHCII from PSII core through interaction of PsbS with LHCII M-trimers. Detached and aggregated LHCII complexes likely represent the PsbS-dependent quenching site Q1 (Holzwarth et al., 2009). To what extent the detached/aggregated LHCII contains additionally the minor antenna complexes CP 24 and CP 29, cannot be judged from our data. Two possible scenarios for LHCII aggregation in the light-adapted state are shown, one containing M-trimers only and one binding additionally CP24. Other PsbS monomers might interact additionally through CP47 with the RC core. Green color of LHCII proteins indicates violaxanthin binding, orange color zeaxanthin binding. The proposed model integrates data from (Caffarri et al., 2009; Holzwarth et al., 2009; Horton, 2012; Johnson et al., 2011; Pagliano et al., 2014). For further details see text.

Figure 1

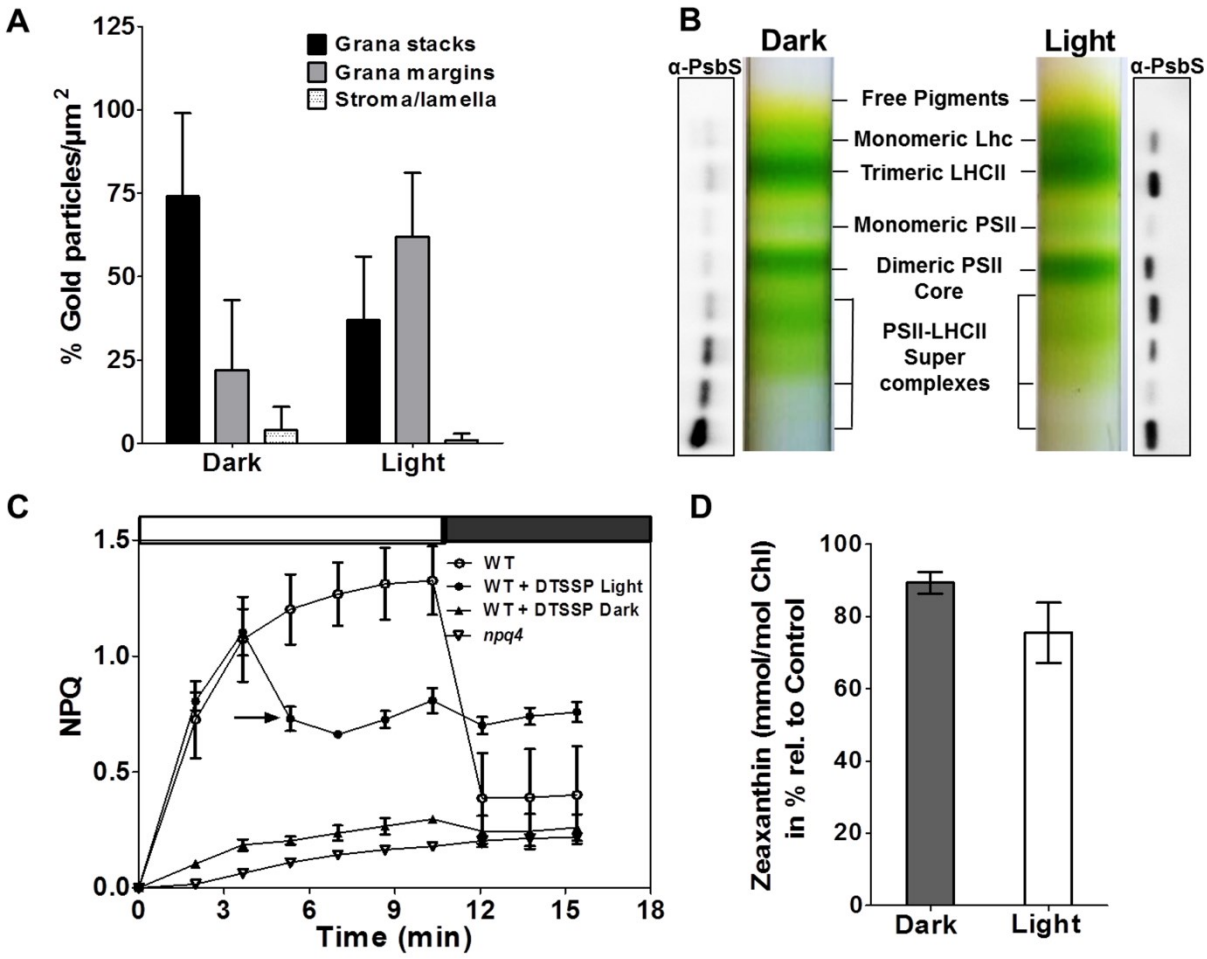
A
125
100
75
50
25
0
% Gold particles/µm 2
Grana stacks
Grana margins
Stroma/lamella
Dark
Light
B
Dark
Light
α-PsbS
α-PsbS
Free Pigments
Monomeric Lhc
Trimeric LHCII
Monomeric PSII
Dimeric PSII Core
PSII-LHCII Super complexes
C
1.5
1.0
0.5
0.0
NPQ
WT
WT + DTSSP Light
WT + DTSSP Dark
npq4
0
3
6
9
12
15
18
Time (min)
D
100
80
60
40
20
0
Zeaxanthin (mmol/mol Chl) in % rel. to Control
Dark
Light

Figure 2

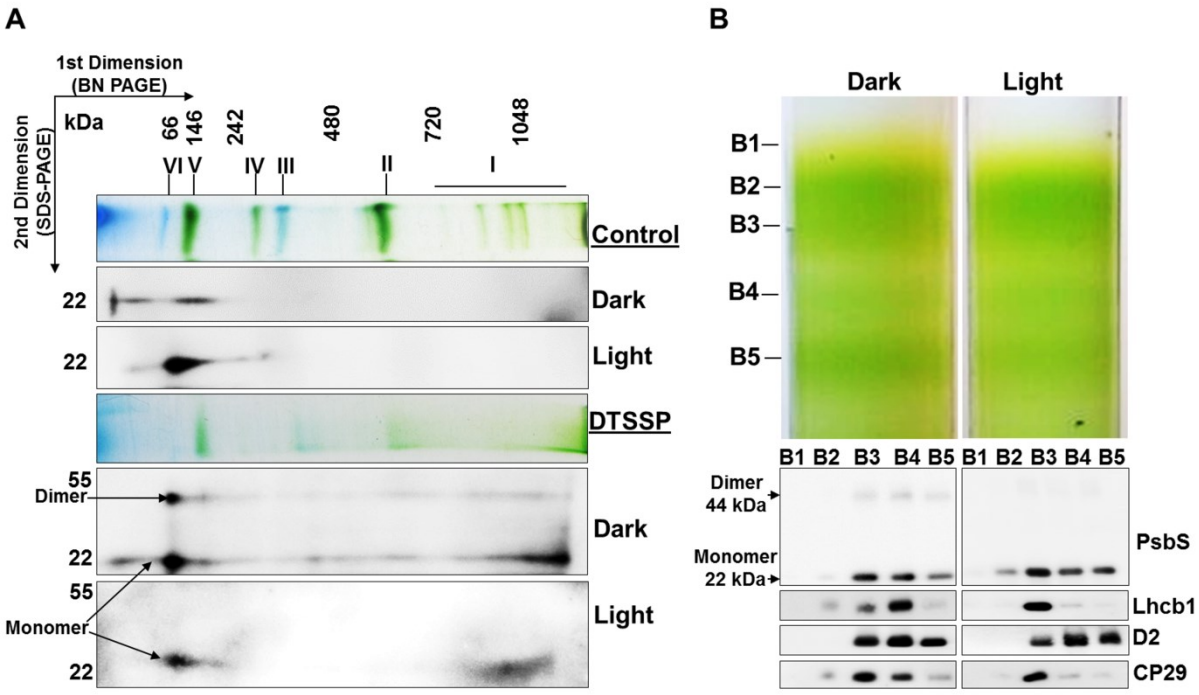
A
1st Dimension
(BN PAGE)
kDa
66
146
242
480
720
1048
VI V IV III II I
2nd Dimension
(SDS-PAGE)
Control
22
Dark
22
Light
DTSSP
55
Dimer
22
Dark
55
Monomer
22
Light
B
Dark
Light
B1
B2
B3
B4
B5
B1 B2 B3 B4 B5 B1 B2 B3 B4 B5
Dimer
44 kDa
Monomer
22 kDa
PsbS
Lhcb1
D2
CP29

Figure 3

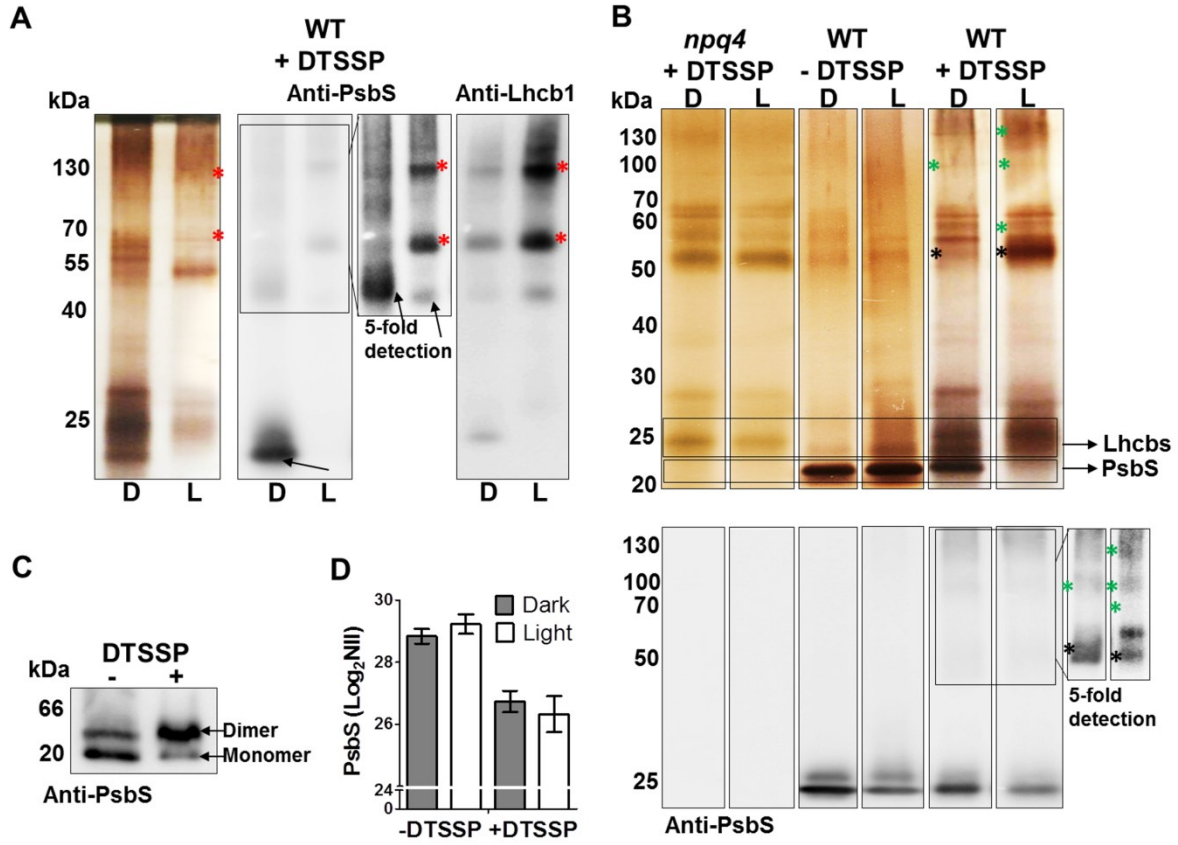
A
WT
+ DTSSP
Anti-PsbS
Anti-Lhcb1
kDa
130
70
55
40
25
5-fold
detection
D
L
B
npq4
+ DTSSP
WT
- DTSSP
WT
+ DTSSP
kDa
130
100
70
60
50
40
30
25
20
Lhcbs
PsbS
5-fold
detection
Anti-PsbS
C
DTSSP
kDa
-
+
66
20
Dimer
Monomer
Anti-PsbS
D
PsbS (Log2NII)
Dark
Light
-DTSSP
+DTSSP

Figure 4

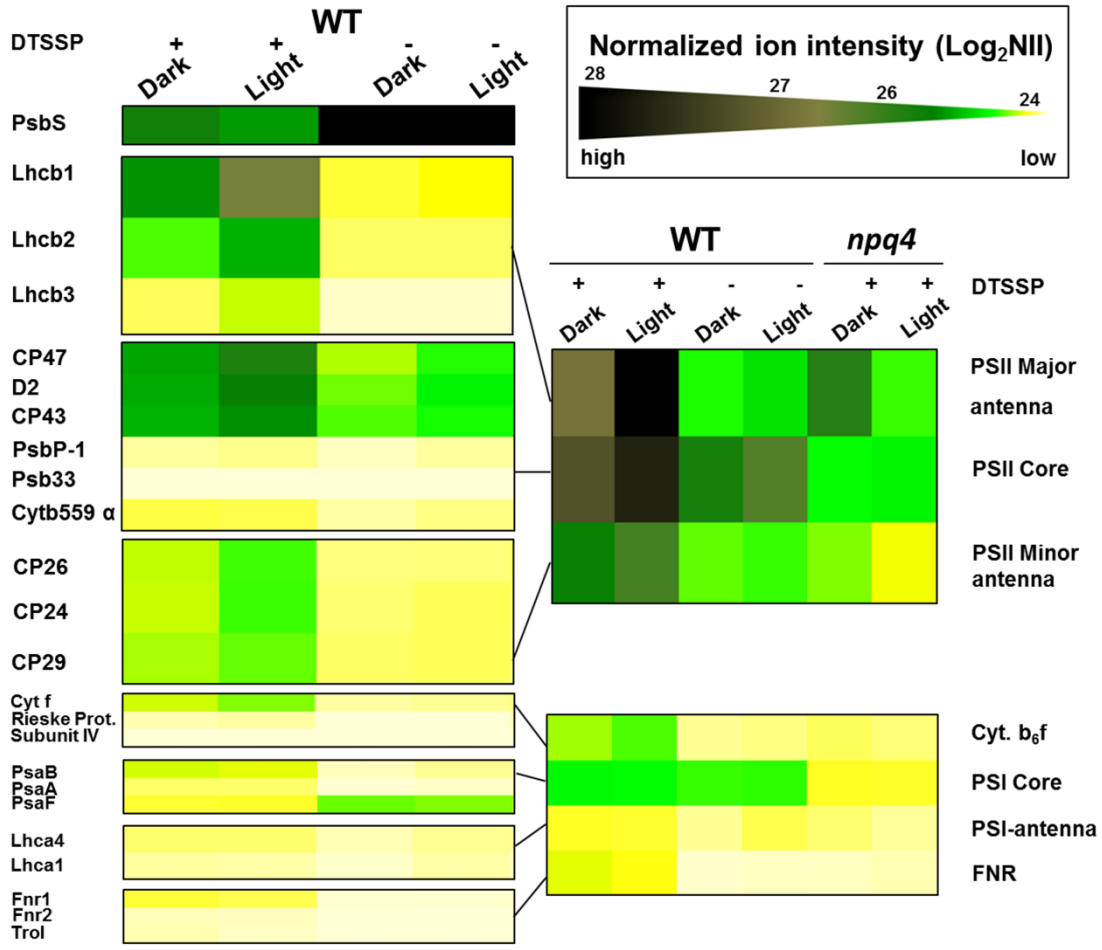
WT
DTSSP
+ Dark
+ Light
- Dark
- Light
PsbS
Lhcb1
Lhcb2
Lhcb3
CP47
D2
CP43
PsbP-1
Psb33
Cytb559 α
CP26
CP24
CP29
Cyt f
Rieske Prot.
Subunit IV
PsaB
PsaA
PsaF
Lhca4
Lhca1
Fnr1
Fnr2
Trol
Normalized ion intensity (Log2NII)
28
27
26
24
high
low
WT
npq4
DTSSP
PSII Major antenna
PSII Core
PSII Minor antenna
Cyt. b6f
PSI Core
PSI-antenna
FNR

Figure 5

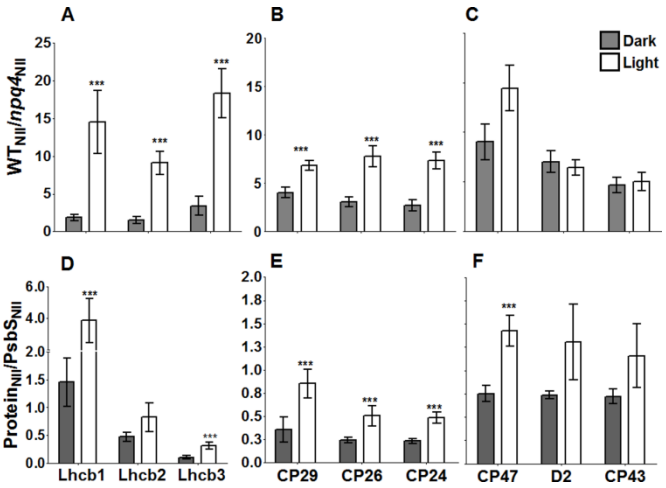
A
B
C
Dark
Light
WT_NII/npq4_NII
D
E
F
Protein_NII/PsbS_NII
Lhcb1
Lhcb2
Lhcb3
CP29
CP26
CP24
CP47
D2
CP43

Figure 6

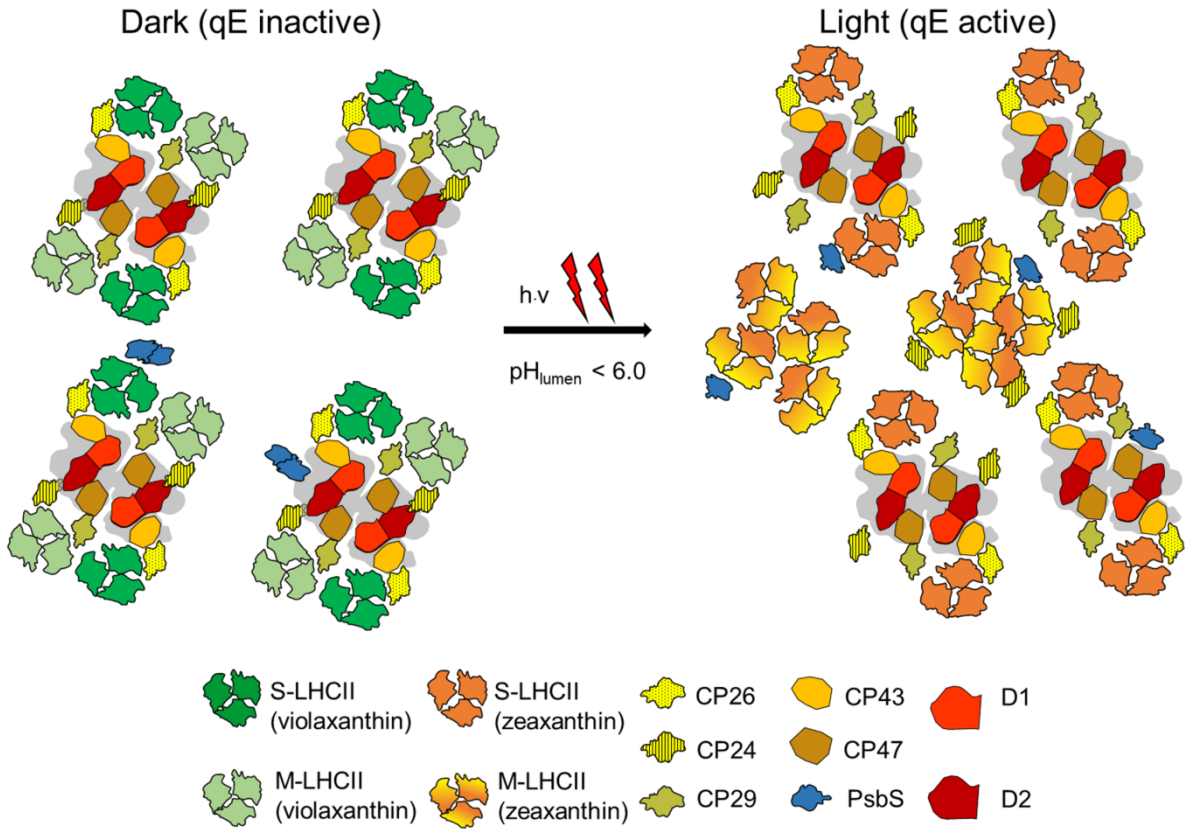
Dark (qE inactive)
Light (qE active)
h·v
pH lumen < 6.0
S-LHCII (violaxanthin)
S-LHCII (zeaxanthin)
M-LHCII (violaxanthin)
M-LHCII (zeaxanthin)
CP26
CP24
CP29
CP43
CP47
PsbS
D1
D2

SUPPLEMENTAL DATA

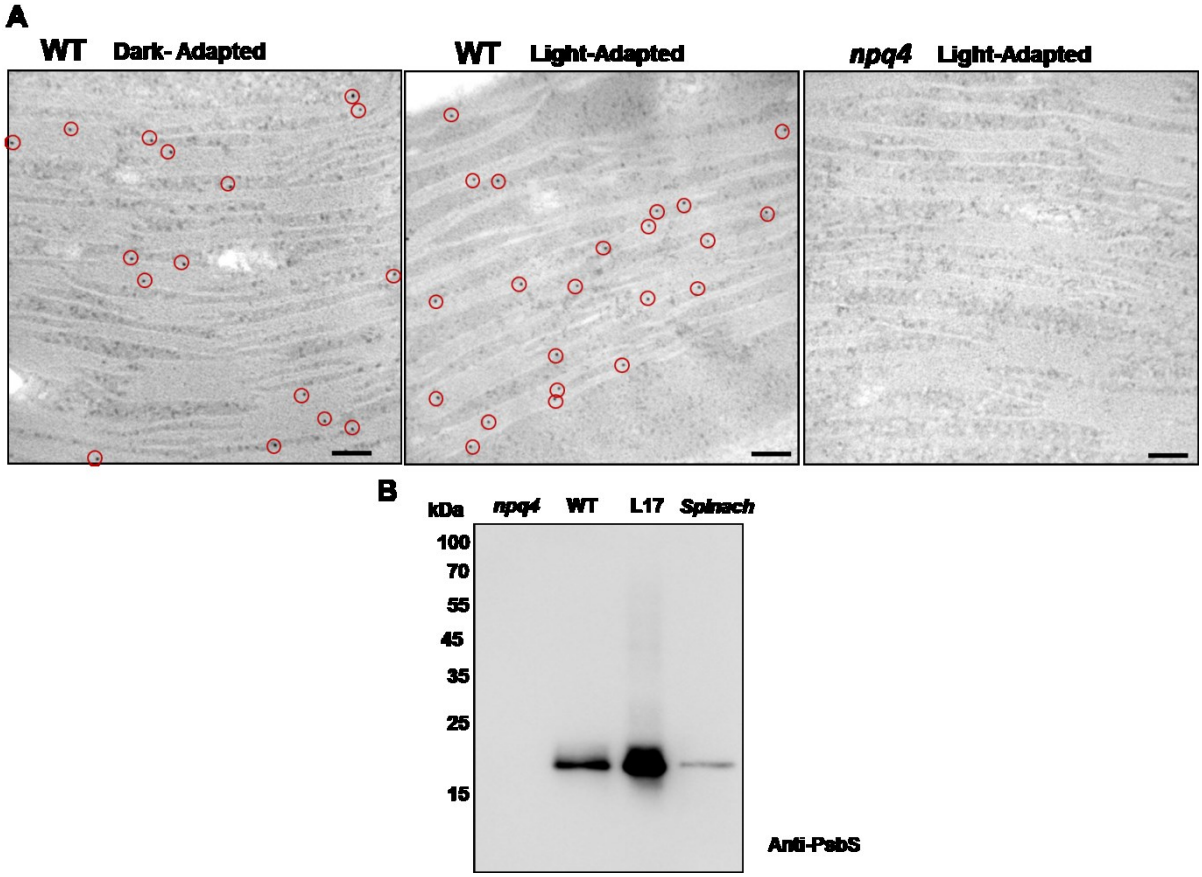

Figure S1. **Immunolocalization of PsbS in chloroplasts**. **(A)** Representative images from a total of 38 images of PsbS immunogold labeling performed in dark- and light-adapted WT Arabidopsis chloroplasts (left) and light-adapted *npq4* Arabidopsis chloroplasts (right, negative control). The gold particles are highlighted by red circles. Scale bar = 100 nm. **(B)** The antibody specificity was confirmed by western blot analysis of isolated thylakoids (10 µg Chl loaded) from the PsbS-deficient mutant *(npq4*), WT Col-0 and the PsbS overexpressing line *L17*.

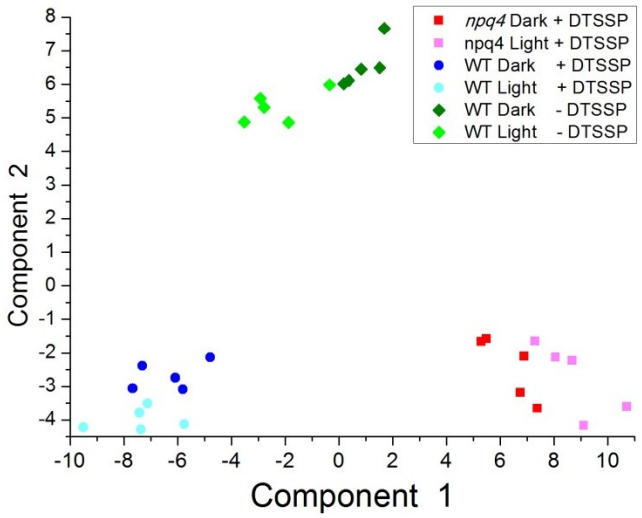

Figure S2. **Principal component analysis (PCA) of MS data from individual Co-PsbS immunoprecipitation samples**. Relative mass spectrometric intensity on protein level was used as input for PCA calculation. Individual samples are marked by circles (WT samples with DTSSP), squares (*npq4* samples with DTSSP) and diamonds (WT samples without cross-linker). Principal component 1 explains 50 % and principal component 2 25 % of the total variance.

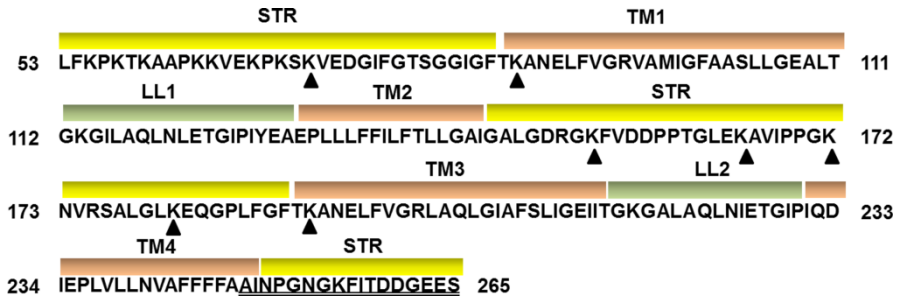

Figure S3. **PsbS sequence showing DTSSP binding sites and the antibody epitope**. The DTSSP modified lysine residues (= DTSSP binding sites) are marked with black triangles. The epitope which is recognized by the antibody is indicated by the underlined sequence. Stroma exposed regions (STR), trans membrane helices (TM) and luminal loops (LL) were predicted from (Fan et al., 2015; Li et al., 2000).

Supplemental Table 1. PsbS co-purified proteins. Proteins are enlisted according to their normalized ion intensity (i.e. relative amount) from higher to lower abundant proteins within each complex. Intensity ratios between WT and *npq4* samples express the values present in all WT samples i.e. including values from eluted proteins in thylakoids with and without cross-linking. Intensity values for PsbS co-purified proteins but excluded as plausible interaction partners during qE induction are also included (below black line).The reported q values include the correction by the method of Benjamini and Hochberg. Mean values from 5 independent experiments are given. ** Proteins without a DTSSP modification in cross linked samples.

Complex/ Function	Protein	Protein identification data			Normalized ion intensity (Log_2 NII)						Ratios NII		q Values		
		Unique peptides	Razor + unique peptides	Peptides	*npq4* Dark + DTSSP	*npq4* Light + DTSSP	WT Dark - DTSSP	WT Dark + DTSSP	WT Light - DTSSP	WT Light + DTSSP	Light WT/*npq4*	Dark WT/*npq4*	WT/*npq4*	WT + DTSSP Light/dark	WT - DTSSP Light/dark
	PsbS	18	18	18	----	----	28.9	26.8	29.3	26.4	----	----	1E-08	0.99	0.44
PSII-Major antenna	Lhcb1.1. 1.2. 1.3	5	16	16	25.8	24.7	23.9	26.5	24.3	27.5	7.0	1.6	3E-05	0.51	0.30
	Lhcb1.5	0	4	15	25.2	22.1	24.1	26.1	24.7	26.8	26.0	1.9	4E-06	0.51	0.20
	Lhcb2	1	8	13	24.8	23.2	23.4	25.3	23.5	26.3	8.2	1.4	2E-04	0.51	0.44
	Lhcb3	7	7	8	22.2	20.7	21.2	23.5	21.1	24.7	15.9	2.5	2E-06	0.51	0.44
PSII Core	CP47	24	24	24	23.4	23.0	24.8	26.4	25.5	26.9	14.3	7.5	1E-10	0.51	0.14
	D2	13	13	13	23.6	24.0	25.1	26.3	25.7	26.7	6.2	6.5	1E-11	0.52	0.09
	CP43	20	20	20	24.2	24.3	25.3	26.3	25.5	26.5	4.5	4.2	5E-09	0.56	0.23
	D1**	8	8	8	21.9	21.8	23.1	23.8	23.5	24.1	5.2	3.7	3E-07	0.51	0.23
	PsbP-1	11	11	11	21.9	21.9	21.7	22.6	22.6	22.9	2.1	1.6	2E-03	0.51	0.01
	Cyt_{b559} β**	2	2	2	18.8	19.0	19.6	20.8	20.6	21.2	4.7	3.9	3E-06	0.46	0.04
	Cyt_{b559} α	2	2	2	20.6	21.6	22.5	23.8	23.1	23.7	4.4	9.0	6E-09	0.97	0.08
	Psb33	12	12	12	18.8	17.8	19.0	19.3	19.6	19.6	3.5	1.4	9E-06	0.51	0.08
PSII- Minor antenna	CP29.2	18	21	21	23.0	22.6	23.4	24.9	23.5	25.2	6.0	3.7	3E-09	0.56	0.34
	CP24	18	18	18	23.1	22.4	23.3	24.7	23.5	25.4	7.8	2.8	2E-08	0.52	0.20
	CP26	24	24	24	23.5	22.5	23.1	24.7	23.1	25.3	7.1	2.4	1E-07	0.54	0.34
	CP29.1	12	12	15	22.4	21.7	22.8	24.2	23.1	24.5	6.9	3.6	1E-09	0.63	0.18
	CP29.3	7	7	8	19.1	17.7	20.4	21.4	20.8	21.8	17.2	5.0	3E-07	0.40	0.12
Cytocrome b_6f	Cyt f	30	30	30	23.0	22.9	22.5	24.6	22.8	25.1	4.6	3.2	2E-07	0.63	0.21
	Rieske Protein	10	10	10	21.8	20.6	19.9	22.1	20.4	22.5	3.8	1.2	6E-05	0.63	0.14
	Subunit IV	2	2	2	18.8	18.8	18.5	20.1	17.8	19.5	1.6	2.4	5E-04	0.56	0.91
PSI Core	Psaf	14	14	14	23.4	23.1	25.2	23.9	25.1	24.0	1.9	1.4	3E-03	0.99	0.65
	PsaB	16	16	16	21.9	22.4	22.0	24.6	22.8	24.5	4.2	6.5	1E-09	0.99	0.08
	PsaA	13	13	13	20.9	21.2	21.0	23.4	21.6	23.4	4.7	5.8	5E-09	0.99	0.08
PSI-Antenna	Lhca4	13	13	13	22.7	22.1	22.0	23.4	22.8	23.3	2.3	1.6	2E-03	0.82	0.03
	Lhca1	8	8	8	21.8	21.0	21.3	22.6	22.5	22.4	2.7	1.7	1E-03	0.99	0.02
FNR	Fnr1	23	27	27	21.2	21.9	20.5	23.9	20.8	23.6	3.2	6.2	6E-08	0.99	0.34
	Fnr2	16	16	20	18.7	18.9	18.4	21.8	19.3	21.7	7.0	8.3	2E-10	0.99	0.13
	Trol	14	14	14	18.3	16.9	18.4	22.1	18.9	21.3	21.3	13.8	6E-12	0.77	0.21
PGR	Pgr5-Like	9	10	10	18.8	18.4	19.6	20.9	19.9	20.4	4.0	4.6	2E-11	0.52	0.16

Supplemental Table 1 (Cont.). PsbS co-purified proteins. Proteins are enlisted according to their normalized ion intensity (i.e. relative amount) from higher to lower abundant proteins within each complex. Intensity ratios between WT and *npq4* samples express the values present in all WT samples i.e. including values from eluted proteins in thylakoids with and without cross-linking. Intensity values for PsbS co-purified proteins but excluded as plausible interaction partners during qE induction are also included (below black line).The reported q values include the correction by the method of Benjamini and Hochberg. Mean values from 5 independent experiments are given. ** Proteins without a DTSSP modification in cross linked samples.

Complex/ Function	Protein	Protein identification data			Normalized ion intensity (Log_2 NII)						Ratios NII		q Values		
		Unique peptides	Razor + unique peptides	Peptides	*npq4* Dark + DTSSP	*npq4* Light + DTSSP	WT Dark - DTSSP	WT Dark + DTSSP	WT Light - DTSSP	WT Light + DTSSP	Light WT/*npq4*	Dark WT/*npq4*	WT/*npq4*	WT + DTSSP Light/dark	WT - DTSSP Light/dark
Ca^{++} Receptor	CaS	31	31	31	22.6	21.3	24.4	24.2	24.9	23.7	5.5	2.9	3.0E-06	0.63	0.25
Pigment Synthesis	Ptac16	41	41	41	21.8	20.6	23.5	24.5	24.4	23.5	7.4	6.5	3.7E-09	0.51	0.16
	AT1G74470.1	24	24	24	20.1	19.1	21.6	22.7	22.2	22.4	10.2	6.0	9.7E-10	0.63	0.20
FTSH Proteases	FtsH2	20	42	42	19.4	17.4	20.4	22.3	21.4	22.9	44.9	7.6	6.3E-12	0.52	0.08
	FtsH5	13	36	36	19.7	19.0	20.7	22.5	21.6	22.9	14.7	6.9	9.6E-11	0.55	0.08
Oxidative Stress	Dde2	39	39	39	19.8	19.9	21.9	22.3	22.2	22.4	5.5	5.6	2.5E-09	0.63	0.23
	AT3G26070.1	9	12	12	17.0	16.8	17.8	21.3	19.3	20.8	15.5	19.7	8.4E-09	0.99	0.06
	Apx4	15	15	15	19.6	20.0	19.2	20.6	20.0	20.6	1.5	2.0	2.8E-06	0.63	0.08
Photosynthesis Acclimation	Ape1	15	15	15	19.0	17.9	20.0	20.5	20.2	20.7	7.1	2.8	1.7E-09	0.52	0.23
Membrane biogenesis	Thf1	13	13	13	17.3	18.0	19.1	19.2	18.3	19.2	2.4	3.6	1.1E-05	0.63	0.34
Tic/Toc	TIC 62	22	22	22	19.6	18.9	18.9	21.1	19.1	20.4	3.0	2.7	6.2E-05	0.63	0.34
Unknown	AT4G35250.1	16	16	16	19.2	18.3	20.4	20.6	21.2	20.4	4.3	2.6	1.2E-08	0.99	0.13
	Enh1	9	9	9	19.1	18.4	19.5	19.8	19.2	19.5	2.2	1.6	3.2E-03	0.52	0.65
Transporter	KEA3	7	7	7	-----	-----	15.6	17.8	16.0	17.0	-----	-----	2.3E-07	0.07	-----
PSI	PGRL1B	3	3	4	-----	-----	15.6	16.3	15.6	16.0	-----	-----	2.0E-04	0.70	-----
PSII Core	PsbP	3	3	3	-----	-----	15.1	15.1	16.1	16.3	-----	-----	9.2E-04	0.00	-----

Expression of the PsbS Protein upon High Light Acclimation in *Chlamydomonas reinhardtii*

Viviana Correa Galvis[a], Petra Redekop[a], Annika Grieß[a] , Viktor Koch[a], Ben Lucker[b], David Kramer[b], Krishna K. Niyogi[c,d], and Peter Jahns[a]

[a]Plant Biochemistry, Heinrich-Heine-University Düsseldorf, 40225 Düsseldorf, Germany

[b]Department of Plant Biology and Plant Research Laboratory, Michigan State University, East Lansing, Michigan 48824,USA

[c]Department of Plant and Microbial Biology, Howard Hughes Medical Institute, University of California, Berkeley, CA 94720-3102, USA

[d]Physical Biosciences Division, Lawrence Berkeley National Laboratory, Berkeley, CA 94720, USA

ABSTRACT

Non-photochemical quenching (NPQ) of excess excitation energy is an important photoprotective mechanism active in photosynthetic organisms. In *Arabidopsis thaliana,* NPQ is a constitutive mechanism and depends on the PsbS protein. In the green algae *Chlamydomonas reinhardtii,* NPQ has to be activated upon high light acclimation and essentially requires the accumulation of the LHCSR proteins. Expression of the PsbS protein in *C. reinhardtii* has not been reported so far. In this work, we show that PsbS is a light induced protein in *C. reinhardtii*, whose accumulation under high light is further controlled by CO_2 availability. PsbS accumulated after several hours of high light illumination at low CO_2. At high CO_2, however, PsbS was only transiently expressed under high light and was degraded after 1 h of high light exposure. PsbS accumulation correlated with an enhanced NPQ capacity in high light acclimated cells grown at low CO_2. However, PsbS could not compensate the function of LHCSR in LHCSR-deficient mutants. Our data suggest that PsbS might be involved in the regulation of the qE capacity in *C. reinhardtii* by promoting conformational changes required for NPQ activation in the antenna of photosystem II, similar to its counterpart in land plants.

INTRODUCTION

Sunlight is the ultimate energy source for photosynthesis. Although efficient light absorption and utilization is essential for efficient photosynthesis, the absorption of light energy in excess of efficient utilization for photosynthesis may lead to the production of reactive oxygen species which cause generate cell damage (Møller et al., 2007). Oxygenic photosynthesis has evolved from cyanobacteria (and other prokaryotes) to eukaryotes (Blankenship and Hartman, 1998) along with photoprotective mechanisms allowing the quenching of excess energy (Niyogi and Truong, 2013). One of the most important and pervasive mechanisms of minimizing photo-oxidative damage by excess light energy is the harmless de-activation of singlet excited chlorophylls in the light harvesting antenna as heat, known as non-photochemical quenching (NPQ). NPQ is composed of different components, with the so-called qE-component being the dominant mechanism under most natural conditions (Nilkens et al., 2010). The qE mechanism is strictly regulated by changes in the ΔpH across the thylakoid membrane and thus operates on a very short time scale allowing a rapid response of the photosynthetic machinery to rapid changes in light intensities (Kulheim et al., 2002; Li et al., 2000). Although the function of qE is the same in all organisms carrying out oxygenic photosynthesis, the underlying mechanisms differ among the Chlorophyta clade (Goss and Lepetit, 2015). In the green algae *Chlamydomonas reinhardtii*, qE depends on light induced accumulation of the LHCSR proteins, specifically LHCSR3 (Peers et al., 2009). LHCSR3 is a pigment binding member of the LHC family that is activated via protonation of a C-terminus subdomain upon acidification of the lumen, allowing for the reversible switch from a light harvesting to a dissipative state (Bonente et al., 2011; Liguori et al., 2013). In land plants, the qE mechanism differs between vascular and non-vascular plants. In the moss *Physcomitrella patents*, qE is independently and additively activated by two types of proteins: LHCSRs (as in green algae) and PsbS, a non-pigment binding protein from the LHC family (Alboresi et al., 2010; Gerotto et al., 2012). Both proteins are activated in parallel by changes in the luminal pH, but contrary to *C. reinhardtii* (Anwaruzzaman et al., 2004; Niyogi et al., 1997), pH-regulated synthesis of zeaxanthin from violaxanthin also significantly contributes to qE. In particular zeaxanthin binding to LHCSR enhances the LHCSR-dependent qE capacity (Pinnola et al., 2013). PsbS, on the other hand, is supposed to enhance the quenching of excess energy by direct interaction with LHCII trimer proteins (Gerotto et al., 2015). In vascular plants, qE activation essentially requires pH-regulated activation of PsbS by protonation of two glutamate residues at its two luminal loops (Fan et al., 2015; Li et al., 2000; Li et al., 2004) and is further modulated by zeaxanthin synthesis (Niyogi et al., 1998). The qE mechanism has been vastly studied in *A. thaliana*, being a model organism for the study of energy dissipation mechanisms since the essential role of PsbS in qE activation was described (Li et al., 2000). In the current model for qE activation, dimeric PsbS monomerizes

upon acidification of the lumen (= active PsbS) and by that facilitates conformational changes in the LHCII-PSII supercomplexes, thereby promoting aggregation of LHCII. These changes, along with the synthesis of zeaxanthin, lead to activation of the quenching state in PSII-LHCII complexes (Bergantino et al., 2003; Johnson et al., 2011; Morosinotto et al., 2002; Xu et al., 2015) (see also manuscript 2).

A. thaliana PsbS homologs have been found in several lineages of green algae (Anwaruzzaman et al., 2004; Bonente et al., 2008; Teramoto et al., 2002). Transcriptomic analysis have revealed that mRNA levels of the two PsbS encoding genes in *C. reinhardtii* (*PSBS1* and *PSBS2*) are upregulated upon nitrogen starvation (Miller et al., 2010) and after a shift from low to higher light intensities (Mettler et al., 2014). However, expression and accumulation of the PsbS protein has not been reported so far, and earlier work showed that over-expressed PsbS does not localize to the thylakoid membrane in *C. reinhardtii* (Bonente et al., 2008). In this work, we show that PsbS transiently accumulates in *C. reinhardtii* during high light acclimation and that the accumulation and degradation of PsbS is regulated by CO_2 availability. Our data suggest that PsbS regulates the activation of the qE capacity elicited by the LHCSR protein upon high light acclimation in *C. reinhardtii.*

RESULTS

Constitutive expression of the PsbS protein

Based on the predicted PsbS protein sequence (Anwaruzzaman et al., 2004), we designed an antibody that specifically recognizes PsbS of *C. reinhardtii*. The antibody binds to the C-terminal sequence of the protein and its reactivity was confirmed by immunodetection of recombinant *Cr*PsbS (Fig. 1A, C). The antibody showed no cross reaction with the *A. thaliana* PsbS (Fig. 1B).

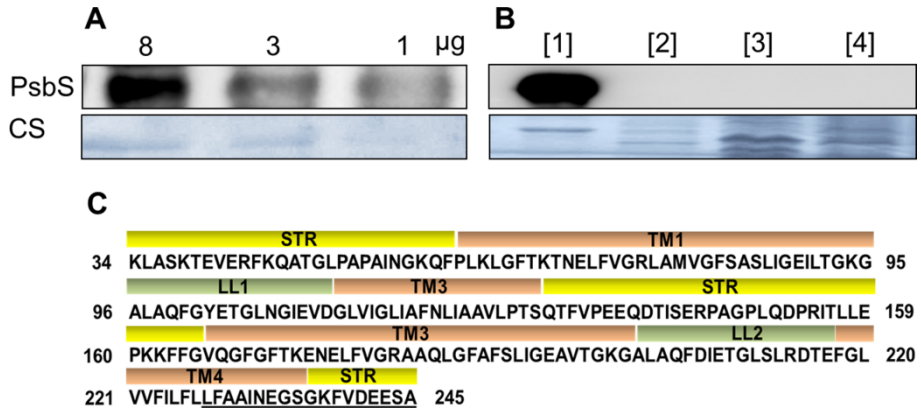

Figure 1. Immunoblot detection of the PsbS protein. **(A)** Immunodetection of recombinant PsbS (r-*Cr* PsbS) by the anti-PsbS antibody raised against the C-terminal peptide of *C. reinhardtii* PsbS. **(B)** Reactivity of the PsbS antibody to [1] r-*Cr* PsbS from *E.coli* cells, [2] *C. reinhardtii* WT cells (2.9 x 10^5 cells grown under low light in TAP media), [3] thylakoids isolated from *C. reinhardtii* cells (10 µg chlorophyll, cells grown as in [2]), and [4] thylakoids isolated from *A. thaliana* (10 µg chlorophyll). The r-*Cr* PsbS signal was detected after 1-2 sec of exposure to the chemioluminescence reagent. CS: Coomassie staining. **(C)** *Cr* PsbS sequence according to (Anwaruzzaman et al., 2004) shows the binding site of the antibody (underlined). (STR) Stroma exposed regions; (TM) transmembrane helices; (LL) luminal loops.

According to the information available at the transcript level, PsbS mRNA increased upon nitrogen starvation under mixotrophic growth (Miller et al., 2010) and after transferring autotrophically grown cells from lower to higher, non-saturating light (Mettler et al., 2014). In order to identify specific conditions that trigger constitutive expression of the PsbS protein, we designed an experiment combining different light conditions, C and N availabilities. Cells were grown under low light (LL) or high light (HL), under either mixotrophic (TAP medium with acetate as a carbon source) or autotrophic (high salt medium – HS) conditions, and in the presence or absence of a nitrogen source. In wild-type cells (WT), PsbS was constitutively expressed in HL acclimated cells grown under photoautotrophic conditions and PsbS accumulation was reduced upon nitrogen starvation (Fig. 2A). No PsbS protein was detected in LL-grown cells or in mixotrophically-grown cells (Fig. 2A). The amount of PsbS protein, however, was obviously lower compared to other members of the LHCII PSII complexes, since PsbS could only be detected by immunoblot analysis when the amount of

total protein loaded on the gel was increased to 40 µg of total protein instead of 5 µg for other proteins (Fig. 2).

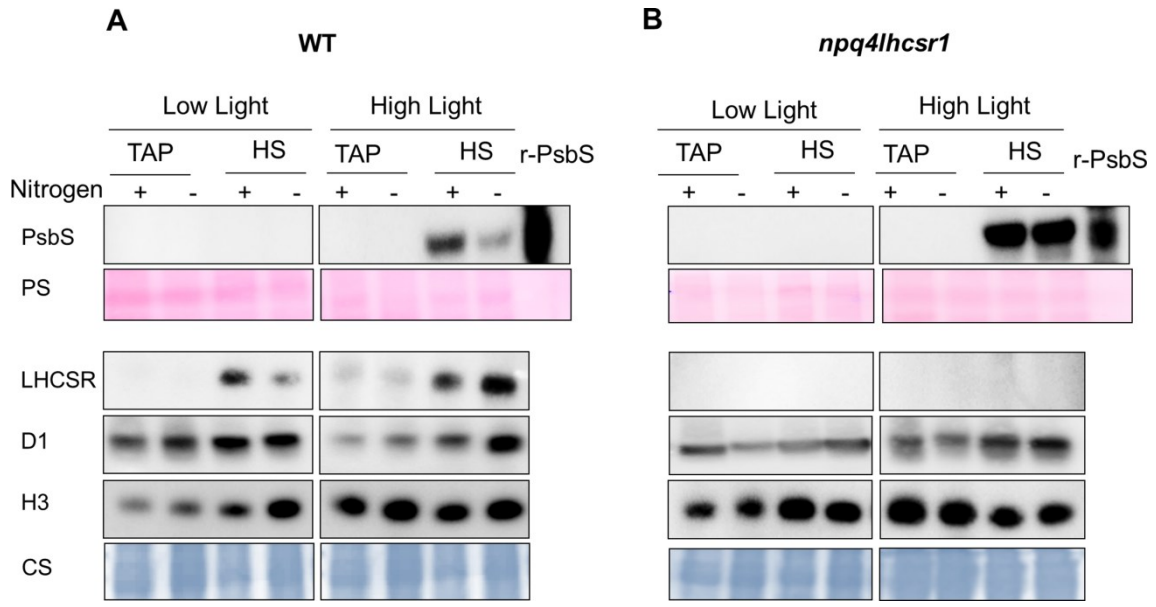

Figure 2. PsbS expression under different light, carbon, and nitrogen conditions. Cells were grown under LL (30 µmol photons m^{-2} s^{-1}) or HL (480 µmol photons m^{-2} s^{-1}) in either TAP (containing acetate as a carbon source) or HS medium (low carbon). Each growth condition was tested in presence (+N) or absence (-N) of nitrogen by depriving the cells for 48 h in a medium without NH_4^+. **(A)** WT ($4A^+$). **(B)** *npq4lhcsr1* mutant. 40 µg of total protein was loaded in each lane for PsbS detection, and 5 µg for LHCSR, D1 and Histone H3 detection. As a positive control, 0.2 µg of recombinant *Cr* PsbS (r-PsbS) were additionally loaded. The PsbS signal was detected after 60 sec of exposure to the chemoluminescence reagent. CS: Coomassie staining; PS: Ponceau staining.

In *C. reinhardtii*, NPQ is a light-dependent process activated only in photoautotrophically-grown cells acclimated to HL (Finazzi et al., 2006; Peers et al., 2009). The level of ΔpH-dependent quenching (qE) requires mainly the light-induced expression of the LHCSR3 protein and to a lower extent the equally light dependent expression of the LHCSR1 protein (Peers et al., 2009). Since also PsbS is exclusively expressed under strictly HL conditions, PsbS expression might be correlated with the quenching capacity. To address this hypothesis we analyzed protein expression under all the different conditions as previously described (Peers et al., 2009). In the *npq4lhcsr1* double mutant, where the qE response was completely impaired (Fig. 3), PsbS was more strongly expressed in the *npq4lhcsr1* mutant compared to the WT and it was not degraded upon nitrogen starvation (Fig. 2B). Consequently, the light-induced expression and accumulation of PsbS does not depend on the accumulation of LHCSR proteins, but was enhanced in their absence. Nonetheless, this PsbS increase could not compensate and/or complement the function of LHCSR, since no NPQ induction was observed in the *npq4lhcsr1* mutant under conditions leading to PsbS expression (Fig. 3). Therefore, although PsbS expression was induced by HL, the accumulation of PsbS was not sufficient for qE induction.

Additionally, LHCSR amounts were higher under photoautotrophic conditions (HS medium) in both LL and HL grown cells compared to cells grown under mixotrophic conditions (TAP medium) in HL. However, NPQ induction was only triggered under HL growth (Fig. 3) (Peers et al., 2009) and was slightly higher upon nitrogen starvation (Fig. 3). These findings are in agreement with earlier observations that NPQ induction in *C. reinhardtii* is not only a HL dependent mechanism (Allorent et al., 2013; Iwai et al., 2007) but is also regulated by photosynthetic activity and CO_2 availability. The latter is likely a result of the CO_2 regulated expression of LHCSR proteins (Allorent et al., 2013; Iwai et al., 2007; Maruyama et al., 2014; Yamano and Fukuzawa, 2009).

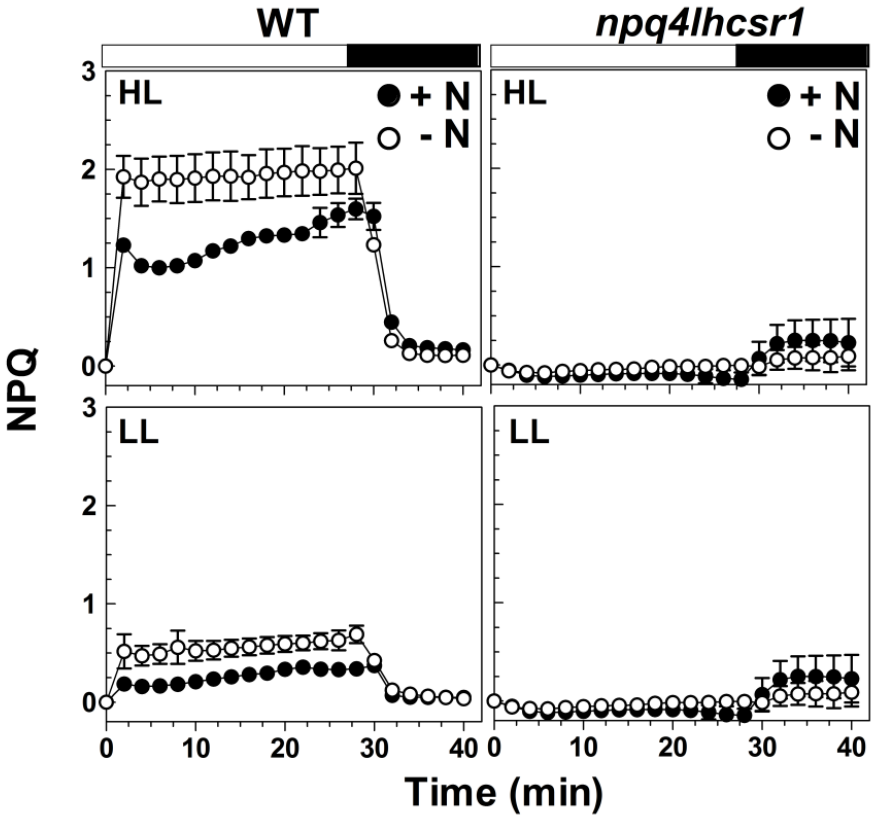

Figure 3. NPQ induction in cells grown under different light, carbon, and nitrogen conditions. WT (4A$^+$) and *npq4lhcsr1 c*ells were grown under low light (LL, 30 µmol photons m^{-2} s^{-1}) or high light (HL, 480 µmol photons m^{-2} s^{-1}) in HS medium until reaching the exponential phase. Cells were then separated and resuspended in media with (+N) or without (-N) nitrogen (NH_4^+) for additional an 48 h. Chlorophyll a fluorescence was subsequently measured by resuspending 2 x 10^7 cells in 1 ml fresh HS media, followed by 15 min incubation in the dark. Values represent mean ± SD (n =3 biological replicates).

Regulation of protein expression by carbon availability under high light acclimation

The responses of *C. reinhardtii* to HL are commonly studied by transferring LL grown cells to HL, thus simulating long-term acclimation to HL upon increases in light intensities in aquatic environments. Monitoring the constitutive expression of PsbS (and other proteins) under constant HL growth may thus not be an appropriate system to study the function of this

protein, since it might reflect changes in cell metabolism in response to extreme irradiance, but not adaptive changes to HL. In *C. reinhardtii*, *PSBS* mRNA is transiently upregulated upon transition from lower to higher light intensities (Mettler et al., 2014). Hence, if the PsbS protein has a role in adaptive responses to higher light intensities, it can be expected that changes in the protein expression must also be light-activated. Additionally, the energy quenching capacity in *C. reinhardtii* also depends on CO_2 availability (Maruyama et al., 2014; Minagawa and Tokutsu, 2015). Thus, if the function of PsbS is related to the activation of qE capacity under HL, changes in its expression patterns in CO_2 concentration dependent manner are expected. To address these questions, WT and *npq4lhcsr1* cells were grown in photoautotrophic media under LL under different carbon regimes. These regimes are, for the purpose of this study, defined as: low CO_2 (no additional CO_2 input into the media), ambient CO_2 (supplied by air bubbling in the media) and high CO_2 (bubbling with air containing 5 % CO_2). After reaching an exponential phase, cultures were transferred to HL, and the accumulation of PsbS and other proteins was analyzed by immunoblotting at different time points after HL illumination (Figs. 4 and 5).

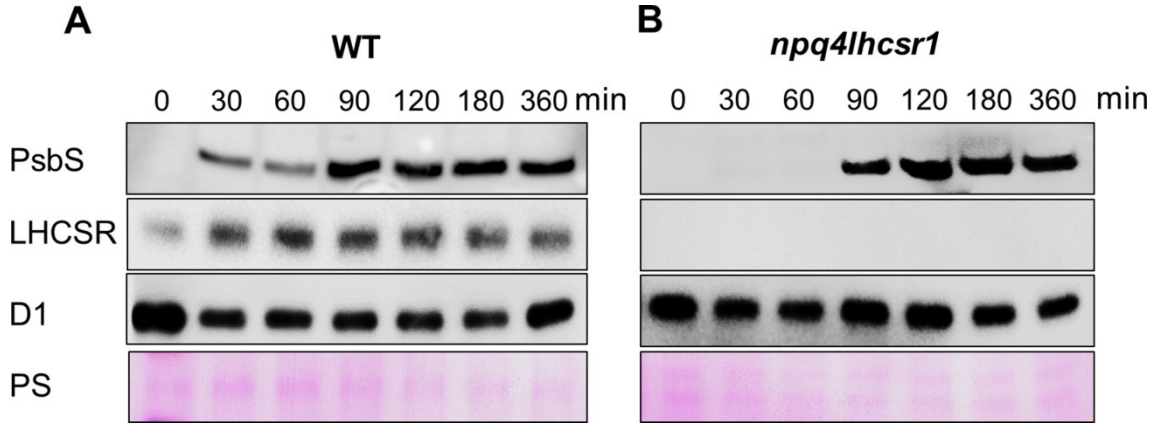

Figure 4. Protein expression in cells grown at low CO_2 after transfer to high light. **(A)** WT (dw15.1) and **(B)** *npq4lhcsr1* cells were grown in HS medium in low light (30 µmol photons m^{-2} s^{-1}) and low CO_2 (no additional air input) until reaching exponential growth (5 x 10^6 cells/ml). Cell cultures were transferred to high light (480 µmol photons m^{-2} s^{-1}) and equal culture volumes were used for protein extraction after 0, 30, 60, 90, 120, and 360 min of HL exposure. For immunoblot analysis of PsbS, 40 µg total protein were loaded onto the gels, while 5 µg were used for the other proteins. PS: Ponceau staining.

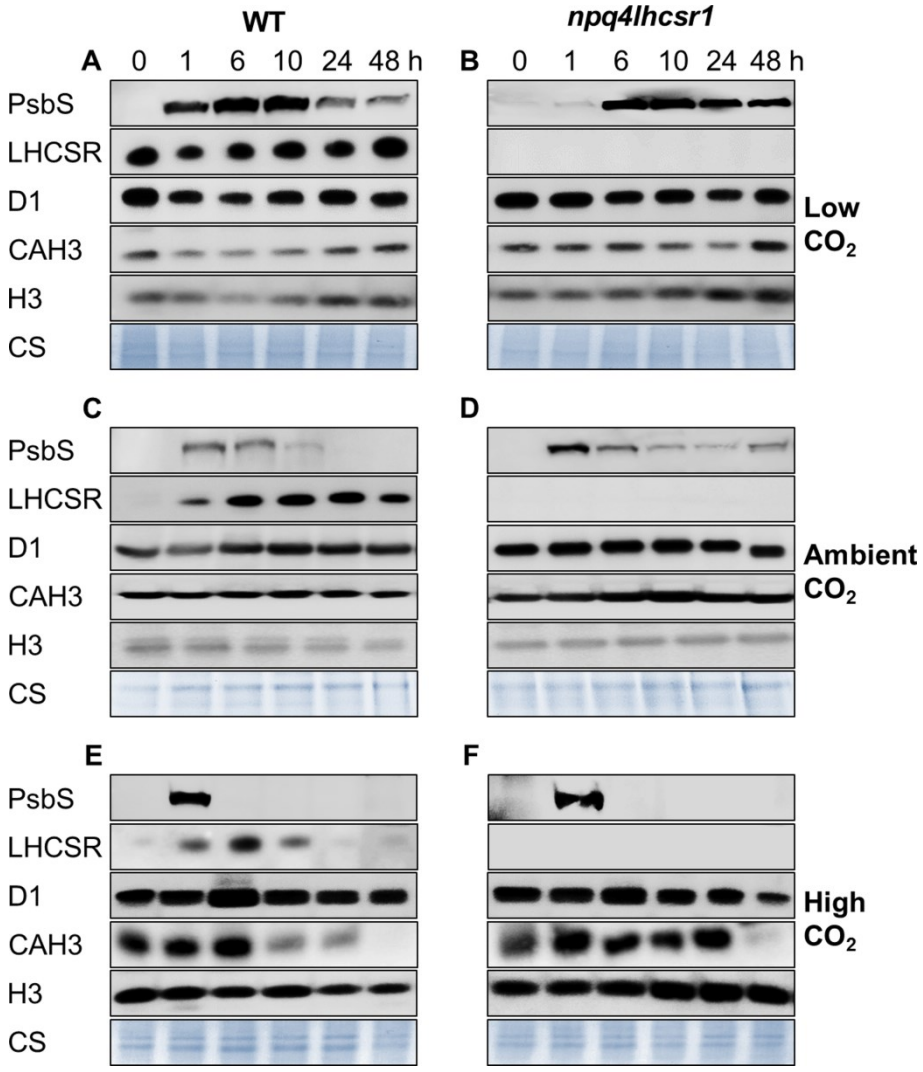

Figure 5. Protein expression after transfer to high light in cells grown at different CO_2 concentrations. WT ($4A^+$) **(A, C, E)** and *npq4lhcsr1* **(B, D, F)** cells were grown in HS medium under low light (30 µmol photons m^{-2} s^{-1}) at either **(A, B)** low CO_2 (no additional air input), **(C, D)** ambient CO_2 (bubbling with air) or **(E, F)** high CO_2 (bubbling with air containing 5 % CO_2). After reaching a cell density of 5 x 10^6 cells/ml, cultures were transferred to high light (480 µmol photons m^{-2} s^{-1}) and equal culture volumes were taken for protein extraction at 0, 1, 6, 10, 24, and 48 h after transfer to HL. For immunoblot analysis of PsbS, 40 µg total protein were loaded onto the gels, while 5 µg were used for the other proteins. Coomassie staining (CS) and the Histone 3 protein (H3) were used as loading controls for each time point.

The expression of PsbS was induced in WT and *npq4lhcsr1* mutant cells within 30 to 90 min after transfer of cells to HL, independent of the CO_2 concentration in the medium (Figs. 4 and 5). However, the PsbS content did not remain at a constant level, but decreased at longer HL exposure time, and the dynamics of PsbS accumulation showed a pronounced dependence on the CO_2 concentrations (Fig. 5). In WT and *npq4lhcsr1* cells grown under low CO_2, PsbS expression reached maximum levels after about 10 h and decreased to lower levels after 48 h of HL exposure (Fig. 5 A, B). At ambient CO_2 concentrations, maximum PsbS levels accumulated between 1 and 6 h after HL illumination. In WT cells, PsbS

disappeared completely after 24 h, while low levels of PsbS were retained up to 48 h in *npq4lhcsr1* mutant cells (Fig. 5 C, D). Growth at high CO_2 concentrations, however, led to a pronounced accumulation of PsbS after 1 h of HL exposure and, complete degradation at longer illumination times in both WT and mutant cells (Fig. 5 E, F). The expression of LHCSR proteins in WT cells was regulated by light as well as carbon availability. In low CO_2 grown cells, LHCSR proteins were already expressed under LL growth, likely due to the fact that the intensity of 30 µmol photons m^{-2} s^{-1} is already saturating photosynthesis under limiting CO_2, and their expression levels increased only slightly upon HL exposure (Figs. 4A and 5A). With increasing CO_2, the expression of the protein was activated upon transfer to HL (Fig. 5 C, E), where it accumulated gradually in ambient CO_2 grown cells (Fig. 5C) but was degraded after 10 h of HL in high CO_2- grown cells (Fig. 5E). Remarkably, the expression of the CAH3 protein, a carbon anhydrase located in the thylakoid lumen known to be essential for the carbon concentration mechanism under low CO_2 (Karlsson et al., 1998; Park et al., 1999), was also expressed in cells under high CO_2 growth but degraded after 24 h of HL exposure (Fig. 3 E, F). In contrast, no protein changes were observed for the PSII core subunit D1 (Figs. 4 and 5).

Since both, PsbS and LHCSR had similar expression patterns in response to HL exposure at different CO_2 concentrations, we further investigated if those changes correlated with the quenching capacity during HL acclimation. The activation of NPQ was strongly dependent on CO_2 availability (Fig. 6) and required the accumulation of LHCSR proteins (Fig. 6B, D, F), emphasizing the essential role of these proteins, specifically LHCSR3, for qE activation (Peers et al., 2009). In WT, NPQ induction was inversely proportional to CO_2 availability: NPQ induction under HL conditions was fully suppressed in the presence of 5 % CO_2 (Fig. 6E). At low CO_2 (Fig. 6A) and ambient CO_2 grown cells (Fig. 6C), however, activation of NPQ capacity (amplitude of about 1.0) was induced after 6 h of HL exposure. The rapid dark reversibility of this NPQ indicates that predominantly the pH-dependent qE quenching was activated under these conditions (Allorent et al., 2013). Only low CO_2 grown cells showed higher qE quenching (amplitude of about 1.5) upon longer illumination times (48 h, Fig. 6A) compared to ambient CO_2 grown cells, which did not show a significant increase in qE capacity after 6-10 h of HL exposure (Fig. 6C). Interestingly, the gradual increase in qE capacity in low and ambient CO_2 grown cells correlated with the time frame for maximal PsbS accumulation (Fig. 5 A, C). This suggests that the PsbS protein might be either directly involved in the activation of qE, or in other responses required for HL acclimation of cells, especially under low CO_2 availability, and thus limited photosynthetic capacity.

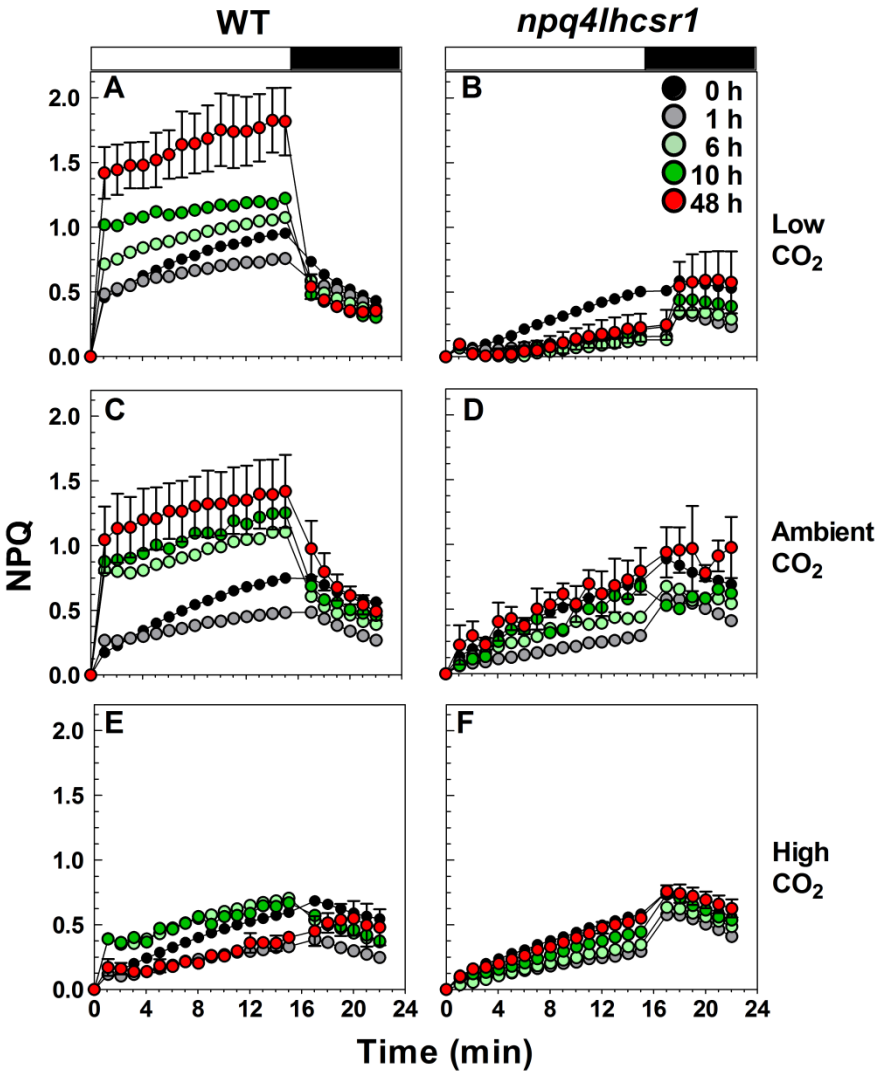

Figure 6. NPQ induction in *C. reinhardtii* cells grown at different CO_2 concentrations. Cells were grown in HS medium either at low CO_2 (A, B), ambient CO_2 (C, D) or high CO_2 (E, F). After growth under low light, cells were transferred to high light. NPQ was determined during 15 min of illumination at 825 µmol photons m^{-2} s^{-1} and a subsequent dark period of 5 min after 0, 1, 6, 10, and 48 h transfer to high light. Values represent mean ± SD (n = 4 biological replicates). For clarity, SD is only shown for samples after 48 h under HL, but was in the similar range for all other conditions.

Localization of PsbS in *C. reinhardtii*

The PsbS protein was detected in isolated solubilized thylakoids and its distribution among the PSII/PSI-LHC complexes was determined after separating protein complexes under native conditions by sucrose gradient ultracentrifugation (Fig. 7). In WT cells exposed to HL, most of the PsbS comigrated with PSII core enriched protein fractions rather than with LHCSR or LHCII proteins (Fig. 7 B, C), suggesting an association of PsbS with PSII. Conversely, in HL acclimated qE-deficient cells (*npq4lhcsr1*), PsbS was mainly co-migrating with light harvesting proteins (Fig. 7C). The differential PsbS distribution among complexes in cells with and without quenching capacity suggests that changes in the localization of PsbS might be related to the rearrangement of proteins during qE activation upon HL exposure.

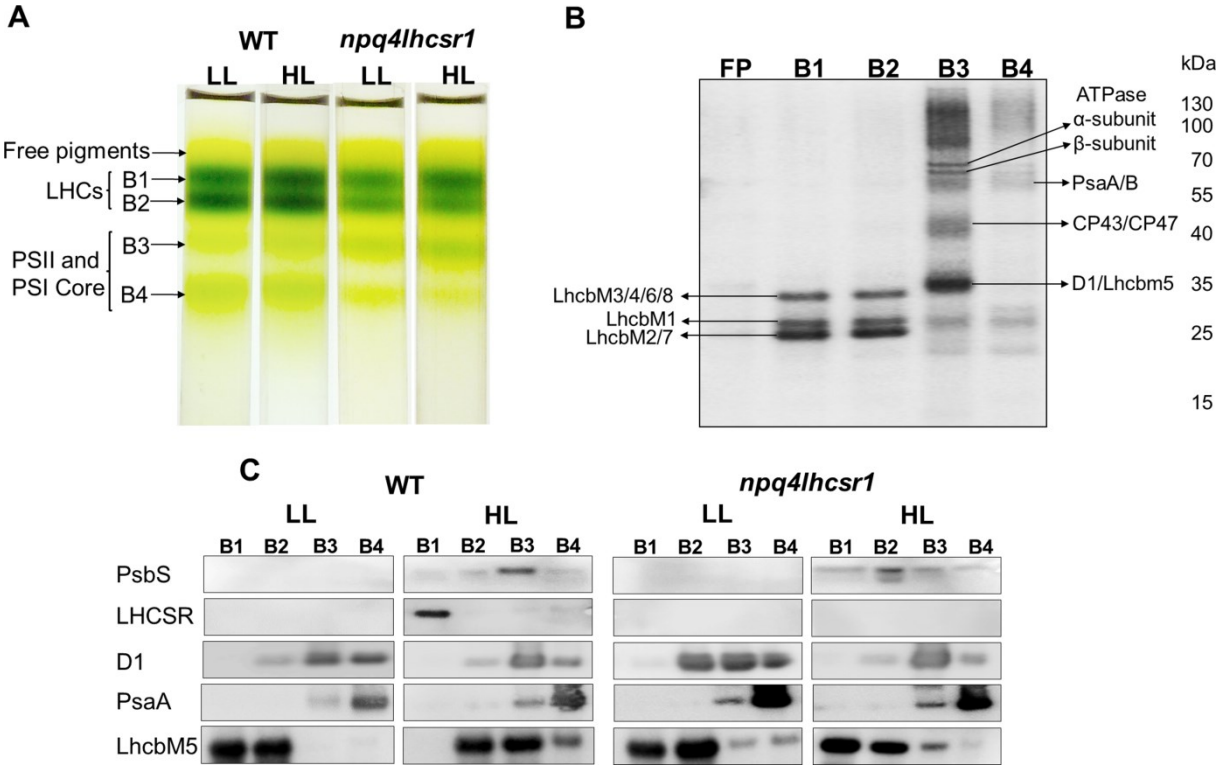

Figure 7. Localization of PsbS in *C. reinhardtii*. Thylakoids from WT ($4A^+$) and *npq4lhcsr1* cells grown under low light and ambient CO_2 were extracted before and after a 4 h exposure of cells to HL (480 µmol photons m^{-2} s^{-1}). Thylakoid membranes were solubilized with 1 % α-DM and protein complexes (corresponding to 200 µg chlorophyll) were separated by sucrose gradient centrifugation. **(A)** Separated bands were identified according to (Tokutsu et al., 2012; Tokutsu and Minagawa, 2013) as: free pigments (FP), dissociated LHCs (B1 and B2: monomers and trimers, respectively), and PSII and PSI enriched fractions (B3 and B4, respectively). **(B)** Proteins in each band were analyzed by NuPAGE® and visualized using a Sypro® Ruby protein staining. The distribution of the proteins is representative for all light treatments and both genotypes. Individual proteins were identified based on their molecular mass as previously reported (Drop et al., 2014). **(C)** Immunoblot analysis of representative proteins in each fraction.

DISCUSSION

The pH-regulated qE-mechanism of energy dissipation in C. *reinhardtii* is mediated by the LHCSR3 protein (Peers et al., 2009), contrary to land plants where this function is performed by either both PsbS and LHCSR as in mosses (Alboresi et al., 2010; Gerotto et al., 2012) or only PsbS as in vascular plants (Li et al., 2000). In this work, we presented evidence that the PsbS protein in *C. reinhardtii* is a light induced protein, which likely regulates the activation of the LHCSR dependent qE capacity without being sufficient to induce qE in the absence of LHCSR proteins.

HL irradiances elicit a combination of two strategies that allow *C. reinhardtii* cells to deal with excess light energy: the Δ pH-dependent quenching (qE) and state transitions (qT) (Allorent et al., 2013). State transitions are characterized by a redox dependent phosphorylation and movement of LHCII from PSII (in state 1) to PSI (in state 2), which balances the distribution of excitation energy between the two photosystems (Wollman, 2001). In state 2, LHC proteins, including LHCSR3, are predominantly associated with PSI (Allorent et al., 2013; Bonente et al., 2011; Takahashi et al., 2006) and move gradually to PSII upon transition to state 1, e.g. in response to HL (Allorent et al., 2013). The gradual transition of LHC proteins to PSII can be followed by monitoring the changes in chlorophyll fluorescence (Allorent et al., 2013). In HL adapted cells under autotrophic conditions, chlorophyll fluorescence might slowly increase in the first minutes of illumination (transitions from state 2 to 1) followed by a rapid decrease once LHCII have reached PSII (state 1). This is reflected as a low NPQ at the beginning of illumination, followed by a rapid increase until steady state quenching in the light (Allorent et al., 2013). In this work, cells were pre-illuminated with far red light prior to NPQ measurements, which promotes the association of LHCII with PSII (Peers et al., 2009). Consequently, a high proportion of LHCII was in state 1 before the onset of actinic light illumination. The rapid induction of NPQ observed within the first minute of illumination (Figs. 3 and 6A) thus represents a qE type quenching under conditions where NPQ is fully activated.

The regulation of qE responses (induction and capacity) is controlled at different levels in *C. reinhardtii*. At the transcript level, *LHCSR* and *PSBS* genes (specifically *PSBS1*) are upregulated in response to changes from low to high light (Maruyama et al., 2014; Mettler et al., 2014; Peers et al., 2009). In the present work, this became visible at the protein level after a few hours of HL illumination (Figs. 4 and 5). In addition to a shift in light intensity, the availability of CO_2 (and hence the efficiency of photosynthesis) plays an important role in the regulation of the qE machinery. In the absence of HL, *LHCSR3* transcription could be triggered even under low CO_2 conditions (Figs. 2A; 4A and 5A, C) thanks to an EEC motive (enhancer element of low CO_2-inducible genes) in its promoter region (Kucho et al., 2003; Maruyama et al., 2014) and possibly due to the possibility that a LL intensity of 30 µmol

photons m^{-2} s^{-1} used here may already saturate photosynthesis at limiting CO_2 availability. PsbS expression is exclusively light-dependent (Figs. 1; 2A; 4A and 5A) but its accumulation under HL depends on CO_2 availability as well (Fig. 5). CO_2-dependent accumulation of PsbS might also be controlled at the transcript level, since the EEC motive is also present in the promoter region of both *PSBS* genes (Fig. 8). Additionally, the accumulation of LHCSR requires Ca^{2+} (Petroutsos et al., 2011), however, whether or not HL induced accumulation of PsbS is also Ca^{2+}-dependent remains to be elucidated.

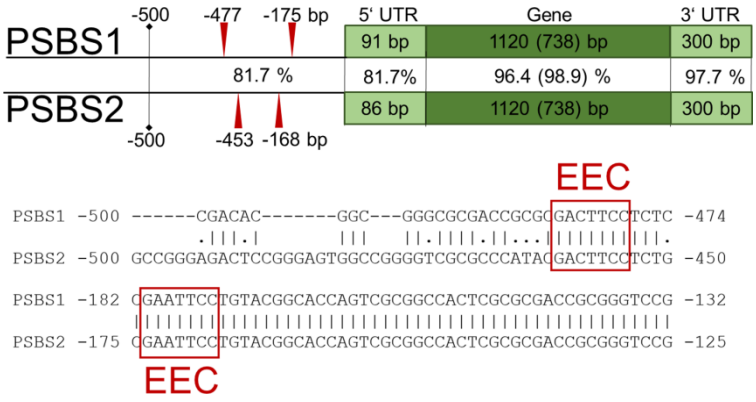

Figure 8. Conserved motifs in the promoter region of *PSBS* genes that respond to low CO_2. Two EEC conserved motifs corresponding to enhancer elements of low CO_2 inducible promoters were identified for *PSBS1* (at -477 and -175 bp) and *PSBS2* (-453 and -168 bp) genes (Merchant et al., 2007). The EEC motif sequence is shown for both genes by a nucleotide sequence alignment upstream of the 5' UTR region. The diagram was modified for the PsbS encoding genes after (Maruyama et al., 2014).

Change from lower to higher light intensities under high CO_2 (5 %) activates a shift in the metabolism from light utilization towards optimal ATP production (Mettler et al., 2014), so that quenching of excess energy is not activated. In a system where high ATP synthesis is favored by high CO_2 availability, lumen acidification was insufficient to trigger qE, thus this mechanism has a less important role in HL (Fig. 6E). Further studies of the regulation of carbon concentrating mechanisms (CCM) under HL are required to understand changes in CCM-related proteins, such as the degradation of CAH3, upon long term HL acclimation (Fig. 5E, F).

In addition to light and carbon availability, nitrogen starvation has been reported to upregulate the transcription of *PSBS* genes in mixotrophic growth (Miller et al., 2010). Under nitrogen starvation, transcription of genes encoding Calvin-Benson cycle enzymes and light-harvesting proteins decrease rapidly after a few hours upon nitrogen deprivation (Miller et al., 2010), but changes at the protein level are rather slow (Schmollinger et al., 2014). So even though PSBS transcripts were upregulated, those changes may be insufficient to activate the synthesis of proteins (Fig. 2). Nevertheless, a decrease of light-harvesting protein levels,

except for LHCSR3 and LHCSR1, along with lower levels of the carbon metabolism enzymes (Schmollinger et al., 2014) increased NPQ induction under nitrogen starvation in HL, compared to cells without nutrient deficiency (Fig. 3).

The analysis of NPQ induction curves in comparison with the accumulation of PsbS and LHCSR under different growth conditions enables us to identify specific requirements for qE quenching in *C. reinhardtii.* The following important conclusions regarding the induction of qE in *C. reinhardtii* can be drawn:

1. The presence of LHCSR in LL grown cells before the onset of HL illumination (Figs. 2A, 4A and 5A) is not sufficient for qE induction. Consequently, further acclimation processes are required for establishing a high qE capacity.
2. The presence of both PsbS and LHCSR3 after 1 h of HL exposure in high CO_2 grown cells is not sufficient for qE induction (Fig. 5A). Together with the rapid degradation of both PsbS and LHCSR during longer illumination periods, this suggests that qE is generally not activated at high CO_2 concentrations.
3. The presence of PsbS is not sufficient to induce any qE in the absence of LHCSR3, even after longer periods of HL acclimation (Figs. 2B, 3, 5B and D, 6B and D). This underscores the essential requirement of LHCSR for qE.
4. PsbS accumulates only transiently to maximal levels during HL acclimation and undergoes degradation after induction of full qE capacity (Figs. 5A and C, 6A and C), indicating a critical role of PsbS during the establishment of high qE capacity.
5. PsbS accumulation precedes the accumulation of LHCSR concomitant with the establishment of high qE capacity (Figs. 5A and C, 6A and C), suggesting that PsbS controls processes, which might be required to establish a specific interaction of LHCSR with PSII that is required for qE.
6. Complete degradation of PsbS is not required for maintaining high qE capacity, since higher qE can be induced in the presence of low PsbS levels after 48 h of HL acclimation under low CO_2 (Figs. 5A and 6A). This implies that PsbS does not interfere with the quenching site.

Taken together, PsbS in *C. reinhardtii* is transiently expressed during the establishment of qE capacity upon HL acclimation. Similar to LHCSR, the expression of PsbS is regulated by light and CO_2 availability. These characteristics suggest that PsbS is involved in qE activation. It can be speculated, that PsbS might promote qE capacity by controlling conformational changes in high light as proposed to the PsbS in *A. thaliana* (Johnson et al., 2011) (see also manuscript 2). In *C. reinhardtii,* two qE quenching sites have been proposed to be involved in qE: one in the minor light-harvesting complexes and another in aggregated LHCII trimers, detached from PSII (Amarnath et al., 2012), and similar to the situation in *A. thaliana* (Holzwarth et al., 2009). Within the thylakoid membrane, PsbS was

found to co-migrate with PSII core proteins and not with LHCSR in HL-acclimated cells (Fig. 7C), suggesting a preferential interaction of PsbS with the PSII reaction center upon HL acclimation. However, in the absence of LHCSR proteins (*npq4lhcsr1*), this affinity for PSII was reduced (Fig. 7C). Although PsbS did not directly interact with LHCSR proteins in the light (Fig. 7C), its affinity towards PSII in a quenched state could indicate that PsbS is involved in the detachment of LHCII proteins from PSII, which might be essential for qE induction. Such a function of PsbS in the reorganization of PSII antenna proteins would be very similar to that in vascular plants (see manuscript 2). To verify the proposed critical role of PsbS for activation of qE upon HL acclimation in *C. reinhardtii*, the analysis of qE induction in *PSBS* knock-out or knock-down lines will be essential in future work.

The HL-induced expression of PsbS protein in *C. reinhardtii* provides new insights into the evolution of qE quenching in oxygenic photosynthetic organisms. In the clade Viridiplantae (green algae and plants), PsbS homologs are found in organisms of different branches of the Chlorophyta (green algae) and the Streptophyta (the closest algae group to terrestrial land plants) (Bonente et al., 2008; Gerotto and Morosinotto, 2013). However, only in late Streptophyta, PSBS is expressed and accumulated, suggesting a more significant role of PsbS in NPQ in this clade compared to the early Streptophyta and Chlorophyta relatives, where NPQ processes are LHCSR dependent (Gerotto and Morosinotto, 2013; Peers et al., 2009). Here, we reported the HL induced accumulation of PsbS in the model Chlorophyta *C. reinhardtii*. Our data are in agreement with the hypothesis that the LHCSR function was lost, and gradually replaced by PSBS, during the transition from aquatic to terrestrial environments (i.e. from Chlorophyta to late Streptophyta). PsbS-regulated NPQ might have provided a selective advantage in terrestrial environments, acting as a fine-tuning mechanism for fast responses to fluctuating light in a system where carbon access to Rubisco may become limiting upon high light stress.

MATERIALS AND METHODS

Cells and growth conditions

Chlamydomonas reinhardtii wild-type strain dw15.1 (cw15, nit1, mt+) was provided by Barb Sears (Michigan State University). The WT strain 4A+ (137c genetic background) and the double mutant *npq4lhcsr1* lacking the LHCSR3 and LHCSR1 proteins (*LHCSR 3.1, LHCSR 3.2,* LHCSR1 genes) were provided by Kris Niyogi (University of California, Berkeley). For all experiments, cells were grown at 23 °C and constantly stirred on a shaker at 112 rpm. Light regimes were defined as low light (LL: 30 µmol photons m^{-2} s^{-1}) and high light (HL: 480 µmol photons m^{-2} s^{-1}).

Expression and purification of recombinant PsbS protein

Recombinant PsbS cloned into the pET28a (+) vector (Novagen) as described previously (Bonente et al., 2008) was kindly provided by Katrin Gärtner (Michigan State University). Recombinant PsbS (*r*-PsbS) was overexpressed in BL21 gold *Escherichia coli* cells, extracted and purified as follows. After 5 h of IPTG induced expression, cells were resuspended in 30 ml lysis buffer (20 mM sodium-phosphate pH 7.4, 1 % Triton (v/v), 2 M NaCl, 1 mg/ml lysozyme, 1 tablet of protease inhibitor cocktail EDTA-*free*, Roche) and disrupted three times by a French press at a constant pressure between 1200-1500 psi. The sample was centrifuged at 25 000 *x g* and 4 °C for 30 min, and solubilized proteins were collected from the supernatant. Recombinant PsbS was purified by affinity chromatography with a pre-equilibrated nickel–nitrilotriacetic acid column (Bio-Rad) using an imidazol gradient (0, 10, 20, 50, 100, 200, 300, 750 mM) in a buffer containing 40 mM Tris-HCl pH 8, 300 mM NaCl and 100 mM sodium cholate. 5 µl of each eluted fraction were separated on a 12 % acrylamide SDS–PAGE according to (Laemmli, 1970) and elution of the recombinant protein was verified by Coomassie blue staining. Confirmed elutes were desalted (3.5 kDa cut-off dialysis tubing, Spectra/Pro®) and concentrated with a spin column (3 kDa cut off, Vivaspin Protein Concentrator GE Healthcare). Protein concentrations were quantified using the DC™ Protein Assay (Bio-Rad), and *r*-PsbS was identified by immunoblotting as described previously (Schwarz et al., 2015). *r*-PsbS was detected using an anti-His-tag antibody (Miltenyi Biotec*)* and an antibody specifically designed for *C. reinhardtii* (contracted work Pineda antibody service).

Nitrogen starvation experiments

WT 4A+ and *npq4lhcsr1* cells were grown in a 50 ml pre-culture in TAP (Gorman and Levine, 1965) or HS (Sueoka, 1960) media containing 7.2 mM and 9.4 mM NH_4^+, respectively (+N media). Cells were grown under constant low light (30 µmol photons m^{-2} s^{-1}) for 3-5 days until

the culture reached a density of 3-5 x 10^6 cells/ml. 25 ml of the pre-culture were used to inoculate 100 ml of the same media. For each culture, two different intensities of continuous light were used: 30 µmol photons m^{-2} s^{-1} (low light, LL) and 480 µmol photons m^{-2} s^{-1} (high light, HL). Once the cultures reached 5 x 10^6 cells /ml, nitrogen starvation was induced by transferring the cells to media without any NH_4^+ (TAP or HS, -N) and cells were grown for the next 48 h under their respective light regimes. Cells were harvested by centrifugation at 3850 x *g*, frozen in liquid nitrogen and stored at -20 °C for further analysis.

Immunoblot analysis of PsbS expression

For each strain, cells were grown in three 50 ml HS media pre-cultures under LL for 5 days. Each pre-culture was used to inoculate 700 ml of HS media with no additional air input (no CO_2), bubbling with air (ambient CO_2 ≈ 0.035-0.04 %) or air enriched with 5 % CO_2 (high CO_2). Cells were grown in continuous LL until reaching a cell density of 5 x 10^6 cells / ml and subsequently transferred to HL. For protein analysis, 100 ml of sample were taken after 0, 1, 6, 10, 24, and 48 h of HL exposure. After harvesting the samples, 100 ml of fresh HS media was added to each culture. The same procedure was used when sampling cells after 0, 30, 60, 120, 180 and 360 minutes transfer to HL. In this case, cells were grown in HS without additional CO_2. All samples were harvested and stored for further analysis as described for the nitrogen starvation experiments.

200 µl frozen pellet (≈ 1 x 10^9 cells/ml) were resuspended in 500 µl TMK buffer (10 mM Tris/HCl pH 6.8, 10 mM $MgCl_2$, 20 mM KCl) and 0.6 g of glass beads (200 µm), vortexed three times for 1 min with 2 min of ice cooling intervals. The supernatant was removed, the beads washed with 100 µl TMK buffer and the collected supernatants centrifuged for 5 min at 17,000 x *g* at 4 °C. The pellet was resuspended in 200 µl extraction buffer (1.6 % SDS, 1 M urea, 50 mM Tris/HCl pH 7.6, Protease inhibitor cocktail EDTA-*free* Roche), heated for 30 min at 95 °C under stirring and centrifuged 20 min at 17,000 x *g* at room temperature. Protein content of the supernatants was quantified with the DC™ Protein Assay (Bio-Rad). Proteins were separated on a NuPAGE® Novex® 10 % Bis-Tris gel (Life Sciences) according to the manufacturer's instructions. Specific proteins were detected by immunobloting as described previously (Schwarz et al., 2015). PsbS was detected with the *C. reinhardtii* antibody (contracted work Pineda antibody service). The LHCSR antibody was provided by Michael Hippler (University of Münster). For all other proteins, Agrisera® antibodies were used.

Isolation of thylakoid membranes

WT ($4A^+$) and *npq4lhcsr1* mutant cells were grown in 1 L HS medium cultures with air bubbling (ambient CO_2) under LL until reaching the exponential phase (5 x 10^6 cells/ml) and

subsequently illuminated with HL for 4 h. Cells were harvested by centrifugation at 12,000 x *g* for 10 minutes and resuspended in 20-25 ml buffer (250 mM sorbitol, 1 mM $MnCl_2$, 5 mM $MgCl_2$, 35 mM Hepes/NaOH pH 7.8, protease inhibitor cocktail, Roche). Cells were disrupted by pressure in a French press (1000 psi, 4 °C) for three times, centrifuged 10 min at 12,000 x *g*, 4 °C. The pellet was resuspended with a paint brush in 15 ml of 5 mM $MnCl_2$, centrifuged again, resuspended in 200-250 µl aliquots with 5 mM $MnCl_2$, frozen in liquid N_2 and stored at -20 °C.

Sucrose gradient ultracentrifugation

Protein complexes in the thylakoid membrane were separated by sucrose density gradient centrifugation as described by Tokutsu et al. (2012) with some modifications. Stacked membranes were unstacked by adding 1 volume of 5 mM EDTA and centrifuged for 1 min at 17,000 x *g* at 4 °C. Unstacked membranes were solubilized in a medium containing 25 mM MES pH 6.5 and 1 % α-DM at a final concentration of 0.4 mg chlorophyll/ml. Insolubilized material was removed by centrifugation at 17000 x *g* for 10 min. Solubilized thylakoids corresponding to 200 µg Chl were loaded onto a discontinuous sucrose gradient (0.1/0.4/0.7/1.0/1.3 M sucrose, 25 mM MES, pH 6.5, 1 M Betaine, 0.02 % α-DM) and fractionated by ultracentrifugation for 16 h at 130,000 x *g* at 4 °C. After separation, each band was collected and half of the volume was used to quantify the pigment content by reverse HPLC (Färber et al., 1997) whereas the other half was used for protein analysis. Proteins corresponding to 2 µg chlorophyll (and 25 µg chlorophyll for PsbS detection) were separated on a NuPAGE® Novex® 10 % Bis-Tris gel (Life Sciences) and visualized with a Sypro® Ruby protein gel staining, according to the manufacturer's protocol. Proteins were immobilized and detected as mentioned on the

Chlorophyll fluorescence measurements

All spectroscopic measurements were performed with three biological replicates. For the nitrogen starvation experiment, cells were measured after the 48 h treatment with (+N) or without (-N) nitrogen. A volume corresponding to 2 x 10^7 cells was centrifuged for 10 seconds, the cells resuspended in 2 ml of fresh HS media and incubated in the dark in a 1 cm path length glass cuvette under stirring for 30 min. Spectroscopic measurements were performed using a spectrometer/fluorometer as in (Lucker and Kramer, 2013). After the dark adaptation period, cells were exposed to 5 min far red light (> 720 nm, 1 µmol photons m^{-2} s^{-1}) prior to chlorophyll fluorescence measurements. For fluorescence analysis, cells were illuminated with 600 µmol photons m^{-2} s^{-1} actinic light for 30 min followed by 10 min incubation in the dark. Saturation pulses (Red light, 250 ms, 3200 µmol photons m^{-2} s^{-1}) were applied every 90 seconds. For the light shift experiments, chlorophyll fluorescence was measured using a JTS-10 spectrometer (Bio Logic SAS, France). A volume corresponding to

2 x 10^7 cells was dark adapted under stirring under ambient CO_2 for 15 min and then filtrated on a glass fiber filter (PALL Corporation). The filter was placed on the spectrometer and cells were exposed to 5 min of far red light (400 µmol photons m^{-2} s^{-1}) followed by 15 min at 940 µmol photons m^{-2} s^{-1} of red actinic light and 6 min incubation in the dark. Saturation pulses (red light, 7900 µmol photons m^{-2} s^{-1}) were applied every 60 seconds. In the dark relaxation phase, samples were illuminated for 55 seconds with far red light between saturation pulses. NPQ was calculated as (Fm/Fm') – 1 (Krause and Jahns, 2004).

Cell counting

Cells in a 1 ml culture were fixed with 20 µl 0.25 % iodine (w/v in ethanol) and the number of cells/ ml calculated using a Thoma cell counting chamber (Marienfeld, Germany).

REFERENCES

Alboresi, A., Gerotto, C., Giacometti, G.M., Bassi, R., and Morosinotto, T. (2010). *Physcomitrella patens* mutants affected on heat dissipation clarify the evolution of photoprotection mechanisms upon land colonization. Proc. Natl. Acad. Sci. USA *107*, 11128-11133.

Allorent, G., Tokutsu, R., Roach, T., Peers, G., Cardol, P., Girard-Bascou, J., Seigneurin-Berny, D., Petroutsos, D., Kuntz, M., Breyton, C., et al. (2013). A dual strategy to cope with high light in *Chlamydomonas reinhardtii*. Plant Cell *25*, 545-557.

Amarnath, K., Zaks, J., Park, S.D., Niyogi, K.K., and Fleming, G.R. (2012). Fluorescence lifetime snapshots reveal two rapidly reversible mechanisms of photoprotection in live cells of *Chlamydomonas reinhardtii*. Proc. Natl. Acad. Sci. USA *109*, 8405-8410.

Anwaruzzaman, M., Chin, B., Li, X., Lohr, M., Martinez, D.A., and Niyogi, K.K. (2004). Genomic analysis of mutants affecting xanthophyll biosynthesis and regulation of photosynthetic light harvesting in *Chlamydomonas reinhardtii*. Photosynth Res *82*, 265–276.

Bergantino, E., Segalla, A., Brunetta, A., Teardo, E., Rigoni, F., Giacometti, G.M., and Szabò, I. (2003). Light- and pH-dependent structural changes in the PsbS subunit of photosystem II. Proc. Natl. Acad. Sci. USA *100*, 15265-15270.

Blankenship, R.E., and Hartman, H. (1998). The origin and evolution of oxygenic photosynthesis. Trends Biochem Sci *23*, 94-97.

Bonente, G., Ballottari, M., Truong, T.B., Morosinotto, T., Ahn, T.K., Fleming, G.R., Niyogi, K.K., and Bassi, R. (2011). Analysis of LhcSR3, a protein essential for feedback de-excitation in the green alga *Chlamydomonas reinhardtii*. PLoS Biol *9*, e1000577.

Bonente, G., Passarini, F., Cazzaniga, S., Mancone, C., Buia, M.C., Tripodi, M., Bassi, R., and Caffarri, S. (2008). The occurrence of the psbS gene product in *Chlamydomonas reinhardtii* and in other photosynthetic organisms and its correlation with energy quenching. Photochem Photobiol *84*, 1359-1370.

Drop, B., Webber-Birungi, M., Yadav, S.K., Filipowicz-Szymanska, A., Fusetti, F., Boekema, E.J., and Croce, R. (2014). Light-harvesting complex II (LHCII) and its supramolecular organization in *Chlamydomonas reinhardtii*. Biochim Biophys Acta *1837*, 63-72.

Fan, M., Li, M., Liu, Z., Cao, P., Pan, X., Zhang, H., Zhao, X., Zhang, J., and Chang, W. (2015). Crystal structures of the PsbS protein essential for photoprotection in plants. Nat. Struct. Mol. Biol *22*, 729-735.

Färber, A., Young, A.Y., Ruban, A., Horton, P., and Jahns, P. (1997). Dynamics of Xanthophyll-Cycle Activity in Different Antenna Subcomplexes in the Photosynthetic Membranes of Higher Plants (The Relationship between Zeaxanthin Conversion and Nonphotochemical Fluorescence Quenching). Plant Physiol *115*, 1609-1618

Finazzi, G., Johnson, G.N., Dall'Osto, L., Zito, F., Bonente, G., Bassi, R., and Wollman, F. (2006). Nonphotochemical Quenching of Chlorophyll Fluorescence in *Chlamydomonas reinhardtii*. Biochemestry *45*, 1490-1498.

Gerotto, C., Alboresi, A., Giacometti, G.M., Bassi, R., and Morosinotto, T. (2012). Coexistence of plant and algal energy dissipation mechanisms in the moss *Physcomitrella patens*. New Phytol *196*, 763-773.

Gerotto, C., Franchin, C., Arrigoni, G., and Morosinotto, T. (2015). In Vivo Identification of Photosystem II Light Harvesting Complexes Interacting with PHOTOSYSTEM II SUBUNIT S. Plant Physiol *168*, 1747-1761.

Gerotto, C., and Morosinotto, T. (2013). Evolution of photoprotection mechanisms upon land colonization: evidence of PSBS-dependent NPQ in late Streptophyte algae. Physiol Plant *149*, 583–598.

Gorman, D.S., and Levine, R.P. (1965). Cytochrome f and plastocyanin: their sequence in the photosynthetic electron transport chain of Chlamydomonas reinhardi. Proc. Natl. Acad. Sci. USA *54*, 1665-1669.

Goss, R., and Lepetit, B. (2015). Biodiversity of NPQ. J Plant Physiol 172, 13-32.

Holzwarth, A.R., Miloslavina, Y., Nilkens, M., and Jahns, P. (2009). Identification of two quenching sites active in the regulation of photosynthetic light-harvesting studied by time-resolved fluorescence. Chem Phys Lett *483*, 262-267.

Iwai, M., Kato, N., and Minagawa, J. (2007). Distinct physiological responses to a high light and low CO2 environment revealed by fluorescence quenching in photoautotrophically grown *Chlamydomonas reinhardtii*. Photosynth Res *94*, 307-314.

Johnson, M.P., Goral, T.K., Duffy, C.D., Brain, A.P., Mullineaux, C.W., and Ruban, A.V. (2011). Photoprotective energy dissipation involves the reorganization of

photosystem II light-harvesting complexes in the grana membranes of spinach chloroplasts. Plant Cell *23*, 1468-1479.

Karlsson, J., Clarke, A.K., Chen, Z.Y., Hugghins, S.Y., Park, Y.I., Husic, H.D., Moroney, J.V., and Samuelsson, G. (1998). A novel α-type carbonic anhydrase associated with the thylakoid membrane in *Chlamydomonas reinhardtii* is required for growth at ambient CO2. EMBO J *17*, 1208-1216.

Krause, G.H., and Jahns, P. (2004). Non-photochemical Energy Dissipation Determined by Chlorophyll Fluorescence Quenching: Characterization and Function. In Chlorophyll a Fluorescence, G. Papageorgiou, and Govindjee, eds. (Springer Netherlands), pp. 463-495.

Kucho, K., Yoshioka, S., Taniguchi, F., Ohyama, K., and Fukuzawa, H. (2003). Cis-acting elements and DNA-binding proteins involved in CO2-responsive transcriptional activation of Cah1 encoding a periplasmic carbonic anhydrase in *Chlamydomonas reinhardtii*. Plant Physiol *133*, 783-793.

Kulheim, C., Agren, J., and Jansson, S. (2002). Rapid regulation of light harvesting and plant fitness in the field. Science *297*, 91-93.

Laemmli, U.K. (1970). Cleavage of Structural Proteins during the Assembly of the Head of Bacteriophage T4. Nature *227*, 680-685.

Li, X., Björkman, O., Shih, C., Grossman, A.R., Rosenquist, M., Jansson, S., and Niyogi, K.K. (2000). A pigment-binding protein essential for regulation of photosynthetic light harvesting. Nature *403*, 391-395.

Li, X.P., Gilmore, A.M., Caffarri, S., Bassi, R., Golan, T., Kramer, D., and Niyogi, K.K. (2004). Regulation of photosynthetic light harvesting involves intrathylakoid lumen pH sensing by the PsbS protein. J Biol Chem *279*, 22866-22874.

Liguori, N., Roy, L.M., Opacic, M., Durand, G., and Croce, R. (2013). Regulation of light harvesting in the green alga *Chlamydomonas reinhardtii*: the C-terminus of LHCSR is the knob of a dimmer switch. J Am Chem Soc *135*, 18339-18342.

Lucker, B., and Kramer, D.M. (2013). Regulation of cyclic electron flow in *Chlamydomonas reinhardtii* under fluctuating carbon availability. Photosynth Res *117*, 449-459.

Maruyama, S., Tokutsu, R., and Minagawa, J. (2014). Transcriptional regulation of the stress-responsive light harvesting complex genes in *Chlamydomonas reinhardtii*. Plant Cell Physiol *55*, 1304-1310.

Merchant, S.S., Prochnik, S.E., Vallon, O., Harris, E.H., Karpowicz, S.J., Witman, G.B., Terry, A., Salamov, A., Fritz-Laylin, L.K., Maréchal-Drouard, L.*, et al.* (2007). The Chlamydomonas Genome Reveals the Evolution of Key Animal and Plant Functions. Science *318*, 245-250.

Mettler, T., Muhlhaus, T., Hemme, D., Schottler, M.A., Rupprecht, J., Idoine, A., Veyel, D., Pal, S.K., Yaneva-Roder, L., Winck, F.V., et al. (2014). Systems Analysis of the Response of Photosynthesis, Metabolism, and Growth to an Increase in Irradiance in the Photosynthetic Model Organism *Chlamydomonas reinhardtii*. Plant Cell. 26, 2310-2350.

Miller, R., Wu, G., Deshpande, R.R., Vieler, A., Gartner, K., Li, X., Moellering, E.R., Zauner, S., Cornish, A.J., Liu, B.*, et al.* (2010). Changes in transcript abundance in *Chlamydomonas reinhardtii* following nitrogen deprivation predict diversion of metabolism. Plant Physiol *154*, 1737-1752.

Minagawa, J., and Tokutsu, R. (2015). Dynamic regulation of photosynthesis in *Chlamydomonas reinhardtii*. Plant J *82*, 413-428.

Møller, I.M., Jensen, P.E., and Hansson, A. (2007). Oxidative modifications to cellular components in plants. Annu Rev Plant Biol *58*, 459-481.

Morosinotto, T., Baronio, R., and Bassi, R. (2002). Dynamics of chromophore binding to Lhc proteins in vivo and in vitro during operation of the xanthophyll cycle. J Biol Chem *277*, 36913-36920.

Nilkens, M., Kress, E., Lambrev, P., Miloslavina, Y., Müller, M., Holzwarth, A.R., and Jahns, P. (2010). Identification of a slowly inducible zeaxanthin-dependent component of non-photochemical quenching of chlorophyll fluorescence generated under steady-state conditions in Arabidopsis. Biochim Biophys Acta *1797*, 466-475.

Niyogi, K.K., Björkman, O., and Grossman, A.R. (1997). Chlamydomonas Xanthophyll Cycle Mutants Identified by Video Imaging of Chlorophyll Fluorescence Quenching. Plant Cell *9*.

Niyogi, K.K., Grossman, A.R., and Björkman, O. (1998). Arabidopsis Mutants Define a Central Role for the Xanthophyll Cycle in the Regulation of Photosynthetic Energy Conversion. Plant Cell *10*, 1121-1134.

Niyogi, K.K., and Truong, T.B. (2013). Evolution of flexible non-photochemical quenching mechanisms that regulate light harvesting in oxygenic photosynthesis. Curr Opin Plant Biol *16*, 307-314.

Ossenbühl, F., Gohre, V., Meurer, J., Krieger-Liszkay, A., Rochaix, J.D., and Eichacker, L.A. (2004). Efficient assembly of photosystem II in *Chlamydomonas reinhardtii* requires Alb3.1p, a homolog of Arabidopsis ALBINO3. Plant Cell *16*, 1790-1800.

Park, Y.-I., Karlsson, J., Rojdestvenski, I., Pronina, N., Klimov, V., Öquist, G., and Samuelsson, G. (1999). Role of a novel photosystem II-associated carbonic anhydrase in photosynthetic carbon assimilation in *Chlamydomonas reinhardtii*. FEBS Lett *444*, 102-105.

Peers, G., Truong, T.B., Ostendorf, E., Busch, A., Elrad, D., Grossman, A.R., Hippler, M., and Niyogi, K.K. (2009). An ancient light-harvesting protein is critical for the regulation of algal photosynthesis. Nature *462*, 518-521.

Petroutsos, D., Busch, A., Janssen, I., Trompelt, K., Bergner, S.V., Weinl, S., Holtkamp, M., Karst, U., Kudla, J., and Hippler, M. (2011). The chloroplast calcium sensor CAS is required for photoacclimation in *Chlamydomonas reinhardtii*. Plant Cell *23*, 2950-2963.

Pinnola, A., Dall'Osto, L., Gerotto, C., Morosinotto, T., Bassi, R., and Alboresi, A. (2013). Zeaxanthin binds to light-harvesting complex stress-related protein to enhance nonphotochemical quenching in *Physcomitrella patens*. Plant Cell *25*, 3519-3534.

Schmollinger, S., Muhlhaus, T., Boyle, N.R., Blaby, I.K., Casero, D., Mettler, T., Moseley, J.L., Kropat, J., Sommer, F., Strenkert, D.*, et al.* (2014). Nitrogen-Sparing Mechanisms in Chlamydomonas Affect the Transcriptome, the Proteome, and Photosynthetic Metabolism. Plant Cell *26*, 1410-1435.

Schwarz, N., Armbruster, U., Iven, T., Brückle, L., Melzer, M., Feussner, I., and Jahns, P. (2015). Tissue-specific accumulation and regulation of zeaxanthin epoxidase in Arabidopsis reflect the multiple functions of the enzyme in plastids. Plant Cell Physiol *56*, 346-357.

Sueoka, N. (1960). Mitotic replication of deoxyribonucleic acid in *Chlamydomonas reinhardi.* Proc. Natl. Acad. Sci. USA *46*, 83-91.

Takahashi, H., Iwai, M., Takahashi, Y., and Minagawa, J. (2006). Identification of the mobile light-harvesting complex II polypeptides for state transitions in *Chlamydomonas reinhardtii*. Proc. Natl. Acad. Sci. USA *103*, 477-482.

Teramoto, H., Nakamori, A., Minagawa, J., and Ono, T.A. (2002). Light-intensity-dependent expression of Lhc gene family encoding light-harvesting chlorophyll-a/b proteins of photosystem II in *Chlamydomonas reinhardtii*. Plant Physiol *130*, 325-333.

Tokutsu, R., Kato, N., Bui, K.H., Ishikawa, T., and Minagawa, J. (2012). Revisiting the supramolecular organization of photosystem II in *Chlamydomonas reinhardtii*. J Biol Chem *287*, 31574-31581.

Tokutsu, R., and Minagawa, J. (2013). Energy-dissipative supercomplex of photosystem II associated with LHCSR3 in *Chlamydomonas reinhardtii*. Proc. Natl. Acad. Sci. USA *110*, 10016–10021.

Wollman, F. (2001). State transitions reveal the dynamics and fexibility of the photosynthetic apparatus. EMBO J *20*, 3623-3630.

Xu, P., Tian, L., Kloz, M., and Croce, R. (2015). Molecular insights into Zeaxanthin-dependent quenching in higher plants. Sci Rep *5*, 13679.

Yamano, T., and Fukuzawa, H. (2009). Carbon-concentrating mechanism in a green alga, *Chlamydomonas reinhardtii*, revealed by transcriptome analyses. J Basic Microbiol *49*, 42-51.

AUTHOR CONTRIBUTIONS

VC and PJ designed the experiments. VC and PJ wrote the manuscript. PR performed the nitrogen starvation experiment and the short term light induction experiment. VC performed the protein analysis for the CO_2 experiment and the PsbS localization experiments. VC, PR and AG performed the NPQ measurements. VK performed the expression and purification of the recombinant PsbS. KKN generated and provided the *npq4lhcsr1* double mutant .BL and DK collaborated with the NPQ measurements in the nitrogen starvation experiment.

7. ACKNOWLEDGEMENTS

I would like to especially thank my supervisor Prof. Dr. Peter Jahns, who gave me the chance to work on this project, was always willing to discuss with me, and whose support and guidance were invaluable in all the moments when I thought I was diving in a bottle neck. Thanks Peter for being so committed to your *Doktorvater* role. I am also grateful to Prof. Dr. Rüdiger Simon, who agreed to be my co-supervisor and for his guidance during the annual committee meetings.

I would like to thank the financial support of the iGRAD-Plant program that made the execution of this work possible. To all the members of the iGRAD-Plant program, especially to Dr. Sigrun Wegener-Feldbrügge whose support and organization saved me a couple of times from the bureaucratic deluge I had to deal with. I also would like to thank Prof. Dr. Andreas Weber who gave me the opportunity to be part of the iGRAD-Plant program.

I would like to thank Dr. Gereon Poschmann from the BMFZ –Düsseldorf for all the good collaborative work in the PsbS protein –interactions project and Dr. Michael Melzer for his contribution to the PsbS localization studies. To Prof. Barb Sears, Prof. David Kramer and Dr. Ben Lucker who guided me during my stay at Michigan State University.

Special thanks to all the member of the AG Jahns group. Maria, who was always willing to help me with the stuff I asked for during my busy work days, and made delicious coffee for me although I was always too late to drink it warm, *Danke Mutti*. To Nadine, who was the best colleague I could ever ask for. We were always connected as a team although we had two different projects and we always understood each other so well not only at work but on a personal level. I am really going to miss working with you, *lieber Hase.* To Lazar for the nice late evening talks in the lab and for reading some parts of my work. To Petra Redekop who worked so hard in the *Chlamydomonas* project, which could not have come so far without her help. To Andreas Hussner whose critical mind made us pay attention to little details and Lena Tiebel who is the most straight forward person I know. And finally to Annika Grieß and Viktor Koch who also worked in the *Chlamydomonas* project.

I want to thank my friend Sophia Aldous. Her laughs were always the support I needed. Thanks to Lea, David, Pia, Rudi, Lotte, and Julia who made Düsseldorf feel like home, *Ich danke euch!*

I am immensely grateful to Tobias Schumann who besides being a great co-worker, helped me out to correct parts of this work with his incredible eye for detail and translated the

summary into German. I also want to thank him for his wonderful and unconditional support, *MIL GRACIAS MI VIDA.*

Finalmente quiero a gradecer a mi mami Cecilia Galvis, porque es gracias a ella que soy quien soy y su apoyo ha sido lo que me ha permitido llegar hasta este punto, gracias mamá. Tambien quiero agradecer a mi hermano Iván, cuya sinceridad siempre ha sido mi polo a tierra.